ABSTRACT

Title of Document: CHARACTERIZATION OF THE TrxSR TWO-COMPONENT SIGNAL TRANSDUCTION SYSTEM OF STREPTOCOCCUS PYOGENES AND ITS ROLE IN VIRULENCE REGULATION

Kathryn Maureen Gold, Doctor of Philosophy, 2011

Directed by: Dr. Kevin McIver, Associate Professor, Department of Cell Biology & Molecular Genetics

The Gram-positive group A streptococcus (GAS) is a strict human pathogen, which causes a wide variety of infections, ranging in severity from minor to life threatening. In order to cause such a diverse array of diseases, GAS utilizes two-component signal transduction systems (TCS) to coordinately regulate sets of virulence genes in response to changing host conditions. The present study investigates the role of the TrxSR TCS in the regulation of virulence of the GAS. Using an insertional inactivation mutation in TrxR in serotype M1 MGAS5005, transcriptome studies established that TrxR activates transcription of Mga-regulated virulence genes, a separate non-TCS regulatory pathway controlling factors important for immune evasion and colonization. Transcriptional reporter fusions of P*mga* to firefly luciferase revealed that the TrxR regulation occurs through the P*mga* promoter. Additionally, electrophoretic mobility shift assays using purified His-MBP tagged TrxR established specific binding of

TrxR to P*mga*, although the interaction appeared to be transient. To determine the importance of signal transduction for TrxR-mediated regulation of the Mga regulon and virulence, an *in vitro* reconstitution assay was performed with purified TrxR and TrxS. Using both wild type and mutated forms of the TrxSR proteins, we demonstrated that TrxSR is a functional two-component phosphorelay system. Interestingly, phosphorylation of TrxR did not appear to be critical for DNA binding and regulation, since a TrxR D55A mutation did not change the expression of TrxR regulated genes in GAS based on EMSA and qPCR. In order to investigate whether there is a functional conservation of TrxR's involvement in GAS virulence regulation, mutations were made in serotype M4 and M49 strains representing either throat only or generalist strains. We have determined that TrxR regulates *mga* and Mga-regulated genes (*emm*, *arp*) in the M4 and M49 backgrounds, suggesting conservation of TrxR's role in virulence regulation. Overall, TrxSR represents a functional TCS that appears to directly regulate the Mga virulence regulon independent of phosphorelay. Furthermore, the functional conservation of TrxR regulation of Mga in other serotypes suggests a conserved role for its involvement in virulence regulation in GAS.

CHARACTERIZATION OF THE TrxSR TWO-COMPONENT SIGNAL TRANSDUCTION SYSTEM OF STREPTOCOCCUS PYOGENES AND ITS ROLE IN VIRULENCE REGULATION

By

Kathryn Maureen Gold

Dissertation submitted to the Faculty of the Graduate School of the
University of Maryland, College Park, in partial fulfillment
of the requirements for the degree of
Doctor of Philosophy
2011

Advisory Committee:
Professor Kevin McIver, Chair
Professor William Bentley, Dean's Representative
Professor Najib El-Sayed
Professor Vincent Lee
Professor Richard Stewart

DEDICATION

For Jacob,

"What lies behind us, and what lies before us are tiny matters
compared to what lies within us."

~ by Ralph Waldo Emerson

ACKNOWLEDGEMENTS

First and foremost, I would like to thank my advisor, Kevin McIver, for mentoring and guiding me throughout the course of my graduate career. Kevin, you have taught me not only how to survive in science, but how to persevere. You've shown me how to deal with delays and disappointments, and how to turn drawbacks into learning experiences. Also, I'd like to thank my committee members, Drs. Vince Lee, Rick Stewart, Najib El-Sayed, and Bill Bentley, for all of your generous support and suggestions over the years. Special thanks go to Rick and Vince, who provided me with some of the reagents that I needed to help trouble-shoot my experiments.

I would also like to thank my McIver lab members, both past and present. Daria, you were a great help to me in my final years here. I could always count on you to assist me whenever I needed and to set up overnights on Sundays to save me the drive. Lara and Kanika, thank you for all of our much-needed gossip breaks and conversations. They were always a lift, and sometimes a "day-saver." Elise, you enabled me to conquer my "protein fears" and guided me through many of my first protein experiments. Yoann, I would thank you for your endless passion for research. It will ever be an inspiration to me. And Traci, you taught me the ropes of working in microbiology.

Many thanks also go to Megan and Beth, for your support and friendship during our time together in grad school. Your infinite "optimism and enthusiasm" was and always will be much appreciated!

Most importantly, I would like to thank my family. Mom, you've been my rock of encouragement, always there whenever I needed someone to talk to for those extra words of support. Dad, you supported me without fail and could always keep things in perspective in terms of graduating "on time". Most of all, Jacob, thank you for joining me on this wild ride. We've experienced the ups and downs of science together, and I am *eternally* grateful for all of your love and support.

Thank you!

TABLE OF CONTENTS

DEDICATION ..... **ii**

ACKNOWLEDGMENTS ..... **iii**

TABLE OF CONTENTS ..... **v**

LIST OF TABLES ..... **ix**

LIST OF FIGURES ..... **x**

LIST OF ABBREVIATIONS ..... **xi**

CHAPTER ONE: Introduction **1**

CHAPTER TWO: Literature Review **3**

HISTORICAL PERSPECTIVE **3**

CLASSIFICATION **4**

General characteristics 4

Growth requirements 4

Lancefield grouping 4

M, T, and OF typing 5

Class determination 6

GROUP A STREPTOCOCCAL DISEASE **6**

Throat infections 7

Skin infections 9

Invasive diseases 10

Secondary sequelae 13

Vaccines 15

VIRULENCE FACTORS **16**

Cell-associated 17

Secreted factors 23

VIRULENCE REGULATION **27**

Two-component systems 28

Stand-alone regulators..... 33
Other GAS regulators..... 38
TWO-COMPONENT SIGNAL TRANSDUCTION SYSTEMS 40
System architecture..... 41
Genomic distribution..... 43
Phosphotransfer chemistry..... 43
Histidine kinases..... 44
Response regulators..... 48
Regulatory mechanisms..... 51

CHAPTER THREE: Materials and Methods 55

BACTERIAL STRAINS 55
E. coli strains, media, and growth conditions..... 55
GAS strains, media, and growth conditions..... 55
DNA MANIPULATIONS 56
Plasmid isolation..... 56
GAS chromosomal DNA isolation..... 57
Polymerase chain reaction..... 57
PAGE oligonucleotide purification..... 58
Enzymatic DNA modifications..... 60
BACTERIAL TRANSFORMATIONS 60
E. coli competent cells..... 60
GAS competent cells..... 61
Electroporation..... 61
GENETIC CONSTRUCTIONS 62
Plasmid constructions..... 62
Strain constructions..... 69
RNA ANALYSIS 71
RNA extraction and DNase I treatment..... 71
RT-PCR..... 72
Microarray..... 72

Real-time RT-PCR..... 75
5' RACE..... 75
PROTEIN ANALYSIS 76
Protein expression and purification..... 76
GAS protein extracts..... 77
SDS-PAGE gel analysis..... 78
Western Blot..... 79
Co-Immunoprecipitation assay..... 79
Bacterial two-hybrid assay..... 80
TrxS-TrxR *in vitro* phosphorelay..... 80
Electrophoretic mobility shift assays (EMSA) 81
TRANSCRIPTIONAL REPORTER ASSAY 82
Luciferase Assay..... 82

CHAPTER FOUR: Characterization of the *trxTSR* operon and its role in the activation of the Mga regulon 84

INTRODUCTION 84
RESULTS 86
Genetic organization of the *trxSR* operon..... 86
Expression from P*trxT* varies across growth..... 88
Definition of the TrxR regulon in GAS..... 92
Complementation with *trxR* on a plasmid restores expression of the Mga regulon..... 95
TrxR activates the Mga regulon in both throat and generalist strains..... 97
Deletion of *trxT* resembles a *trxR*$^-$ phenotype, however complementation does not restore phenotype..... 99
DISCUSSION 100
trxSR is part of a tightly regulated operon..... 101
Defining the TrxR regulon in GAS..... 103
Involvement of TrxT in the TrxSR TCS..... 105

CHAPTER FIVE: TrxR interacts directly with P*mga* 107

INTRODUCTION **107**

RESULTS **109**

TrxS can dimerize *in vivo* 109

TrxS exhibits autophosphorylation activity and phosphorelay to TrxR *in vitro* 111

TrxS and TrxR can interact *in vivo* 114

TrxR activates P*mga* 116

TrxR binds specifically to P*mga in vitro* 117

The effect of phosphorylation on TrxR's ability to bind to DNA and regulate gene activation 119

TrxR requires its HTH domains to bind to P*mga* 121

TrxR's HTH domains are not needed for *in vivo* activation of P*mga* 123

Truncating TrxR does not affect its ability to rescue a *trxR*$^-$ phenotype 124

DISCUSSION **126**

TrxSR is a functional phosphorelay, yet it may not be needed for TrxR's Mga-specific activity 126

TrxR interacts with the promoter of *mga* 129

Role of TrxR's HTH domains 131

CHAPTER SIX: Conclusions and Recommendations **134**

Complex nature of TrxR protein 134

Global influence of TrxSR on regulation in GAS 137

Summary 141

REFERENCES **143**

LIST OF TABLES

Table 1. Bacterial strains..... 56
Table 2. PCR primers..... 59
Table 3. Plasmids..... 63
Table 4. Real-time PCR primers..... 74
Table 5. SDS-PAGE buffers..... 78
Table 6. MGAS5005.*trxR* vs. MGAS5005 Microarray and Real-time RT-PCR validation..... 94

LIST OF FIGURES

FIGURE 1. Group A streptococcal virulence factors..... 16
FIGURE 2. Two-component system schematic..... 42
FIGURE 3. Crystal structures of the catalytic kinase core..... 48
FIGURE 4. *trxR* mutant in a murine model of streptococcal soft tissue infection..... 86
FIGURE 5. *trxTSR* genomic region..... 87
FIGURE 6. The *trxSR* operon..... 89
FIGURE 7. P*trxT* expression across growth..... 91
FIGURE 8. Validation of microarray studies..... 95
FIGURE 9. Complementation with *trxR* restores expression of the Mga regulon..... 96
FIGURE 10. Real-time RT-PCR analysis of *trxR*$^-$ and cured strains..... 98
FIGURE 11. Role of TrxT in the TrxSR TCS assessed through qPCR..... 100
FIGURE 12. TrxS dimerizes *in vivo*..... 110
FIGURE 13. Predicted catalytic residues of TrxS and TrxR..... 111
FIGURE 14. Histidine 383 of TrxS and aspartate 55 of TrxR are essential for TrxSR phosphorelay..... 113
FIGURE 15. Native TrxS is pulled down by His-MBP-TrxR..... 115
FIGURE 16. P*mga* activity is regulated by TrxR..... 116
FIGURE 17. TrxR binds specifically to P*mga*..... 118
FIGURE 18. Effect of TrxR's phosphorylation state on gene transcription and DNA binding..... 120
FIGURE 19. TrxR requires its HTH domains to bind to P*mga*..... 122
FIGURE 20. TrxR does not require its HTH domains to affect gene transcription of the Mga regulon..... 123
FIGURE 21. Effect of TrxR truncations on the activity of the protein *in vivo*..... 125
FIGURE 22. Model for interacting virulence regulation in GAS..... 139

LIST OF ABBREVIATIONS

aa	amino acid
Ala	alanine
Asn	asparagine
ASPGN	acute post-streptococcal glomerulonephritis
ARF	acute rheumatic fever
ADP	adenosine diphosphate
Asp	aspartate
ATP	adenosine triphosphate
bp	base pair
BSA	bovine serum albumin
B. subtilis	*Bacillus subtilis*
cAMP	cyclic adenosine monophosphate
cDNA	complementary DNA
Cpa	collagen-binding protein of group A streptococci
C. perfringens	*Clostridium perfringens*
C. septicum	*Clostridium septicum*
CovRS	control of virulence two-component system
DEPC	diethyl pyrocarbonate
dH_2O	distilled water
dI-dC	deoxyinosinic-deoxycytidylic acid
DNA	deoxyribonucleic acid
DNase	deoxyribonuclease
dNTPs	deoxyribonucleic acid triphosphate monomers
ds	double-stranded
E. coli	*Escherichia coli*
Emm	M protein
EMSA	electrophoretic mobility shift assay
g	gravity
GAS	the group A streptococcus
gDNA	genomic DNA

GRAB	protein G-related α_2-macroglobulin-binding protein
His	histidine
HK	histidine kinase
HTH	helix-turn-helix
Ig	immunoglobulin
Ihk/Irr	*isp*-associated histidine kinase and response regulator
IL	interleukin
i.p.	intraperitoneal
kb	kilobase
kDa	kilo-Dalton
LB	Luria-Bertani medium
Leu	leucine
LTA	lipotechoic acid
M	molar
µ	micro
MHC	major histocompatability complex
Mga	multiple gene regulator of the group A streptococcus
Mrp	M-related protein
MSCRAMM	microbial surface component recognizing adhesive matrix molecules
NEB	New England Biolabs
NET	neutrophil extracellular trap
ng	nanograms
Ni-NTA	nickel-nitriloacetic acid
NMR	nuclear magnetic resonance
Nra	negative regulator of the group A streptococcus
nt	not tested
OF	opacity factor
ORF	open reading frame
PAMP	pathogen associated molecular pattern
PCR	polymerase chain reaction

pel	pleiotropic effect locus
Phe	phenylalanine
PMN	polymorphonuclear leuokocyte
PNK	polynucleotide kinase
PTS	phosphoenolpyruvate phosphotransferase system
q	quantitative
RALPs	RofA-like proteins
REC	receiver domain
RNA	ribonucleic acid
RR	response regulator
RivR	RofA-like protein
RofA	regulator of protein F
RT	reverse transcriptase
S. aureus	*Staphylococcus aureus*
SDS	sodium dodecyl sulfate
S. pneumoniae	*Streptococcus pneumoniae*
S. pyogenes	*Streptococcus pyogenes*
S. typhimurium	*Salmonella typhimurium*
SclA	streptococcal collagen-like protein
ScpA	streptococcal C5a peptidase
Sic	streptococcal inhibitor of complement
Ska	streptokinase
Slo	streptolysin O
SLS	streptolysin S
Sof	serum opacity factor
Spe	streptococcal pyrogenic exotoxin
Srv	streptococcal regulator of virulence
STSS	streptococcal toxic shock syndrome
TBE	tris/borate/EDTA
TCS	two-component system
TE	tris/EDTA

THY	Todd-Hewitt yeast extract medium
TrxSR	two-component regulatory system X
Tyr	tyrosine
UV	ultraviolet
WT	wild type
ZYP	N-Z-amine/yeast extract/phosphate

CHAPTER ONE:

Introduction

The Group A Streptococcus (GAS), or *Streptococcus pyogenes,* is a strict human pathogen of clinical importance worldwide. GAS causes not only benign, self-limiting infections, such as pharyngitis and impetigo, but also severe, invasive infections like necrotizing fasciitis and streptococcal toxic shock syndrome. Nonsuppurative infections such as acute post-streptococcal glomerulonephritis can also occur following GAS infection. GAS has the ability to infect a broad range of tissues, evidenced by the numerous diseases it can cause. Although typical portals of entry for infection include the throat and skin, the more severe diseases may develop following mild trauma or surgery. GAS can also spread from normally sterile sites of colonization to deeper tissues, as well as throughout the bloodstream and lymphatics, to other organs. Recent estimates of invasive GAS infections indicate that there are over 18 million cases worldwide, resulting in at least 500,000 deaths per year (36). There is no current vaccine that exists to prevent GAS infections, making GAS among the more significant global human pathogens.

In order to rapidly adapt to changing *in vivo* environments encountered during infection, GAS must be able to coordinately regulate the transcription of its virulence genes in response to relevant host signals. One method that GAS employs to accomplish this is through the use of two-component signal transduction systems (TCSs). Several TCSs exist in GAS, with many of their roles previously elucidated. This study addresses the role of the uncharacterized TCS, TrxSR, and its relation to virulence regulation in

GAS. This work begins with a general characterization of the TrxSR TCS, including definition of its operon structure and its regulon. An insertional inactivation mutation within *trxR* was made in a virulent M1 strain of GAS, and determination of its regulon was accomplished through microarray studies. The transcriptome analysis identified that expression of the core Mga-regulated virulence genes is activated by TrxR, and this activation appears to be conserved within GAS, as an M4 and M49 strain shared the same effect. Additionally, *trxSR* is shown to be co-transcribed with an upstream hypothetical membrane protein. However, a potential role for this protein in the TrxSR TCS has not yet been established.

The second focus of this research was an in-depth investigation into the TrxS and TrxR proteins, in relation to their functions within the TCS. TrxS was shown to both autophosphorylate and dimerize, two key functions required for an HK to pass a phosphate to the RR in response to receiving a signal. TrxR was also shown to accept this phosphate, demonstrating that TrxSR form a cognate pair, as they participate in a functional phosphorelay. Further studies of the TrxR protein demonstrate that it can bind directly to the promoter region of *mga* in order to regulate its gene transcription. Moreover, this regulation occurs in the absence of a phosphorylated TrxR, suggesting that TrxR may be active in the absence of interaction with TrxS.

Overall, this work demonstrates that TrxSR represents a functional TCS, which directly regulates the Mga virulence regulon independent of phosphorelay. Furthermore, the functional conservation of TrxR regulation of Mga in other serotypes suggests a conserved role for its involvement in virulence regulation in GAS.

CHAPTER TWO:

Literature Review

HISTORICAL PERSPECTIVE

Throughout history, there have been countless epidemics of Group A Streptococcus (GAS, *Streptococcus pyogenes*) related diseases. Evidence of GAS infection has been found in skulls dating back to 8000-6500 B.C. (233). Perhaps the earliest described epidemic occurred in the times of Hippocrates, in roughly 430 B.C., when it is believed that many people fell victim to an outbreak of what we now recognize as scarlet fever (154). Much later, in the 16^{th}-18^{th} centuries, signs of pharyngitis and its complications were reported in Europe. Although numerous investigators recognized the potential cause of some of these diseases as spherical chain-growing organisms, it was until not 1874 that Billroth named these organisms streptococcus, for *strepto*, meaning twisted or chain and *kokhos*, meaning berry or seed (60). After this, streptococci were frequently classified according to the disease that they caused (e.g. *Streptococcus erysipelatis* - erysipelas, *Streptococcus scarlatinae* - scarlet fever). The classification of GAS began to show more order in 1903 when Schotmüller determined that streptococci could be differentiated based upon their ability to hemolyze red blood cells (60). In 1933 Lancefield developed a system for classifying the β-hemolytic streptococci (60). Those hemolytic strains that belonged to the serotype A group in Lancefield's classification included the majority of the pathogenic strains that infected humans; these collectively became known as *Streptococcus pyogenes*.

CLASSIFICATION OF GAS

General characteristics

GAS is a non-motile, Gram-positive coccus that grows in chains of varying length or pairs. GAS divides in one plane and individual cells range in size from 0.6-1.0 μm in diameter. They are facultative anaerobes and non-spore forming. Additionally, they are both catalase and oxidase-negative. GAS are also β-hemolytic on blood agar plates, as they create a zone of clearance around themselves, caused by lysis of the red blood cells on the agar plate.

Growth requirements

GAS has strict requirements for growth; they are members of the lactic acid bacteria that rely on fermentation of glucose for growth and energy production. They grow in nutrient-rich media, first described by Todd and Hewitt in 1932, that includes neopeptone extracts, dextrose or glucose as the carbon source, and a complex mixture of nutrients from beef-heart infusion (254). Additionally, 2% yeast extract is added to the Todd-Hewitt (THY) media to enhance GAS growth (262). GAS cultures are grown at 37°C with 5% CO_2 or under ambient conditions.

Lancefield grouping

In order to initially categorize the various hemolytic streptococci, Lancefield developed a test to serologically differentiate the various human, animal, and dairy product strains from one another. This test, a precipitin reaction, utilized hot acid to

extract the carbohydrate from each strain. After extraction, the carbohydrate was incubated with C-antigens (to the surface carbohydrate) from various streptococci to determine what it interacted with (131). Lancefield classified the various strains into five groups, named A-E. Those strains that had the group A antigen, correlated with strains isolated from human infection. Lancefield's nomenclature formed the basis for classification of all streptococci and gave the β-hemolytic strep from the human host its name, the Group A Streptococcus (GAS).

M, T, and OF typing

In addition to categorizing streptococci by its surface carbohydrate, individual strains of GAS are characterized by their M protein. This typing has led to the subdivision of GAS strains into more than 180 different recognized M-serotypes (181). Lancefield developed a method for determination of M-antigens in GAS strains which included acid extraction of the M protein followed by a capillary precipitin reaction with known streptococcal sera to determine the specific M-type based upon the presence or absence of precipitate formation (131, 247). More recently, Beall and Facklam developed a method for identification of M-type by means of a PCR reaction in which a primer pair specific to the 5' region of the *emm* gene is used to amplify the hyper-variable epitope (17). This is later sequenced and compared to a database of *emm* genes to determine the GAS *emm*-type.

Along with classifying strains based upon their M-type, GAS strains are also classified according to their T antigen, which was originally defined by its resistance to trypsin (23). While the function of the T protein is not well understood, a recent study

suggests that it may be a component of a pilus-like structure (175). It exists in far fewer variants than the M protein. Additionally, a single T antigen may be found in strains belonging to varying M serotypes. Strains of the same M-type can also contain more than one T antigen. A third typing scheme for GAS strains is based upon the presence of the serum opacity factor (*sof)* gene. Opacity factor (OF) typing generally accompanies M-typing, as SOF production highly correlates with specific M types (18).

Class determination

Serotypes of GAS are divided into two classes based upon the reactivity of their M protein with an antibody directed against the C repeat region and by the presence of serum opacity factor (SOF) (22). Class I serotypes share an M protein that has a surface-exposed C repeat region, whereas Class II serotypes have an M protein that lacks this repeat region. Additionally, it is the Class II serotypes that contain the serum opacity factor gene, as Class I serotypes do not.

GROUP A STREPTOCOCCAL DISEASE

GAS is able to cause a wide range of infections and diseases, ranging in severity from minor to life threatening. Those infections that are minor and typically self-limiting include pharyngitis (infection of the throat) and impetigo and erysipelas (infections of the skin). More serious GAS infections, those that constitute severe and invasive diseases, are puerperal fever, streptococcal toxic shock syndrome (STSS), bacteremia, and

necrotizing fasciitis. Approximately 163,000 deaths occur each year from these invasive diseases (36). Lastly, GAS is associated with several nonsuppurative sequelae, including acute rheumatic fever (ARF) and acute post streptococcal glomerulonephritis (APSGN). For each infection or disease, its symptoms, clinical manifestations, affected population, and potential treatments will be discussed.

Throat infections

Pharyngitis

Streptococcal pharyngitis, otherwise known as "strep throat", is the most common bacterial infection caused by GAS. Roughly 616 million new cases of pharyngitis occur each year (36). It is more prevalent in school-aged children between the ages of 5 and 12, although pharyngitis can affect all age groups (225). GAS colonization can also be asymptomatic (55), increasing carriage rates among the population. Crowding is an important factor in the spread of GAS pharyngitis, as transmission of the bacteria primarily occurs by inhalation of aerosolized droplets or direct contact with respiratory secretions. The usual incubation period for streptococcal pharyngitis is 2 to 4 days. By the end of this period, a pronounced sore throat accompanied by fever, headache, and malaise can occur. In more acute cases of pharyngitis, nausea and abdominal pain can arise. To confirm a streptococcal pharyngeal infection, the current "gold standard" practice involves swabbing the throat and culturing the swab on blood agar plates. Following this procedure, it typically takes 24-48 hours to verify the presence of GAS through the presence of β-hemolytic colonies. Rapid antigen diagnostic tests have also been used. They produce quicker, more immediate results, although they generally lack

sensitivity and can yield a false-positive (225). Antibiotics, most notably penicillin and erythromycin, are used to treat a GAS-mediated pharyngeal infection. Even in the absence of antibiotics, a pharyngeal infection is self-limiting; virtually all signs and symptoms of it disappear within a week.

Scarlet Fever

Today, in developed countries, scarlet fever is generally a mild disease. It is typically described as pharyngitis with a rash or benign scarlet fever. While it was once a considerably more serious and, sometimes, even fatal childhood disease, the malignant toxic forms of scarlet fever have become less common and it is now easily treatable (233). As benign scarlet fever is typically associated with pharyngitis, it is additionally characterized by a sandpaper-like rash that begins on the neck and chest and eventually spreads across the extremities. Moreover, a "strawberry tongue" is observed in patients with benign scarlet fever, as the papillae of the tongue become red and swollen. In more severe cases of the septic and toxic forms of scarlet fever, in addition to the aforementioned symptoms, markedly high fevers and delirium are observed. These cases are typically confounded by more invasive symptoms (septic- local and hematogenous spread of GAS; toxic- exudation of numerous membranous tissues) caused by the streptococcal pyrogenic exotoxins (SPEs) and can lead to systemic toxicity and death (235).

Skin infections

Impetigo

Streptococcal impetigo, also known as pyoderma, is a skin infection of the dermis and epidermis. It is caused by both GAS and *Staphylococcus aureus,* and most commonly affects the lower extremities. Impetigo is characterized by a pus-filled, bacteria-rich blister that forms on the skin, which, with time, oozes and develops a thick golden crust. Typically prevalent in children aged 2-5 years old living in unhealthy conditions, impetigo also manifests in adults following previous respiratory tract infections or skin disorders. Because GAS has been shown to colonize and persist on normal skin for a substantial period of time (6), it has the ability to enter and invade the skin quickly, once minor trauma appears, and cause infection. Itching is the primary symptom associated with impetigo. Although it is a contagious disease, impetigo can be easily treated with penicillin. Moreover, importantly, impetigo is linked to one of the streptococcal secondary sequelae, acute glomerulonephritis, which will be discussed more in detail later, within this chapter.

Cellulitis

GAS is the most common cause of cellulitis, although some cases are caused by *S. aureus*. Cellulitis is a diffuse inflammation of the subcutaneous layers of the skin. Typical symptoms include a pinkish skin color, along with swelling and pain. Predisposing conditions for cellulitis generally include some form of skin irritation, such as a burn, animal bite, rash, or dry skin (233). Additionally, individuals who have poor blood circulation or a weakened immune system, like diabetics or the elderly, are more at

risk for developing cellulitis. Penicillin is generally used to treat cellulitis. However, when is *S. aureus* suspected, nafcillin or oxacillin are used (233).

Erysipelas

Erysipelas is an acute infection of the superficial layer of the skin, characterized by red, raised, well-demarcated lesions. The erythematous lesion is typically accompanied by intense pain and fever. Although the great majority of cases are caused by GAS, erysipelas can also be caused by streptococci of groups G, C, and B and rarely by staphylococci (27). Erysipelas, although relatively uncommon today, affects mainly the elderly. The most common site for infection today is on the lower extremities, including the legs and feet. Historically, however, it was the face (27). The portal of entry for the bacteria is generally the skin, where local trauma or an abrasion occurs. More rarely, when erysipelas occurs on the face, the oropharynx serves as the origin for the bacteria. The erysipelas infection is typically treated with penicillin and resolves completely within a few weeks.

Invasive diseases

Puerperal Fever

Puerperal fever (childbed fever) was one of the most deadly diseases of the 19th century. However, now the disease is seen only sporadically and in isolated instances. Puerperal fever can be contracted during pregnancy, miscarriage, or abortion and is marked by infection of the genital tract and endometrial lining. This acute endometritis is commonly masked by abdominal pain and is thus usually not recognized immediately

following child delivery. Following entry into the women's endometrial lining, GAS can quickly spread to the surrounding structures and into the bloodstream (233). Once sepsis occurs, fever, leukocytosis, and increasingly severe pain typically alert doctors that a more severe infection is present. If left untreated, this infection could result in death. Since the advent of aseptic techniques (pioneered by Semmelweis) and the use of antibiotics, the number of cases of puerperal fever has drastically declined (60). Today it is rarely fatal.

Streptococcal Toxic Shock Syndrome

Streptococcal toxic shock syndrome (STSS) consists of a streptococcal infection followed by rapid onset of shock and organ failure. The latter portion of the infection, in which severe symptoms of shock and failure occur, is generally associated with production of GAS pyrogenic exotoxins (SPEs). These superantigens can over stimulate the immune system to produce numerous inflammatory cytokines, leading to shock and overall tissue damage (122, 235). Unlike the staphylococcal form of toxic shock syndrome that has historically been linked to tampon use, streptococcal TSS is more common following a streptococcal infection of the skin, as it serves as the portal of entry in roughly 25% of streptococcal TSS cases (235). Characterized by rapid onset of fever, high blood pressure, chills, nausea, confusion, and pain, STSS is also commonly present with a deep-seated systemic infection such as bacteremia or necrotizing fasciitis. Because progression of streptococcal TSS is so fast, within 24-48 hours of onset, multiple organ failure and death can occur. In order to treat STSS, numerous measures are taken not only to address the individual symptoms associated with the infection (e.g.

hypotension, renal dysfunction), but also to treat the more aggressive infections (e.g. surgical debridement for necrotizing fasciitis).

Bacteremia

Although GAS infections typically localize in the skin or throat, in more severe cases, when the bacteria enter the bloodstream, bacteremia occurs. Historically, streptococcal bacteremia occurred most commonly in children and the elderly. Today, however, sepsis cases have been increasing in individuals 14-40 years of age. Bacteremia in children typically results from streptococcal pharyngeal infections, whereas cases of the elderly emanate from infections of the skin (234). Bacteremia has also been found in intravenous drug users. This may account for the increase in sepsis cases in the 14-40 year old age group. Typical clinical characteristics of GAS bacteremia include fever, chills, and shock. Mortality rates have been reported as relatively low within the last forty years (234), as antibiotic therapy has been used to widely treat bacteremia.

Necrotizing Fasciitis

Necrotizing fasciitis, also known as the 'flesh-eating disease', is an infection of the subcutaneous tissue that results in the highly progressive destruction of fascia and fat. Within a matter of days, the infection can progress from an apparent benign skin lesion to a highly lethal disease. Although GAS is widely known as the most common causative agent of necrotizing fasciitis, other Gram-positive bacteria such as *S. aureus* and *Clostridium perfringens* and *C. septicum* can elicit similar disease pathology (234).

Characteristically, beginning at the site of a trivial or minor wound, the infection becomes painful. As it swells, it also becomes red and produces heat. Within 24 hours, the infection spreads and migrates outward from the site of the initial infection. During the next 24-48 hours, the redness transitions to purple and eventually to blue, as it forms fluid-filled blisters and bullae. At this point, severe tissue destruction and gangrene, have occurred, accompanied by the extensive necrosis of the subcutaneous tissue, occur, and the patient becomes very weak, as fever and delirium set in. Additional systemic sepsis and toxic shock can also occur. In order to treat necrotizing fasciitis, early detection and treatment are vital. Typically, antibiotic therapy, surgical debridement, and even amputation are used to slow the disease progression and rid the body of the damaged tissue. Although previous mortality rates have been reported as low as 20%, today's mortality rates have risen to >50% (235), most likely due to the emergence of more highly virulent GAS.

Secondary Sequelae

Acute Rheumatic Fever

Acute rheumatic fever (ARF) is a nonsuppurative systemic inflammatory disease that can affect the heart, joints, skin, and central nervous system following an upper respiratory infection with GAS. Roughly, 233,000 deaths occur each year as a result of rheumatic fever (36). Furthermore, it is the leading cause of childhood heart disease globally and thus, most commonly, appears in children between the ages of 5 and 15 (150). Rheumatic fever is believed to be caused by an autoimmune attack, in which host immune cells create antibodies against GAS that also appear to cross-react with self-

epitopes against the myocardium and joints. Due to the numerous clinical manifestations of ARF, diagnosing the disease is accomplished following the criteria set forth by Jones, who outlined specific major and minor clinical signs to identify the disease (159). ARF can also lead to more severe manifestations including congestive heart failure and Sydenham's chorea. Treatment of ARF includes antimicrobial therapy to rid the body of GAS and anti-inflammatory agents and analgesics to control joint pain. For long-term management of ARF, patients are given continuous prophylactic antibiotic treatment to prevent recurrent attacks, as they represent the major cause of deaths and disabilities from rheumatic heart disease.

Acute Post Streptococcal Glomerulonephritis

Acute post streptococcal glomerulonephritis (ASPGN) is an acute inflammatory disease, involving the renal glomeruli that filter waste products from the blood. ASPGN can result after both pharyngeal and GAS skin infections. The latent period between a streptococcal pharyngeal infection and nephritis is roughly 1 to 3 weeks. After a skin infection, it is more prolonged, 3-6 weeks (102). ASPGN occurs primarily in children, young adults, and individuals over 40 years of age, with males affected twice as often as females (55). ASPGN is thought to develop after immune complexes consisting of streptococcal antigens (such as the M protein) complexed with host antibody deposit in the kidney glomeruli, causing the tubules to become inflamed, and impairing the kidney's ability to filter and eliminate waste. Symptoms of ASPGN often include high blood pressure, kidney edema, and presence of blood in the urine. Diagnosis of ASPGN requires urinalysis testing and treatment is generally aimed towards lowering the blood

pressure and reducing edema. Mortality due to ASPGN is very low; less than 0.5% of patients die from the initial disease, and fewer than 2% die or progress to end-stage renal disease (102).

Vaccines

As the number of incidents of invasive GAS disease rise, the need for a vaccine to protect against these diseases intensifies. With the target group for vaccination children 5-15 years old, the ideal vaccine would contain an epitope that is conserved in all GAS strains, is highly immunogenic, induces both IgG and IgA, and most importantly, does not exhibit cross-reactivity with human tissue (232). GAS vaccine development has historically focused on the N-terminal region of the M protein, as Lancefield originally showed that antibodies against this region are not only protective, but bactericidal as well (132). Several potential candidates have since used this region to develop multivalent N-terminal type-specific vaccines. However, even with the latest vaccine (26-valent) incorporating 26 of the most common M-types (107), because of the vast number and flux of M-types in developing countries, this vaccine would have limited effectiveness in the worldwide fight against invasive GAS disease. Additionally, because some antibodies to the M protein are cross-reactive with human myosin (56), a characteristic that is central to the pathogenesis of ARF, the use of the M protein in a vaccine remains problematic. As an alternative, numerous groups have tried to use well-characterized virulence factors for vaccine candidates, including ScpA (48, 110), the GAS carbohydrate (214), the fibronectin-binding protein Sfb1 (87, 164), and various exotoxins (259). In spite of this, none of these candidates has reached human clinical trials. Nevertheless,

there is renewed hope that future developments will lead to a potential vaccine, and in time, will reduce the number of severe GAS infections worldwide.

VIRULENCE FACTORS

In order to cause such a wide range of diseases, GAS utilize numerous virulence factors that enable them to colonize the host, invade the surrounding tissue, evade the host immune system, and disseminate throughout the body, causing further infection. Many of these virulence factors are surface-associated, as they are attached to the streptococcal cell, and others are released and secreted into the extracellular environment (Fig 1). Several of these virulence factors and their role in virulence are presented below.

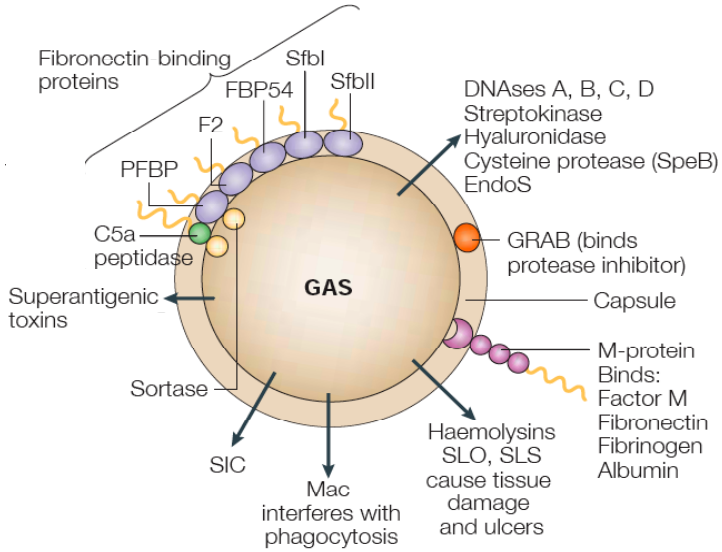

FIGURE 1. **Group A streptococcal virulence factors.** Schematic illustrates many cell-surface associated virulence factors, including the M and M-like proteins, fibronectin-binding proteins (SfbI/II, FBP54, F2, PFBP), capsule, C5a peptidase (SclA), and GRAB. Also shows some of the secreted factors of GAS: streptolysin O (SLO), streptolysin S (SLS), secreted inhibitor of complement (Sic), DNases, Mac/IdeS, and superantigenic toxins. [Figure adapted from (172).]

Cell associated

M and M-like proteins

The major surface protein of GAS involved in both adherence and immune evasion is the M protein, encoded by *emm*. The M protein is an alpha-helical coiled-coil dimer that consists of four different repeat regions (A, B, C, D); one of these repeats, the A region, is hypervariable and confers serotype specificity to the strain (196). Currently, there are over 200 different recognized M-serotypes (171). It has been observed that the size of the M protein can vary, depending on the number of the repeat units in the A and B portions of the protein (100). While the M protein has historically been used for serotyping and classification of GAS, it also plays an important and very significant role in the streptococcal cell.

One of the major functions of the M protein is to protect the GAS cell from phagocytosis by the host. It does this by binding to the complement regulatory protein H to inhibit and interfere with opsonization of the cell (104). Additionally, the M protein can prevent the deposition of the complement factor C3b on the surface of the GAS cell, inhibiting the alternative complement pathway (104). A second key function of the M protein lies in its ability to adhere to different molecules. Many of the A repeats from different M proteins have been shown to bind to plasminogen, IgA, IgG (2), human C4b-binding protein (5), and factor H (165, 181). The B repeats, which are semi-hypervariable, bind to fibrinogen (105) and human serum albumin (2). Lastly, it is believed that the M protein can be released by the cell, in a soluble form (190), to act as a superantigen that contributes to T-cell activation and inflammatory responses during invasive streptococcal infections.

In addition to the M protein, there exist within this gene superfamily many other structurally similar proteins. More than 20 genes have been identified within the *emm* superfamily (e.g. *mrp, arp, emmL, fcrA, sir, enn, and sph)* and have been appropriately named M-like or M-related proteins, due to their highly conserved domain structure within the cell-wall associated region of the proteins (101). These proteins, because of their similar domains, have variable immunoglobulin binding capabilities (29) like that of the M protein.

Lipotechoic acid

Lipotechoic acid (LTA) is the fundamental component of the GAS cell wall, made up of techoic acid molecules attached to the wall via lipid anchors. LTA has been shown to adhere to oral epithelial cells through fibronectin binding (227) and it is believed to be an initial mediator of adhesion, before specific high-affinity receptor adhesins, as it is capable of recognizing a relatively wide range of molecules (95). LTA is also a pathogen-associated molecular pattern (PAMP) recognized by toll-like receptors of the innate immune response (3).

MSCRAMMs

GAS encodes numerous surface-associated adhesin molecules that allow for attachment and adherence to structures on the eukaryotic cell surface or with components of the intercellular matrix. These proteins, known as MSCRAMMs, for *m*icrobial *s*urface *c*omponent *r*ecognizing *a*dhesive *m*atrix *m*olecules, include the fibronectin-binding proteins, protein F (*prtF*) (93), SfbII (128), protein F2 (*prtF2)* (108), Sfbx (109), Pfbp

(212), FbaA (250), FbaB (251), and Fbp54 (52). Other proteins such as the aforementioned M-protein and serum opacity factor (SOF) (53) can bind fibronectin as well. The multitude and extensive array of fibronectin-binding proteins illustrates how important this function is to GAS during human host infection.

In addition, multiple collagen-binding MSCRAMMs have been identified in GAS. One of these proteins, Cpa, is expressed in at least 28 serotypes of GAS and has been found to bind to type 1 collagen (127). Cpa is thought to have a role in attachment and internalization of GAS in tissues containing type 1 collagen, as a *cpa* mutant showed decrease internalization into epithelial cells (127). A second 57 kDa collagen-binding protein has been identified in GAS, which uses collagen on the host eukaryotic cell as its receptor (264). However, no evidence for the role of this protein in GAS virulence has been discovered.

Streptococcal collagen-like surface protein

The group A streptococci produce the streptococcal collagen-like protein, SclA, and as its name implies, SclA is similar to collagen in structure. SclA has been found to be important in adhesion, as it can bind to both fibroblasts (200), lung epithelial cells (147), and respiratory epithelial cells (47). Additionally, *sclA* is up-regulated by Mga (202), the transcriptional regulator of the core virulence genes, suggesting an important role for the protein in bacterial virulence. Furthermore, studies involving mutants in *sclA* have shown attenuation in virulence following a subcutaneous injection and a decrease in epithelial cell adherence, highlighting the importance of this adhesin to GAS pathogenesis. Recently, it has been shown that SclA can bind the human complement

regulatory protein, factor H, to inhibit the alternative complement pathway (39). In addition, SclA is capable of binding a fibrinolysis inhibitor, TAFI, and through its recruitment of plasmin to the surface of the GAS cell (189), can modulate the inflammatory reactions of the host.

C5a peptidase

C5a peptidase, encoded by the *scpA* gene, is a surface-associated and anchored endopeptidase that specifically cleaves and inactivates the C5a chemotaxin of the complement system (49). The peptidase acts on the cell's binding site for PMNs, inhibiting the recruitment of phagocytic cells to the site of infection, and potentially enabling GAS's evasion of the immune system (111). Numerous studies have shown the importance of the C5a peptidase to the virulence of GAS. Not only is the *scpA* gene part of the Mga core-virulence regulon, it has also been demonstrated to be important in the intranasal and subcutaneous models of GAS infection (110, 111).

Capsule

The hyaluronic acid capsule of GAS is encoded by the *has* operon, which is negatively regulated by the CovRS two-component system (21, 97, 139), and is activated under conditions associated with infection (86). The capsule is chemically identical to that found in human connective tissue. Because of this, GAS capsule can bind to CD44, the receptor for human hyaluronic acid, and evade the host response through molecular mimicry, to mediate attachment to the epithelial cells (216). Additionally, capsule has been found to be an important virulence factor of GAS, as acapsular strains fall victim to

phagocytosis and have complete avirulence in the pharyngeal model of infection (270). Likewise, in a skin infection model, acapsular mutants could not produce the local necrosis and systemic infection of the wild type strain (217), suggesting a role for the hyaluronic acid capsule in soft tissue invasion.

Serum opacity factor

The serum opacity factor (SOF), only produced by Class II serotypes, is an important adhesin of GAS as it helps to bind streptococcal cells to high-density lipoproteins through a fibronectin-mediated process (54, 185). SOF is not only bound to the cell surface, but can also be found as a released protein by the cell (89, 272). Bound SOF appears to have two distinct activities, having roles in both serum opacification and fibronectin/fibrinogen binding, as mentioned previously (53, 114, 125, 198). Although its direct role in virulence has been difficult to discern because of its bifunctional nature, studies have shown that inactivation of *sof* resulted in a reduction of virulence in an IP mouse model of infection (53).

Streptolysin S

Streptolysin S (SLS) is an oxygen stable, non-immunogenic toxin that is released from the cell only in the presence of a carrier molecule (1, 26). For this reason, SLS is primarily surface-bound, associated with the LTA. This protein has the ability to lyse and damage the membranes of many cell types, including erythrocytes, lymphocytes, neutrophils, platelets, and even some subcellular organelles (80). Lysis of these cells is mediated by insertion of a lysin complex into the membrane, leading to formation of

transmembrane pores and damage of the cell's integrity(38). SLS mutants have been shown *in vivo* to have impaired lesion formation and decreased pathogenesis within a subcutaneous skin infection model (59). Additionally, SLS has been shown to impair phagocytic clearance, promote epithelial cell cytotoxicity (59)and mediate the cytocidal effect of GAS on neutrophils (173), demonstrating SLS as a potent virulence factor used by GAS for host immune evasion.

Protein G-related α_2-macroglobulin-binding protein (GRAB)

The Protein G-related α_2-macroglobulin-binding protein (GRAB) is a cell-surface associated protein that enables GAS to protect its own surface-associated virulence factors by regulating proteolytic activity at the streptococcal surface (201). As an inhibitor of both GAS and human proteases, GRAB has been shown to be an important virulence factor, as studies involving *grab* mutants showed an attenuation in virulence in both a localized subcutaneous skin infection model and a systemic infection model within mice (201, 255).

S. pyogenes cell envelope protease (SpyCEP)

The *S. pyogenes c*ell *e*nvelope serine *p*rotease (*SpyCEP*, *scpC*) was recently described as a widely-expressed (257) CovR-regulated protease capable of cleaving the neutrophil-recruiting chemokines, IL-1, IL-2, IL-6, and IL-8 (66, 257). Additionally, it has been shown to cleave the granulocyte chemotactic protein 2 (GCP-2) and growth-related oncogene alpha (GROα), two potent chemokines rich in the human tonsils (66). *In vivo*, a knockout mutant lacking *SpyCEP* was shown to be attenuated for virulence in a

subcutaneous mouse skin lesion model (275). Furthermore, in a mouse upper respiratory tract infection model, SpyCEP was shown to enhance bacterial dissemination from the nasopharynx to the lungs (257). Thus, SpyCEP has shown to be necessary for bacterial dissemination, as it is involved in interfering with the innate immune response by decreasing inflammatory neutrophils, which results in enhancement of GAS disease severity.

Secreted factors

Streptolysin O

Streptolysin O (SLO) is an oxygen-labile, thiol activated hemolysin that interacts with membrane cholesterol and aggregates to form pores in the membranes of host cells (219). Like SLS, SLO can target numerous cell types, including erythrocytes, macrophages, leukocytes, and platelets. SLO has been shown to be important for invasive disease in a mouse skin infection model (141). However, the exact role of SLO is still unknown, as it does not appear to be involved in the formation of necrotic lesions or bacterial dissemination for GAS (141). Recently, it was discovered that SLO is involved in cytolysin-mediated translocation (CMT), a pore-forming process that mediates translocation of an effector molecule (*S. pyogenes* NAD-dehydrogenase/Spn) into the cytoplasm of the eukaryotic host cell (170). It was found that SLO not only acts as a hemolysin to form the pore necessary for translocation, but that it plays a more active, presently unknown role in the process, beyond just forming the pore (153). Additionally, new evidence suggests that SLO interferes with the internalization of GAS,

through local perturbation of the keratinocyte cell membrane, and disruption of a clathrin-dependent uptake pathway (142).

Streptococcal pyrogenic exotoxin B

SpeB is a cysteine protease, one of the many proteolytic enzymes of GAS. Although its role in GAS is somewhat ambiguous, some studies have shown that a *speB* mutant decreased mouse lethality (148), resistance to phagocytosis (146), and even eliminated fibrinogen cleavage (163). Other studies, however, have shown no significant effect on virulence (9, 10). Additionally, SpeB has been shown to cleave and degrade streptococcal IgG-binding proteins. For this reason it is thought to promote prevention of complement activation at the bacterial surface, thereby preventing antibody-mediated phagocytosis, leading to the survival of GAS (50, 67). Furthermore, SpeB was shown to be involved in the spread of GAS, as it can cleave surface-attached fibrinogen-binding proteins (Protein F, Fba), releasing GAS from attachment to host cells, and thus facilitating bacterial spread (199, 269).

Streptococcal inhibitor of complement

The secreted inhibitor of complement-mediated lysis, encoded by *sic*, incorporates into the membrane attack complex of complement to inhibit complement-mediated lysis (71). It has also been shown to inactivate two antibacterial peptides of the innate immune response, LL37 and human neutrophil alpha-defensin (74). Additionally, Sic aids in bacterial survival at mucosal surfaces (99) and has been shown to bind and alter the activities of lysozyme and the secretory leukocyte proteinase inhibitor (70). Due

to the various roles of Sic, it can be said to be a multifunctional virulence factor, able to interact with various host cell proteins and members of the immune system.

Streptokinase

Streptokinase (Ska) has been considered a virulence factor of streptococci, as far back as the 1930's, because of its ability to lyse fibrin clots (253) and subsequently, to spread the GAS infection. The protein acts as an activator, as it forms a complex with plasminogen to convert the plasminogen to its active proteolytic form plasmin (143). GAS streptokinase is specific for human plasminogen (244), as it exhibits little or no activity against other mammalian species. Studies using a transgenic mouse expressing human plasminogen increased mortality in mice. This response was dependent on the expression of streptokinase (244). Streptokinase has also been implicated in the development of acute post-streptococcal glomerulonephritis, as it has been shown to be deposited in renal glomeruli, resulting in local activation of the complement cascade, and ultimately nephritis (182).

S. pyogenes NAD-glycohydrolase

Along with SLO, *S. pyogenes* NAD-glycohydrolase (NADase/Spn) is involved in CMT, where SLO forms the pores necessary to deliver NADase to the cytoplasm of the host epithelial cell. The GAS NADase has been found not only to cleave NAD to produce nicotinamide and ADP-ribose, but also to produce cyclic ADP-ribose (112). *In vivo* mouse models of invasive soft-tissue infection and septicemia showed that mutants lacking NADase activity were significantly attenuated for virulence (30), suggesting an

important role of NADase to streptococcal infection. Additionally, it has been discovered that NADase is involved in numerous host cell changes that enhance GAS pathogenicity, including actin rearrangement to inhibit bacterial internalization, augmentation of SLO-mediated cytotoxicity, and induction of keratinocyte apoptosis (31).

Immunoglobulin G-degrading enzyme

IdeS (*i*mmunoglobulin G-*d*egrading *e*nzyme of *S*. pyogenes/MAC) was identified based upon its similarity to the human leukocyte adhesion receptor, Mac-1 (265). As an extracellular proteinase, IdeS has been shown to cleave the opsonizing IgG antibody at the hinge region to produce two Fab fragments and the Fc portion (265). This cleavage results in inhibition of opsonophagocytosis and production of reactive oxygen species, allowing GAS to avoid killing by PMNs (137), thus, enhancing its survival within the host.

Superantigens (pyrogenic exotoxins)

Streptococcal pyrogenic exotoxins were originally named based upon their presumed role in the development of scarlet fever. There exist numerous exotoxins within GAS, including (although not limited to): SpeA, SpeC, SpeF (79), SpeJ (166), SMEZ (176), SpeL and SpeM (230). Not all exotoxins are present in all strains, due to the fact that some are phage-encoded. Additionally, based upon sequenced genomes, some exotoxins are shown to have more than one allele, suggesting varied functions. Although no clear role of these toxins/superantigens in the disease process has been established, as superantigens, these proteins are believed to bind nonspecifically to the T-

cell receptor and class II MHC. This results in the release of numerous interleukins and cytokines, leading to shock in STSS (122).

DNases

Although GAS encode four antigenically distinct DNases (A, B, C, and D) capable of degrading DNA, it is unknown whether any of them is an important virulence factor. However, recent studies in two murine models of infection and in cynomolgus macaques have shown that a GAS strain lacking DNase production exhibits a decrease in virulence (241). Additionally, it is believed that the DNases degrade neutrophil extracellular traps, or NETS, and aid in evasion of the innate immune response (33, 241). Moreover, the Sda1 DNase has been shown to be involved in the switch to invasive GAS infection (268).

VIRULENCE REGULATION

In order to cause such a wide range of diseases, GAS has evolved numerous mechanisms to regulate its virulence genes. Unlike other prokaryotes, GAS has not been shown to utilize alternative sigma factors to control virulence gene expression. Alternatively, the majority of regulation for GAS is controlled by transcriptional regulators and signal transduction networks. These virulence regulators include classical two-component regulatory systems and stand-alone regulators.

Two component systems (TCS)

Two component systems (TCS) are one of the best-characterized signal transduction systems within bacteria. A classical TCS consists of two proteins. The first of the two proteins, the histidine kinase (HK), typically exists in the membrane of the cell and it generally receives signals front the external environmental, causing autophosphorylation. The second protein, the response regulator (RR), resides inside the cell and upon transfer of a phosphate from the histidine kinase, produces an internal effect, typically through transcriptional regulation. GAS contains 13 TCSs, and those that have been connected to virulence are described below. A more extensive, in-depth review of the bacterial TCS follows this section.

CovRS

The most studied, and best-described TCS of GAS is the CovRS system (TCS 2), named for its *c*ontrol *o*f *v*irulence in GAS. Originally named CsrRS for its role in *c*apsule *s*ynthesis *r*egulation, the TCS was later renamed to emphasize its more widespread role in virulence regulation (69). Believed to respond to environmental stresses such as changes in pH, temperature, and osmolarity (58), CovRS has been shown to directly or indirectly influence expression of approximately 15% of the GAS genome (81), with the majority of the genes being repressed. This has led to CovR being considered the major negative global regulator of virulence genes within GAS. Numerous studies have elucidated the significance of CovR to expression of virulence factors within a host. In the mouse soft tissue model of infection, CovRS was shown to be repressed, leading to an increase in virulence factor production (83). In a longitudinal macaque pharyngitis model,

expression of CovRS varied, but correlated with the course of colonization and infection (263). Additionally, exposing GAS to human blood resulted in global changes to allow for bacterial survival and adaptation to the protein-rich conditions (82).

Increasing evidence also suggests that spontaneous mutations in CovRS allow GAS to become more invasive (14, 58, 243, 268). These GAS strains containing mutations also appear to become more dominant within the population. Recent data have shown that a pharyngeal isolate and blood isolate from the same individual, isolated 13 days apart, were genetically similar, but differed by the presence of an 11 bp insert within *covS* leading to a truncated mutant version of CovS (78). Additionally, to determine the *in vivo* impact of a *covS* mutation, a murine subcutaneous chamber model was employed, comparing a wild type M1 strain to a previously isolated animal-passaged *covS* mutant. Bacteria were collected 24 hours post inoculation, allowing ample time for the bacteria to sense their environments, yet not long enough to allow for restructuring of the bacterial community and selection of mutants. Differences in gene expression dynamics were observed between a wild type and animal-passaged *covS* mutant, indicative of transcriptional changes within gene sets associated with GAS invasion, immune evasion, tissue-dissemination, and metabolic reprogramming (13). Thus, the overwhelming amount of *in vivo* data suggests that CovRS has an important and extremely significant role in modulating gene expression during GAS infection.

FasBCAX

The FasBCAX system (TCS 1), which exhibits homology to the quorum-sensing TCS of *S. aureus* (Agr) and *S. pneumoniae* (Com) (124), is unlike other conventional

TCSs. The operon consists of two genes encoding histidine kinases (*fasB* and *fasC*), one gene encoding a response regulator (*fasA*), and a fourth gene encoding the effector of the operon, a small monocistronic RNA transcript (*fasX*). Named for its ability to regulate *f*ibronectin /fibrinogen binding, hemolytic *a*ctivity, and *s*treptokinase transcription (124), the TCS regulates genes in a growth-phase dependent manner. FasBCAX down-regulates genes encoding GAS adhesins (*fbp54*, *mrp*) and activates genes encoding secreted aggressins (*sagA*, *ska*) and cytotoxins at the end of exponential growth (124). It is thought that the TCS may be involved in local tissue destruction because of its strong cytotoxic and apoptotic phenotype (121).

Ihk/Irr

The Ihk/Irr TCS (TCS 13) is named for its proximity to *isp*, a gene encoding an immunogenic secreted protein: *i*sp-adjacent *h*istidine *k*inase and *i*sp-adjacent *r*esponse *r*egulator, respectively. It has been shown to be important in GAS as it is involved in the evasion of polymorphonuclear leukocyte (PMN)-mediated killing during exposure to the innate immune response. More specifically, using phagocytosis assays, Ihk/Irr was shown to enhance GAS survival by controlling expression of genes critical for GAS survival after phagocytosis (267). Additionally, *irr* was shown to be highly expressed in 16 patients during GAS-induced acute pharyngitis (267), suggesting that Ihk/Irr is critical for GAS survival and pathogenesis in humans. Moreover, a separate study using a *irr* mutant showed attenuation of virulence in both soft tissue infection and bacteremia mouse models (266). The study also suggested that *ihk/irr* are induced by neutrophil-derived ROS (266), resulting in expression of genes that enable GAS to survive host cell

lysis, and to disseminate to cause further disease. Thus, GAS is able to detect and evade the human innate immune system through the aid of the Ihk/Irr TCS.

SptRS

The SptRS TCS (TCS 4) links metabolism and virulence factor production to bacterial persistence in saliva. Named for its involvement in *s*aliva *p*ersistence, the SptRS TCS has been shown to regulate multiple genes encoding proteins involved in acquisition and processing of complex carbohydrates (222), including *amyA, malE, araD,* and *asaD.* Additionally, a study of GAS gene expression over a period of 86 days in the monkey oropharynx confirmed a role for SptRS in GAS pathogenesis of the upper respiratory tract (263). Furthermore, an *in vivo* study using a subcutaneous mouse infection model determined that a mutation in M5005_Spy_0680 (SptR) caused a significantly larger skin lesion than its wild type parental strain (229) and either directly or indirectly affected several genes involved in GAS pathogenesis (e.g. *scpA, sic, prtS*) (229). Thus, it appears that the SptRS TCS allows GAS to alter its metabolic pathways upon entering the oropharynx and to aid in the production of virulence factors necessary for its survival.

TrxSR

TCS 10, previously known as Spt10SR, and renamed TrxSR for *t*wo-component *r*egulatory system *X*, is the latest GAS TCS studied to be directly linked to GAS virulence. TrxSR is the homolog to a pneumococcal TCS that has been shown to be essential for full virulence in several models of pneumococcal infection (96, 252). It is

also a homolog of a *Enterococcus faecalis* TCS involved in resistance to bacitracin (91). Based upon its homology to known virulent TCSs, a preliminary study was undertaken to determine if TrxR played a role in streptococcal infection. Using an *in vivo* murine model of GAS soft tissue infection, a *trxR* mutant was found to be attenuated for virulence (135). Additionally, *trxSR* was shown to be directly repressed by CovR (135). Thus, the data suggest that TrxSR is involved in GAS virulence, although its mechanism of action has yet to be determined.

Other GAS TCS

Of the 13 conserved TCSs of GAS, only five have been studied in detail, with little information known about the remaining systems in relation to a role or involvement in virulence. Recently, a study assessed the role of three previously uncharacterized TCSs by expression microarray analysis (229). Although they did not appear to have direct roles in virulence, putative roles can be inferred for the TCSs based upon the genes that they regulate. TCS 5 (M5005_Spy_0784/0785) is believed to directly activate a nearby mannose/fructose-PTS system, while TCS 7 (M5005_Spy_0832/0833) is thought to be involved in malate metabolism due to its activation of a malate-sodium symporter homolog (229). A role for the third TCS in the study, TCS 9 (M5005_Spy_1280/1281), could not be determined based upon its regulon, although it appears to function as a switch for the cell late in growth, as it has a regulon roughly 30 times bigger in stationary phase as it does in early logarithmic phase (229).

Stand-alone regulators

In addition to the aforementioned TCSs involved in virulence regulation, GAS encode for almost 30 stand-alone transcriptional regulators. These proteins have no known or identified sensor component and typically exist as regulators within existing signal transductions networks, or on their own as 'one-component' systems. In this type of system, the regulators interact with or respond directly to signals, to alter their activity within the cell. Those stand-alone regulators that have been characterized and shown to be involved in virulence regulation are detailed below.

Mga

Mga, or the *m*ultiple *g*ene regulator of G*A*S, was the first virulence regulator found in *S. pyogenes*. Originally called *mry* to reflect its regulation of the M-protein (194), another study identified the same region upstream of *emm* to regulate ScpA and termed the gene *virR* (46). Later, *mry* and *virR* were found to be the same gene and it was renamed *mga* to indicate that it was a multi-virulence factor regulator (218). To date, *mga* has been found in all sequenced GAS strains (24) as two divergent alleles (88). Additionally, several homologs of Mga exist in other pathogenic streptococci and Gram-positive pathogens. They have been shown to be essential for infection, suggesting that Mga belongs to a common family of virulence regulators.

Mga is activated by both growth phase and environmental conditions, as it responds to varying environmental signals such as elevated CO_2, increased iron levels, temperature, and sugar availability (35, 167). Several studies have shown that Mga regulates many genes important for the early stages of infection, a time at which GAS

would encounter such conditions within the human body, as listed above. These Mga-regulated virulence genes include *sof, sic, sclA, fba,* and the aforementioned *emm* and *scpA* (46, 169). They have been shown to be very highly activated by Mga and have collectively become known as the 'core' Mga regulon. Additionally, Mga was found to influence the expression of several metabolic operons and genes important in the transport and utilization of sugar, albeit at low-levels (207).

Numerous studies have shown the *in vivo* relevance of Mga in a variety of animal models of GAS disease. Initial studies using a mouse model of infection demonstrated that the loss of *mga* caused attenuation of virulence (118). More recently, experiments using a large-scale signature-tagged mutagenesis screen in zebrafish established that Mga is important *in vivo* for disease pathogenesis and that a *mga* mutant exhibited attenuated virulence (120). To gain an understanding of Mga during the course of an infection, several studies have looked at the growth of GAS in both *ex vivo* and *in vivo* environments. During growth in whole human blood, maximal levels of *mga* transcript were found 30 minutes post blood exposure (82), correlating with data that suggest maximal expression of the Mga regulon occurs *in vitro* during exponential growth (169, 260). Additionally, a cynomolgus macaque pharyngeal model was used to demonstrate that the Mga regulon is maximally expressed during the acute phase of pharyngitis infection (263). Taken together, these data prove that Mga is indispensable for GAS, as it is needed for successful infection and colonization within the host.

Rgg/RopB

Rgg, also known as RopB for *r*egulation *o*f *p*roteinase, is homologous to other Gram-positive transcriptional regulators that have been shown to regulate expression of extracellular products during the stationary phase of growth (151). In the M49 strain, Rgg is involved in production of SpeB (43). Additionally, it has been shown to regulate the expression of other virulence factors and even transcriptional regulators, like Mga. This suggests that some of Rgg's affect may be indirect (45). Furthermore, Rgg activates several amino acid catabolism operons (44) and contributes to utilization of alternative sugars associated with secondary metabolism and thermal stress responses (42), making it a global regulatory factor of not only virulence, but of genes involved in secondary metabolism and stress as well. Recently, a new role for Rgg has emerged, as it has been proposed that Rgg may be involved in quorum-sensing, by regulating competence of GAS through binding of small pheromone peptides(162).

RofA

RofA was first identified in an M6 strain as a positive transcriptional activator of its own transcription, and of *prtF*, a gene encoding for a fibronectin-binding protein (72). It has since been shown to also repress important virulence genes, including *mga*, *sagA*, and *speB* (19), also in an M6 strain. Additionally, the same study showed that a *rofA* mutant exhibited reduced eukaryotic cell internalization rates in combination with decreased host cell viability (19). However, it was later shown that there appeared to be strain-specific variation in RofA-regulation, whereas a *rofA* mutant in an M2 strain

showed significantly increased affinity for adherence to the host cells with no change in bacterial internalization rates (123).

Since the discovery of RofA in GAS, three other homologs of RofA have been described, and designated as members of the RALP (*R*of-*A* *l*ike *p*rotein) family. These regulators act at the transition from exponential growth to stationary phase and most often serve as negative regulators of virulence. The three other members of the RALP family are described below.

Nra

Nra, the second member of the RALP family, is predominately found in opacity factor (OF)-negative serotypes (123) and is encoded within the FCT genomic region (197). Nra shares homology with RofA. However, it is a *n*egative *r*egulator of genes in the M49 serotype, unlike the activator RofA, and regulates its own expression and such adhesin genes as Cpa (collagen-binding protein) and PrtF2, a fibronectin-binding protein (197). Like RofA, Nra regulates not only Mga, but other virulence genes such as SpeA, SpeB, and SLS that are involved in host cell damage (174). Furthermore, a transcriptome study on an M49 strain showed that Nra also repressed transcript levels of pilus and capsule synthesis operons, as well as two important GAS regulator systems, Rgg and the Ihk/Irr TCS (126). In addition to repressing, Nra was found to induce expression of metabolic enzymes and several stress response-associated proteins (126). In contrast to the findings from the M49 serotype, recent data suggest an opposing effect in the M53 serotype, as Nra appears to function as a positive regulator of pilus gene transcription and inactivation of *nra* leads to loss of virulence in a mouse model of superficial skin infection (149). Thus, while it appears that the regulatory effects between the two

serotypes are polar opposites, there is a conservation of Nra's regulation of pilus gene transcription, suggesting a role for Nra in virulence gene expression.

RALP3

RALP3, also a member of the RofA-like family, has been shown to negatively control hyaluronic acid capsule and cysteine protease expression (130). Its presence is currently limited to only a few of the sequenced serotypes (M1, M4, M12, M28, and M49) and seems to have varied affects in different strains. In an M1T1 strain, the *ralp3* mutant exhibited greater survival in human whole blood and serum. This behavior also correlated with reduced *covR* transcription in the *ralp3* mutant, suggesting CovR as a potential linker between RALP3 and the *hasA* and *speB* genes (130). Additionally, in an M49 strain, RALP3 was shown to repress expression of *msmR,* the multiple sugar metabolism regulator, yet to activate expression of *nra* (126). It was also shown to regulate the ERES region of the chromosome (*epf ralp3 eno sagA*) (126), which contains important known virulence factor genes.

RivR

RivR, *r*alp *IV*, is the fourth member of the RofA-like protein family of transcriptional regulators to be discovered. RivR is directly repressed by the CovRS TCS (209). It is believed that GAS requires expression of RivR for growth in situations where CovR is dephosphorylated (209). It has been shown that RivR can not only activate expression of the Mga regulon (210) but can also act in concert with Mga to enhance its ability to activate transcription. Additionally, a *rivR* mutant was attenuated for virulence in the invasive subcutaneous mouse model of infection (210).

Other GAS Regulators

Along with TCSs and stand-alone regulators, there are several other factors that have been shown to be involved in virulence factor regulation in GAS. These regulators (e.g. small RNAs, metal regulators) do not fit neatly into the aforementioned categories. A few of these will be discussed below.

Pleiotropic effect locus

The *p*leiotropic *e*ffect *l*ocus (*pel*) represents a unique positive regulator in GAS that has an effect on the expression of multiple surface and secreted proteins involved in virulence (140). Interestingly, *pel* is an untranslated mRNA located within the promoter region of *sagA* (157), the first gene in a nine gene operon responsible for SLS production and secretion (180). Initial studies using a *pel* mutant in an M49 strain resulted in a loss of transcription for the *speB* and *emm* genes, and reduced secretion of Ska (140). Additionally, *in vivo* studies using a mouse skin air sac model showed that a *pel* mutant had reduced virulence compared to a wild type strain (65). Furthermore, this RNA was shown to be regulated in a growth-phase dependent manner and is induced by conditioned media (157), suggesting regulation of *pel* by other regulatory molecules of GAS. Regulation by *pel* appears to be serotype specific, however, as *pel* had no regulatory activity in M1T1 GAS isolates (193).

MtsR

MtsR is a metal-dependent regulator that was found to regulate the streptococcal iron acquisition (*sia*) operon in response to iron availability (16). As iron has been shown

to influence the production of various virulence factors such as the M-protein (167) and SLS (85), *in vivo* studies using an *mtsR* mutant in an M49 strain have shown attenuation for virulence in both intramuscular and intraperitoneal zebrafish infection models (16). Additionally, microarray studies on the mutant broaden the MtsR regulon beyond metal homeostasis to include essential virulence and pathogenesis genes of GAS (*mga, emm49, ska*) (256). Moreover, in an M3 strain, MtsR was shown to be linked to necrotizing fasciitis in mice and non-human primates (187), implicating MtsR as an important regulator in GAS pathogenesis.

CodY

CodY is a pleiotropic regulator that has been shown to be involved in the amino acid starvation response, in which the organism faces nutrient limitation, in several low G+C Gram-positive bacteria. Numerous studies have looked at the relationship between the acquisition of nutrients and virulence gene expression, as it is believed that this process is the primary event in the establishment of infection. One such study showed that CodY affects the transcription of numerous transcriptional regulators involved in virulence (*mga, covRS, rgg/ropB), pel*) when grown in complex or defined media (156). Additionally, it was shown that CodY contributed to virulence gene regulation in human blood and extended the previously found *in vitro* regulon (155). Although it is not apparent whether CodY is exerting direct affects on its regulon, or if its regulation is through a secondary network, CodY represents a global regulator within GAS that is involved in virulence gene regulation.

Srv

Srv, the *s*treptococcal *r*egulator of *v*irulence, is another transcriptional regulator of GAS that was identified based upon its homology to the PrfA virulence regulator of *Listeria monocytogenes* (204). Using an intraperitoneal mouse model of infection, Srv was shown to be required for full virulence in an M1 strain, as loss of *srv* resulted in a significant decrease in GAS virulence (204). Additionally, microarray studies show that inactivation of *srv* results in a reduction of Sic and in increase in SpeB (203), two widely known virulence factors. Furthermore, Srv was shown to be necessary for GAS biofilm formation (61), as it regulates the production of SpeB, a protease involved in degradation of GAS and host proteins necessary for the biofilm. After testing this *in vivo* using both a chinchilla model of otitis media and a murine model of soft tissue infection, it was concluded that Srv-mediated regulation of SpeB contributes to biofilm stability, as it may play a role in producing SpeB when dispersion and dissemination of the bacteria is needed during active infection (51, 208).

TWO-COMPONENT SIGNAL TRANSDUCTION SYSTEMS

Signal transduction systems function as intracellular information processing pathways that link an outside stimulus to an internal response. They typically exist as a series of phosphorylation steps to move the signal into a successful effect. As early as the 1980s, researchers found and named a new class of regulatory systems in bacteria as 'two-component system' (TCS). Two-component systems serve as a basic stimulus-

response coupling mechanism that allows organisms to sense and respond to changes in environmental conditions. As the name suggests, a TCS involves two proteins to elicit a response. The histidine kinase is the primary connector of stimuli within the cellular environment. It passes the 'signal' along in the form of a phosphate to a response regulator, which produces the adaptive response. This mechanism and its constituent proteins will be discussed in further detail below.

System Architecture

The majority of TCSs have a very simple design. A transmembrane sensor kinase activates a cytoplasmic RR through a single phosphoryl transfer, leading the activated RR to elicit its adaptive response (Fig 2A). This transfer occurs via three phosphotransfer reactions and two phosphorylation intermediates:

1. Autophosphorylation: HK-His + ATP ⟷ HK-His~P + ADP
2. Phosphotransfer: HK-His~P + RR-Asp ⟷ HK-His +RR-Asp~P
3. Dephosphorylation: RR-Asp~P + H_20 ⟷ RR-Asp +P_i

Adapted from (237)

In the first step of autophosphorylation, the γ-phosphate of ATP is transferred to the conserved histidine residue within the HK. The RR then catalyzes the transfer of the phosphate group from the histidine residue of the HK to its own conserved aspartate residue. In the final step of the reaction, the phosphate is transferred from the aspartate residue of the RR to water in a hydrolysis reaction (237). A classic example of this basic scheme is that of the well-studied EnvZ-OmpR osmosensing TCS of *E. coli*. In this system, upon autophosphorylation of EnvZ, EnvZ transfers its phosphate to OmpR. The activated OmpR then modulates the expression of two outer membrane porin proteins in

response to the osmolarity of the cellular environment (40). In a slightly more complicated version of the basic TCSs, some HKs can not only phosphorylate one RR, but also have the ability to competitively phosphorylate another (e.g. CheA-CheB/CheY).

More elaborate versions of the TCS are the multiple phosphotransfer pathways known as phosphorelays. The basic design of a phosphorelay pathway incorporates five phosphoryl transfer reactions and four phosphoprotein intermediates (Fig 2B). These TCSs are composed of His- and Asp-containing domains that are used as phosphotransfer elements in either isolated domains or as part of a hybrid kinase. The *Bacillus subtilis* sporulation control system is an example of a phosphorelay system that contains two HKs and a single RR, along with additional receiver His-containing phosphotransfer protein (HPt) elements (34).

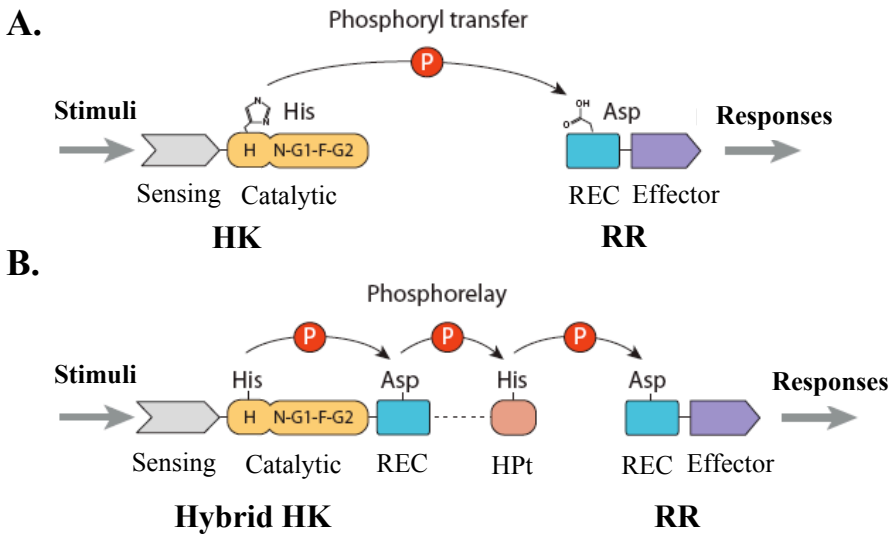

FIGURE 2. **Two-component system schematic.** *A*, The classical TCS pathway in which a HK receives a signal through its sensing domain and phosphorylates at a conserved histidine within its catalytic domain. This phosphate is then transferred to the receiver domain (REC) and activates the RR, which allows the protein to elicit its cellular response. *B*, A phosphorelay in which a hybrid HK involving an additional REC and histidine phosphotransfer (HPt) domain is used for multiple phosphotransfer events before the RR becomes activated. [Figure adapted and modified from (77).]

Genomic Distribution

TCSs are found in the three domains of life: prokaryotes, archaea, and eukaryotes. In prokaryotes and archaea, several hundred two-component proteins have been identified. In *E. coli*, there are 30 HKs and 32 RRs (237). In other sequenced organisms, the number of HKs and RRs differs significantly, ranging anywhere from 0 (*Mycoplasma genitalium*) to 80 (*Synechocystis* sp.) (237). In contrast to the numerous two-component proteins found in prokaryotes, only a small number have been identified in eukaryotes. Those that have been described are predominantly in microorganisms, with only a few found in plants (e.g. *Arabidopsis thaliana*) and none in animals (237). Eukaryotic TCSs typically have hybrid kinases that contain RR domains and do not contain DNA-binding domains. Although there are differences between prokaryotic and eukaryotic TCSs, as will be mentioned in more detail later, the overall mechanism is still the same: to sense and respond to environmental changes.

Phosphotransfer Chemistry

Histidine kinases were named for the important role that the histidine residue plays in the overall function of the protein. Typically, phosphorylation occurs on the N3-position of the imidazole ring of the histidine (246), which creates a phosphoamidate bond. This bond is important because it contains a large negative free energy of hydrolysis, making it relatively unstable (239). Because of this, the phospho-histidine residue is much more suitable as a phosphotransfer intermediate, that can drive phosphorylation of its cognate aspartate residue within the RR, than as a stoichiometrically phosphorylated site for protein interaction. While HKs are

catalytically similar to Ser/Thr/Tyr protein kinases, the chemistry and catalytic mechanism of phosphoryl transfer differ between the two. For Ser/Thr/Tyr kinases, phosphorylation results in a phosphoester bond. This bond has a smaller free energy for the isolated residue than that of the protein. Because of this, the phosphate is transferred from ATP directly to the protein substrate.

Phosphorylation of the aspartate, on the other hand, produces a high-energy acyl phosphate. The best-characterized phospho-aspartate intermediate is found in the P-type ion-translocating ATPases (248). In these proteins, the free-energy of the phospho-aspartate is significantly less than measured in a small-molecule acyl phosphates. With the energy, the acyl phosphate bond is able to drive a conformational change within the protein. It is hypothesized that this energy is also able to cause long-range conformational changes, and not just local electrostatic effects, to activate the RR and elicit its cellular response.

Histidine Kinases

Sensory domains

Most prokaryotic and eukaryotic HKs contain an amino-terminal signal-sensing domain, a region of the protein that is connected to the cytoplasmic kinase core through a transmembrane helix and a cytoplasmic linker (237). The more complicated hybrid HKs, which are typically found in but not limited to eukaryotes, have an additional phosphorylatable receiver module and/or phosphotransfer unit attached to the cytoplasmic transmitter core (73) (Fig 2B). Whether the kinase is of the classical type or a hybrid model, the stimuli are sensed directly through these sensory domains, and/or can

be sensed indirectly through a protein-protein interaction with an accessory protein. Thus, owing to the multitude of HKs specific for distinct signals, the sensing domain of the HK shares very little primary sequence similarity from one protein to another, allowing for diverse, yet specific ligand/stimulus interaction within the organism.

HKs are able to sense a wide variety of stimuli, including but not limited to small molecules, cell envelope stress, light, turgor pressure, redox potential, and electrochemical gradients (77). The sensing domains of HKs can be classified into three major groups based upon their membrane topologies (161). The largest group of sensory domains is represented by the classical HKs, where the sensory domain typically lies within the periplasm, between two transmembrane helices, and transduction of the signal occurs across the membrane. The second group contains not two transmembrane helices, but several (237), with no apparent extracellular domain. In these sensory domains, it is believed that these stimuli are membrane associated, such as a change in cell envelope integrity. The last type of sensory domain does not lie within the membrane, rather, it exists in the cytoplasm for sensing diffused and internal stimuli, like the chemotaxis kinase CheA (236) or the nitrogen regulatory kinase NtrB (152). These HKs take part in protein-protein interactions with other cytosolic components to initiate a response.

In order to respond to such an enormous, diverse group of signals, HKs have evolved several mechanisms of signal perception, occurring at either their own sensor domain, one of their transmembrane regions, or through auxiliary proteins (i.e. three-component system) (129). For the most common form of signal perception, in which HKs sense their signal through an obligatory sensory domain, PAS domains are most frequently used (258). These domains exist as an α/β fold, capable of incorporating

signals by many mechanisms, including direct binding to the PAS domain cavity, binding through a co-factor containing PAS domain, binding at the PAS domain-membrane interface, and signal-mediated modulation of inter-PAS domain disulfide bonds (129). The well characterized PhoQ HK of *Salmonella typhimurium* utilizes the sensor domain-membrane interface to control inducible resistance through its signal, host antimicrobial peptides (15). Here, in the absence of the antimicrobial peptides, the PhoQ sensor domain is attached to the membrane surface. However, once the peptides are present, they have the ability to displace bound metal ions and release the sensor domain from the membrane, thus promoting signal transduction across the membrane to activate the HK (129). Regardless of the sensing mechanism used, signal perception by the HK initiates its own kinase domain activation, ultimately leading to autophosphorylation and signal transduction.

Linker domains

The sensor domains of membrane HKs are generally connected to their cytoplasmic kinase core through a linker domain. This linker typically starts at the end of the last membrane-spanning region in the sensory domain and ends at the conserved histidine residue within the catalytic core. These domains are of variable lengths, ranging from less than 40 amino acids to more than 150 (68). Based upon computational analyses of sequence similarities between several linker domains, there appears to be a 50-residue α-helical, coiled-coil motif lying within this region (228). Although little is known about the linker domain, it has been hypothesized, based upon this coiled-coil motif, that they

may aid in promoting intramolecular protein-protein associations and/or act in structural relays between the sensing and kinase domains (191).

The kinase domain, the catalytic core of the HK

The kinase domain of the histidine kinase typically lies at the carboxy-terminal end of the protein. This region houses the catalytic core of the protein. It is responsible not only for phosphorylation and dimerization, but also for ATP/ADP-binding and phosphotransfer. This domain can typically be split into two separate regions, one for dimerization and an adjacent second half that comprises the nucleotide-binding pocket. The main body of the phosphotransfer domain is an α/β-sandwich fold consisting of a four-stranded antiparallel β sheet and three α helices (237, 271), reminiscent of the ATPase domains of such proteins as DNA gyrase and Hsp90 (25). Due to the function of this domain, the catalytic core is much more conserved between HKs than the sensory domain. As such, it can be identified by a set of conserved primary sequence motifs, which include the H, N, G1, F, and G2 boxes (211) (Fig 3). The H box, which is typically found in the dimerization region of the core, contains the conserved His residue that is the site of phosphorylation. It is this invariant histidine that is the site of the autophosphorylation reaction. The four other conserved boxes comprise the nucleotide-binding pocket within the active site. These residues are all located in close proximity to each other, as can be seen in Figure 3. Part of this region (the "ATP lid") is also highly flexible and permits conformational changes to occur upon ATP binding.

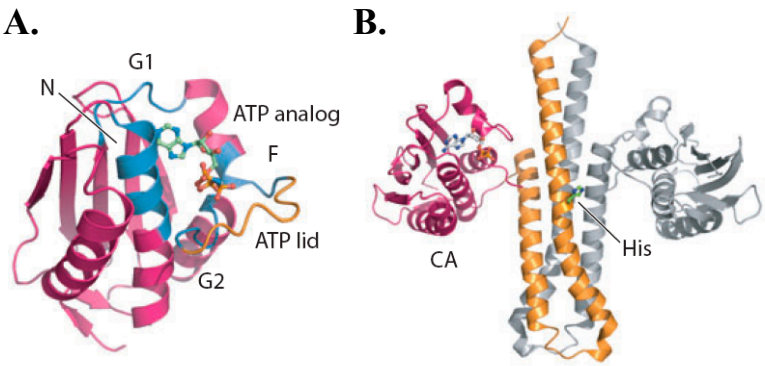

FIGURE 3. **Crystal structures of the catalytic kinase core.** *A,* Structure of the catalytic domain and nucleotide-binding pocket from *E. coli* PhoQ; shown with bound ATP analog. *B,* Structure of the entire kinase core of *Thermatoga maritima* HK853. Shown as a dimer of two monomers, the first is orange and pink (catalytic domain) and the second is shown in gray. [Figure adapted from (77).]

Response Regulators

Receiver domain

Once the catalytic His of the HK becomes phosphorylated, it transfers the phosphate to a conserved Asp residue within the receiver domain of the RR. This N-terminal domain, also referred to as its regulatory domain, is well-conserved between RRs, like that of the HK's kinase domain. CheY, a single-domain RR involved in chemotaxis, serves as a representative model for the RR regulatory domains and has had its crystal structure determined. Based upon its crystal structure, the receiver domain is a doubly wound α/β protein that has a central five-stranded parallel β sheet surrounded by five α helices (238). Numerous highly conserved residues, along with the catalytic Asp, participate in receiving the phosphate within the active site of the domain. The active-site cleft is formed by loops that extend from the C-terminal ends of the β strands β1, β3

and β5 (271). This cleft contains the site of phosphorylation, Asp57, located in the solvent-exposed loop between β3 and αC (215, 237). This residue also lies adjacent to other acidic residues, Asp12 and Asp13, which aid in coordination of the Mg^{2+} that is required for phosphoryl transfer to the catalytic aspartate. Additionally, residues Thr87, Tyr106, and Lys109 complete the active-site cleft, and have been shown to be involved in the phosphorylation-induced conformational change of the RR (8, 274). Although the residues outlined above are those of CheY, numerous X-ray and NMR structures for other RR receiver domains (e.g. PhoB, FixJ) suggest an importance for the identical residues, albeit in slightly different locations, for those proteins.

Effector domain

Once the Asp within the receiver domain has become phosphorylated, conformation changes occur within the RR to order to elicit an appropriate response. Members of the RR family have a diverse set of output responses, as dictated by their effector domains. Although a small percentage of RRs exist as stand-alone CheY-like receiver domains, the majority of RRs (63%) are transcription factors, which have DNA-binding activity to regulate gene expression (77). These RRs can be divided into three major subfamilies based upon the homology of their DNA-binding domains: the OmpR/PhoB winged-helix domains, the NarL/FixJ four-helix domains, and the NtrC ATPase-coupled helical DNA binding domains (239). These domains are well studied and have known three-dimensional structures that feature different variants of the helix-turn-helix DNA-binding structural motif. Other widespread, but far less common DNA-binding domains include the AraC, LytR, and PrrA domains (76). Interestingly, the LytR

DNA-binding domain completely lacks an HTH motif, and appears to consist mostly of β-strands (226).

Those RRs that have an RNA-binding domain, rather than DNA-binding domain, exist relatively rarely within RRs (1%) and commonly belong to the ANTAR family of regulators (77). In transcriptional regulators of the AmiR and NasT type, these domains stimulate transcription by preventing transcriptional termination at rho-independent terminators (184, 224). RRs that contain a enzymatic domain are found in roughly in 13% of RRs (77). The majority of these RRs have domains involved in the regulation of cyclic diguanylate (c-di-GMP) levels within cells, as they have c-di-GMP-specific phosphodiesterase activity (76). The remaining enzymatic subfamilies include the chemotaxis methylesterase CheB domains, HK domains attached C-terminal to receiver domains, and protein phosphatase domains of the PP2C family (77). Lastly, a small and diverse group of RRs contains output domains that have protein-binding capabilities. These RRs exert their effects through protein-protein interactions, and can include such domains as PAS, GAF, and TPR (76).

Activation by phosphorylation

Once the receiver domain of the RR becomes phosphorylated by phosphate transfer from the HK, many structural changes occur within the RR to promote its activation. While phosphorylation generally leads to an active protein, for some RRs, phosphorylation causes the protein to be in the "off" state. For most RRs, though, when the protein is not phosphorylated, the effector domain is typically inhibited by the unphosphorylated receiver domain, which blocks the C-terminal effector region of the

protein from carrying out its effect. Upon phosphate transfer, long-range structural perturbations within the protein occur, repositioning the N- and C-terminal domains of the RR. Recently determined structures of the phosphorylated receiver domain of NtrC elucidated these changes. Displacement of β4, β5, αC, and αD away from the active site of NtrC exposes a hydrophobic surface that is thought to allow transmission of the activation signal to the effector domain (117). This slight repositioning causes dramatic changes to the molecular surface of NtrC and alters the protein topology to allow for signal transmission to its transcriptional effector domain and subsequent protein activation. Additionally, the conformation of two highly conserved switch residues, Ser/Thr on β4 and Phe/Tyr on β5, reorient towards the active site upon phosphorylation to hydrogen bond with the oxygen on the phosphate (77, 94). While these changes have been experimentally demonstrated for NtrC, the range and magnitude of structural changes upon phosphoryl activation can vary among RRs, although the general mechanism of activation by phosphorylation is thought to be conserved.

Regulatory Mechanisms

Regulation of HK activities

As has been discussed in detail above, the main role of the HK is that of an autokinase, in which it transfers a phosphate from ATP to itself, and then this phospho-HK serves as a phospho-donating substrate for the RR. However, many HKs are bifunctional. In addition to their autokinase activity, they possess phosphatase activity toward their cognate phosphorylated RRs. Both the autokinase and phosphatase activities of HKs can be regulated directly or indirectly by stimuli. Regulation of the

autophosphorylation can allow for optimization of signal transmission. One example of this appears in the chemotaxis TCS involving the HK CheA. For this system, CheA is either inhibited or stimulated by signals transmitted from its chemoreceptors, in order to regulate its signaling intensity (28). Additionally, for kinases that possess phosphatase activity, the ability to decrease the level of RR phosphorylation provides a swift mechanism to essentially shut down the signaling pathway. The phosphatase activity for these proteins typically involves amino acid residues located in the dimerization region of the kinase domain, and through interaction with the ATP-binding region, enables it to regulate its activity (77). As has been demonstrated by the osmosensor HK EnvZ, the catalytic histidine residue is used for reverse transfer that sends the phosphoryl group from the RR back to the HK (64). Together, these mechanisms allow individual TCSs to meet their specific needs and optimize signal transmission between the HK and RR.

Regulation of RR dephosphorylation

Separate from the phosphatase activity of the HK, many RRs utilize their own autophosphatase activity in order to allow for fine-tuning of their specific systems. Their ability to catalyze autodephosphorylation occurs at varying rates, as it can happen very quickly, within a matter of seconds, or occur more slowly, taking as long as a few hours (77). Although RR dephosphorylation can be influenced by the phosphatase activities of the HKs, in most cases the mechanism appears to be different, as it does not involve the catalytic histidine of the HK's kinase domain (106). Additionally, for some HKs, it has been shown that their phosphatase activity is stimulated by ATP (116). Moreover, dephosphorylation of the RRs can also be effected by auxiliary proteins. In the *B. subtilis*

sporulation system, a set of three highly regulated phosphatases (RapA, RapB, and RapE) dephosphorylate Spo0F (192), while an additional phosphatase (Spo0E) dephosphorylates Spo0A (186). Thus, a significant number of RR dephosphorylation mechanisms exist, adding to the numerous regulatory strategies employed within a TCS to meet the specific needs of the system.

Other modes

In addition to regulating the HK and RR activities, certain systems employ additional regulatory mechanisms to control the signal output of the TCS. Not all TCSs have a defined reaction to a stimulus. Some systems can create a graded response upon signal activation while others may produce an all-or-nothing response. In addition to altering the level of RR phosphorylation, an alternative strategy used by numerous TCSs is to control the level of gene expression of the RR. In these systems, the TCS genes are subject to autoregulation. Phosphorylated forms of the RR can function as an either an activator or repressor of their own operon (e.g. PhoPQ system of *S. typhimurium* (231)), controlling the amount of their own gene expression. Moreover, another non-traditional regulatory mechanism employed by TCSs such as the *E. coli* chemotaxis system involves one HK phosphorylating more than one RR. In these 'branched' systems, competition for phosphoryl groups can influence the activation of both RRs, creating a precise and defined reaction in response to potentially complex stimuli. More elaborate forms of these intrinsically branched pathways can exist, with "many-to-one", "one-to-many", and "many-to-many" relationships occurring. These added regulatory strategies allow each

individual TCSs to create a specific response and modulate signal transmission within its environment.

CHAPTER THREE:

Materials and Methods

BACTERIAL STRAINS

E. coli strains, media, and growth conditions

E. coli strains used in this study are listed in Table 1. Strain DH5α was used as the host strain for plasmid constructions and was cultured in Luria-Bertani (LB) medium (EMD Biosciences). C41 [DE3] was used for protein expression and cultured in ZYP-5052 auto-induction media (240). BTH101 was used for the bacterial two-hybrid studies and was plated at 30ºC on MacConkey agar (Difco) supplemented with 1% maltose (Sigma). *E. coli* was grown at 37ºC with shaking under normal aerobic conditions. Growth was measured by a spectrophotometer (Ultraspec 10, Amersham Biosciences) at OD_{600} nm. Antibiotics were used at the following concentrations: ampicillin 100 μg/ml; spectinomycin 100 μg/ml; kanamycin 50 μg/ml, and erythromycin 500 μg/ml.

GAS strains, media, and growth conditions

GAS strains used and constructed in the study are listed in Table 1. GAS was cultured in Todd-Hewitt medium supplemented with 0.2% yeast extract (THY; Difco). Growth was assayed by optical density with a Klett-Summerson photoelectric colorimeter with the A filter. C media was prepared using a previously described method (151). Prior to use, magnesium sulfate (0.4 mM), potassium phosphate (10 mM), and sodium chloride (150 mM) were added and the pH of the media was buffered to 7.5 with HEPES to achieve a final concentration of 0.1 M. Antibiotics were used at the following

concentrations: spectinomycin 100 µg/ml, kanamycin 300 µg/ml, and erythromycin 1 µg/ml.

Table 1. Bacterial strains

Strains	Description	Reference
5448-AN	M1T1 GAS, clinical isolate, SpeB(+) SpeA(-) Sda1 (low)	(14)
5448-AP	M1T1 GAS, clinical isolate, SpeB(-) SpeA(+) Sda1 (high)	(14)
BTH101	*E. coli,* F^- *cya-99 araD139 galE15 galK16 rpsL1* (Str^R) *hsdR2 mcrA1 mcrB1*	(113)
C41 (DE3)	*E. coli, F⁻ ompT gal dcm hsdS$_B$* (r_B^- m_B^-) (DE3)	(63)
DH5α	*E. coli, hsdR17 recA1 gyrA endA1 relA1*	(90)
GA19681	M6 GAS, clinical isolate	(207)
GA19681.*trxR*	M6 GAS, $TrxR^-$	This study
GA19681.*trxR*c	M6 GAS, $TrxR^+$ cured strain	This study
GA40634	M4 GAS, clinical isolate	(207)
GA40634.*trxR*	M4 GAS, $TrxR^-$ (insertional inactivation of *trxR*)	This study
GA40634.*trxR*c	M4 GAS, $TrxR^+$ cured strain	This study
KSM165-L.5005	M1T1 GAS, clinical isolate, Mga^-	(135)
MGAS5005	M1T1 GAS, clinical isolate, *CovS*	(222)
MGAS5005.*trxR*	M1T1 GAS, $TrxR^-$ (insertional inactivation of *trxR*)	(135)
MGAS5005.*trxT*	M1T1 GAS, $TrxT^-$ (Δ*trxT* strain)	This study
NZ131	M49 GAS	(249)
NZ131.*trxR*	M49 GAS, $TrxR^-$ (insertional inactivation of *trxR*)	This study
NZ131.*trxR*c	M49 GAS, $TrxR^+$ cured strain	This study

DNA MANIPULATIONS

Plasmid Isolation

Plasmid DNA was isolated from *E. coli* by alkaline lysis using either the Wizard Miniprep (Promega) or the Midi/Maxi prep purification systems (Qiagen) according to

the manufacturer's instructions. DNA fragments were isolated from agarose gels using either the QIAquick (Qiagen) or Wizard SV (Promega) gel extraction kits.

GAS Chromosomal DNA Isolation

GAS chromosomal DNA was isolated as previously described (11, 41). Briefly, 15 ml cultures were grown overnight at 37°C with 20 mM glycine and pelleted in the morning. Cells were washed in 10 mM Tris, resuspended in Solution I (1 M Tris, pH 8, 0.25 M EDTA pH 8, and 50% Sucrose) supplemented with fresh lysosome (130 mg/ml), and incubated for 90 minutes with rotation at 37°C. Cells were pelleted and resuspended in Solution II (1 M Tris pH 8, 0.25 M EDTA pH 8, 20% SDS) and incubated at 37°C for 15 minutes. To the suspension, RNase A (10 mg/ml) and Proteinase K (20 mg/ml) were added and were placed at 55°C for 30 minutes with frequent inversion. The cell lysate was then extracted once with an equal volume of TE-saturated phenol, with 1:1 phenol-chloroform until the interface cleared, and once with 24:1 chloroform-isoamyl alcohol. The DNA was then ethanol precipitated overnight, pelleted, and resuspended in water. DNA concentrations were measured by the A_{260} absorbance on a spectrophotometer (Ultraspec 2100 pro, Amersham Biosciences).

Polymerase Chain Reaction

Polymerase chain reaction (PCR) was performed using Phusion high-fidelity polymerase (New England Biolabs, NEB) for cloning and Taq DNA polymerase (NEB) for diagnostic assays. To use Phusion polymerase, annealing temperatures for primers were determined using the Finnzymes TM calculator

(https://www.finnzymes.fi/tm_determination.html). Amplification was carried out by an initial denaturation step at 98°C for 4 minutes, followed by 35 cycles of denaturation at 98°C for 10 seconds, a 30 second annealing step at a pre-determined temperature, and an extension step at 72°C for approximately 15-30 seconds per kb of DNA. A final extension step for 4 minutes completed the reaction to ensure production of the full-length product. To use Taq polymerase, the PCR protocol was modified slightly from Phusion: briefly, 30 cycles were used, denaturation was performed at 95°C, and longer extension times were used (~1 kb/minute). Annealing temperatures for use with Taq polymerase were determined through Vector NTI software (version 11.0). PCR reactions were purified either by QIAquick PCR purification kit or Wizard SV PCR clean-up systems according to manufacturer's instructions. DNA sequencing was performed by Genewiz, Inc.

PAGE oligonucleotide purification

The oligonucleotides used in the construction of the mutated HTHs and mutated catalytic signaling residues for TrxS and TrxR were PAGE purified prior to annealing. Briefly, the lyophilized oligonucleotides pellet (Integrated DNA Technologies) were resuspended in 100 µl dH_20 with 20 µl formamide stop solution (SequiTherm Excel II kit, Epicentre). The oligonucleotides were then loaded and run on a 10% sequencing gel (42% (w/v) urea, 20% (v/v) 5x TBE, 25% (v/v) 40% acrylamide bis solution). After running for 75 minutes, the gel was placed on an intensifying cassette and a short-wave UV light was used to locate the DNA bands. The bands were then excised, crushed, and soaked in 10 mM Tris, pH 8.0 overnight, followed by a phenol-chloroform extraction.

Table 2. PCR primers

Target	Primer	Sequence (5'-3')	Reference
aad9	*aad9*-L2-bglII	gcgcagatctGGGTGACTAAATAGTGAGGAG	This study
	aad9-R2-bglII	gcgcagatctGGCATGTGATTTTCC	This study
bgaA	βgal-L	ACACCGCTGTCGATCTT	(135)
emm	P*emm*1-L2	AATAAAAGCCAAAAGGTAA	This study
(EMSA)	P*emm*1-R2	AAGCGATTATTGACAAGCTC	This study
mga	OYL-25	TACCATAAAATACCTTTC	(168)
(EMSA)	OYR-25	GGTTGTACCATAACAGTC	(168)
trxT	*Spy1589*-R	TGGACTGATTGTGTTTG	(135)
(Spy1307)	*Spy1307* 1a	agatctGGTTTTTTCAATGCCATTCATATGA	This study
	Spy1307 1b	gggcCCGCTTGATGCACAAA	This study
	Spy1307 2a	ccgcCCATGTGGCTGTTGTCGAT	This study
	Spy1307 2b	tgaaaaaaccagatctGCTTGGACTTTGTCAC	This study
	Spy1307 3a	tctagaCCGCCCATGTGGCTGTTGTCG	This study
	Spy1307 3b	ctcgagGGGCCCGCTTGATGCA	This study
	Spy1307-L	TGCTTAAAGTGGTTAGTCA	This study
	Spy1307-R	AAGTGTGCTATATTAGAAGAGTC	This study
	M1 P*Spy1307*-Xho-L	ctcgagATAGCAGTTTCAGGGACCA	This study
	M1 P*Spy1307*-Bgl-R	agatctATGCACATGGGTGCTTGG	This study
	M1 P*Spy1307*-Xho-L2	cccagatctATGCACATGGGTGCTTGGAATACTGGT	This study
	M1 P*Spy1307*-Bgl-R2	ccctcgagTTTACTCTGATTAATAGTTTAGACTC	This study
	Spy1307-Eco	cccgaattcCTTCCAAAACTTCTT	This study
	Spy1307-Xba	ccctctagaAGTCGATTAATCAAAAAAC	This study
	Spy1307 SP1	AAGGTTAATCTCATAGCTCACTGC	This study
	Spy1307 SP2	GCCCTTTTCAAAGAATAGTGGTTTT	This study
	Spy1307 SP3	GCCCCACCCCAAACACAATC	This study
	Spy1307 SP4	CAGGTTTTTTCAATGCCATTCATATG	This study
	Spy1307 SP5	AGTCCTCTTTTTCTTGTTAACACTTATAGCAGTTT	This study
	Spy1307 SP6	CCCAGTAAGATGCTGGTATTAGTTT	This study
	Spy1307 SP7	CTCTGATTAATAGTTTAGACTCTTCTAATATAGCA	This study
trxR	His-MBP-TrxR-effector	accgcatgcTTACTGGTCGCCCTTGATGG	This study
	His-MBP-TrxR-linker	cccgcatgcTCAGCAATCAATGGTTTCAC	This study
	His-MBP-TrxR-Hind	cccaagcttAAGAAGGAGATATACCATGGGCCA	This study
	His-MBP-TrxR-Sph	ggccgcatgcTTAATCAGGATCCTCGAGCT	This study
	M1 *trxR* effector-nde	cgcccatatgATTCGCAAGGAATACCATCA	This study
	M1 *trxR* effector-xho	ccctcgagTTACTGGTGGCCCTTGATGG	This study
	M1 *trxR* linker-nde	acccatatgCAATTTAAAGACTGGTTGGATGCC	This study
	M1 *trxR* linker-xho	ccctcgagTCAGCAATCAATGGTTTCACTAACTAAA	This study
	M1 *trxR* Nde-L	cgcccatatgATGTATAAGGTACTATTAGTTGACG	This study
	M1 *trxR* Xho-L	gaactcgagCTGGTCGCCCTTGATG	This study
	Spt10PE	CTATATAATTTCATCAGTCG	(135)
	Spt10R-L1	gaactcgagTCAAGGCTTTAGATGAGACG	(206)
	Spt10R-R1	TTGGTAGCCAGTCACTGTCT	(206)
	srxR-Spy1586 RT-L	AAGCATGTTTCGTTC	(135)
	srxR-Spy1586 RT-R	AGAACTGGGAACCTT	(135)
	trxR D55A L	GTGGATGTCATGATTTCAGCTGTTACCATGCCTGGAATG	This study
	trxR D55A R	CATTCCAGGCATGGTAACAGCTGAAATCATGACATCCAC	This study
	trxR D55E L	GGATGTCATGATTTCAGAAGTTACCATGCCTGGAATG	This study
	trxR D55E R	CATTCCAGGCATGGTAACTTCTGAAATCATGACATCC	This study
	TrxR HTH-1 YL413AL-L	GCTATCGCTGATAGGTTACATGTCAATGGGGTTGCTCTAGGGCAATGCTTTAAAAA	This study
	TrxR HTH-1 YL413AL-R	TTTTTAAAGCATTGCCCTAGAGCAACCCCATTGACATGTAACCTATCAGCGATAGC	This study
	TrxR HTH-1 AL413AA-L	AGGTTACATGTCAATGGGGTTGCTGCAGGGCAAT	This study

		GCTTTAAA	
	TrxR HTH-1 AL413AA-R	TTTAAAGCATTGCCCTGCAGCAACCCCATTGACAT GTAACCT	This study
	TrxR HTH-2 NH461AA-L	GCTTATGAAACAGGTTACAATACCGCTGCTTATTT TATCAAGATGTTTAAA	This study
	TrxR HTH-2 NH461AA-R	TTTAAACATCTTGATAAAATAAGCAGCGGTATTGT AACCTGTTTCATAAGC	This study
	trxR M1 RT-R	AATCAATAATCATGGTGAGCCC	This study
trxS	M1 *trxS* Nde-L	ggcgcatatgATTGACGAAGTTTATG	This study
	M1 *trxS* Xho-R	gcgctcgagAGCATCCTTTCTAATC	This study
	T18C-*trxS*-trun-BamHI	cccggatccATTGACGAAGTTTATGTG	This study
	T18C-*trxS*-XmaI	ccccccgggTCAAGCATCCTTTCTAA	This study
	trxS H383A L	CTCTGCAGTCTCAAATCAACCCTGCTTTTTTATAC AACACGTTAGAGT	This study
	trxS H383A R	ACTCTAACGTGTTGTATAAAAAAGCAGGGTTGAT TTGAGACTGCAGAG	This study
	trxS M1 RT-L	TGACAGCCACATAAGCCAAG	This study

Lowercase letters represent additional sequence added. Underline text denotes added restriction sites.

Enzymatic DNA modifications

Enzymatic DNA modifications were performed using enzymes according to the manufacturer's suggested conditions. Restriction digests were performed using enzymes and buffers from NEB for 2 hours at their optimal temperatures. Ligation reactions using T4 ligase (NEB) were performed at 16°C overnight. T4 polynucleotide kinase (PNK, NEB) was used for radioactive end-labeling of probes at 25°C for 10 minutes.

BACTERIAL TRANSFORMATIONS

E. coli competent cells

To prepare DH5α or C41 [DE3] competent cells, 500 ml of LB broth was inoculated with a 5 ml overnight starter culture and grown to an OD_{600} of around 0.6. Cells were placed on ice for 30 minutes in order to cool them and stop their growth minutes prior to centrifugation at 6,000 x *g* for 15 minutes at 4°C. After the initial

pelleting, cells were washed three times in ice-cold sterile 10% glycerol. After the final wash, cells were resuspended in 800 µl of 10% glycerol and split into 50 µl aliquots. Aliquots were stored at -80°C for no more than one year.

GAS competent cells

To prepare competent GAS cells for transformations, 150 ml of THY broth containing 20 mM glycine was inoculated with a 7.5 ml overnight starter culture and was incubated static at 37°C until OD_{600} reached between 0.2 and 0.3. Cells were placed on ice for 30 minutes in order to cool them and to stop their growth prior to centrifugation at 8,000 x *g* for 20 minutes at 4°C. The pelleted cells were washed three times with 20 ml of cold 10% glycerol. After the final wash, the cells were resuspended in 800 µl of 10% glycerol and split into 200 µl aliquots. Aliquots were stored at -80°C for no more than one year.

Electroporation

To remove excess salts prior to electroporation of DNA into either *E. coli* or GAS, DNA was drop-dialyzed over dH_20 on a 0.025 µM membrane filter (Millipore) for 30-60 minutes. Electroporation of both *E. coli* and GAS were performed using a GenePulser Xcell (Bio-rad). For electroporation of *E. coli*, the 50 µl competent cell aliquot was mixed with the drop-dialyzed DNA in a pre-chilled 2 mm cuvette and transformed using the following settings: 2.5 kV, 200 Ω, and 25 µF. Cells were immediately added to 1 ml LB broth and outgrown for 1 hour at 37°C shaking, prior to centrifugation at 6,000 x *g*. Pelleted cells were resuspended in 100 µl saline and plated

on the appropriate antibiotic for selection. For electroporation of GAS, a similar protocol was used with the 200 µl competent cell aliquot with the following electroporator settings: 1.75 kV, 400 Ω, and 25 µF. Cells were placed in 10 ml THY broth and outgrown static for 2 hours at 37°C. Cells were pelleted at 8,000 x *g* and resuspended in 100 µl THY broth prior to plating on the appropriate antibiotic for selection.

GENETIC CONSTRUCTIONS

A. Plasmid constructions

Construction of P*trxT-luc* vectors, pKSM637 and pKSM670

Wild type P*trxT* was amplified from MGAS5005 (Table 1) using primers M1 PSpy1307-Xho-L and M1 PSpy1307-Bgl-R (Table 2). The 620 bp promoter PCR fragment was BglII/XhoI digested and ligated into BglII/XhoI-digested luciferase plasmid pKSM720 (Table 1) to form pKSM637.

Truncated P*trxT* was amplified from MGAS5005 (Table 1) using primers M1 PSpy1307-Xho-L-2 and M1 PSpy1307-Bgl-R-2 (Table 2), which deleted the last 65 bp from the promoter region. The promoter PCR fragment was BglII/XhoI digested and ligated into BglII/XhoI-digested luciferase plasmid pKSM720 to form pKSM670 (Table 3).

Table 3. Plasmids

Plasmid	Description	Reference
p233-10R	*trxR* insertional inactivation plasmid	(206)
pBluescript II KS (-)	ColE1 ori Ap^R *lacZα*	Stratagene
pCRK	Gene replacement/shuttle vector for *E. coli* and GAS with Km^R	This study
pJRS525	Replicating vector for GAS with Sp^R	(169)
pKSM201	Replicating vector for GAS with Km^R	(119)
pKSM324	GAS replicating plasmid containing P*rpsL*	(261)
pKSM612	GAS replicating plasmid P*rpsL*-TrxR	(135)
pKSM636	Δ*trxT* mutagenic plasmid with non-polar *aad9*	This study
pKSM637	GAS replicating plasmid with P*trxT-luc*	This study
pKSM643	Expression vector M1 GAS His-MBP-TrxS (signaling region)	This study
pKSM649	*trxT* complementing vector	This study
pKSM654	Expression vector M1 GAS His-MBP-TrxS H383A	This study
pKSM655	Expression vector M1 GAS His-MBP-TrxR	This study
pKSM657	Expression vector M1 GAS His-MBP-TrxR D55A	This study
pKSM662	Expression vector M1 GAS His-MBP-TrxR D55E	This study
pKSM670	P*trxT-luc* truncated	This study
pKSM678	GAS replicating plasmid P*rpsL*-His-MBP-TrxR	This study
pKSM680	GAS replicating plasmid P*rpsL*-His-MBP-TrxR D55A	This study
pKSM690	GAS replicating plasmid P*rpsL*-His-MBP-TrxR D55E	This study
pKMS691	GAS replicating plasmid P*rpsL*-His-MBP-TrxR HTH-1 mutant	This study
pKSM694	GAS replicating plasmid P*rpsL*-His-MBP-TrxR HTH-2 mutant	This study
pKSM697	GAS replicating plasmid P*rpsL*-His-MBP-TrxR HTH-1/2 mutant	This study
pKSM699	T25C-tagged TrxS (signaling region) Km^R	This study
pKSM720	GAS replicating plasmid with firefly luciferase and RBS	(119)
pKSM721	GAS replicating plasmid with P*mga-luc* Sp^R	(135)
pKSM733	Expression vector M1 GAS His-MBP-TrxR HTH-1/2 mutant	This study
pKSM734	Expression vector M1 GAS His-MBP-TrxR (Δeffector)	This study
pKSM735	Expression vector M1 GAS His-MBP-TrxR (Δreceiver)	This study
pKSM736	Expression vector M1 GAS His-MBP-TrxR (effector only)	This study
pKSM737	GAS replicating plasmid P*rpsL*-His-MBP-TrxR (Δeffector)	This study
pKSM738	GAS replicating plasmid P*rpsL*-His-MBP-TrxR (Δreceiver)	This study
pKSM739	GAS replicating plasmid P*rpsL*-His-MBP-TrxR (effector only)	This study
pKSM741	T18C-tagged TrxS (signaling region) Ap^R	This study
pOri253	Replicating vector for GAS with Em^R	(138)
pSL60-1	Vector containing non-polar *aad9* gene	(145)
pT18C-link	T18 expressing two-hybrid vector with linker	Gift, D. Kearns
pT25C-link	T25 expressing two-hybrid vector with linker	Gift, D. Kearns
pVL847	Expression vector N-terminal 10x His-MBP	(136)

Construction of allelic exchange vector pKSM636 for creation of MGAS5005.*trxT*

SOE PCR (splicing by overlap extension by the polymerase chain reaction) (98) was used to make a non-polar deletion of the *trxT* gene. The primers Spy1307-1a/b (Table 2) were created to amplify a 1,060 bp upstream region from MGAS5005 (Table 1)

containing the first twenty nucleotides of *trxT*, a BglII site, and a 10 bp overlap with the second fragment at the 3' end. A second set of primers, Spy1307-2a/b (Table 2), were created to amplify a 1,080 bp downstream region from MGAS5005 (Table 1) containing the last 58 nucleotides of *trxT*, with a BglII site at the 5' end. These fragments were then combined as template DNA using the Spy1307-3a/b primers to generate the deletion. The resulting product was then blunt-end ligated into a HincII-digested pBluescript II KS (-) (Table 3). The non-polar, promoterless spectinomycin resistance gene (*aad9*) was amplified from pSL60-1 (Table 3) using primers aad9-L2-bglII and aad9-R2-bglII (145) (Table 2), digested with BglII, and ligated into a BglII-digested pBluescriptΔ*trxT*. The Δ*trxT-aad9* fragment from pBluescriptΔ*trxT* was then PCR amplified using Phusion HF DNA polymerase and ligated with the temperature-sensitive gene replacement/shuttle vector pCRK (Table 3), digested with BamHI, to yield the final pKSM636 Δ*trxT* mutant (Table 3).

Construction of *trxT* complementation vector, pKSM649

trxT along with its native promoter was amplified from the serotype M1 strain MGAS5005 (Table 1) using primers *Spy1307*-Eco and *Spy1307*-Xba (Table 2). Both the PCR product and pKSM201 (Table 3) were EcoRI/XbaI-digested and the two were ligated together to create pKSM649 (Table 3).

Construction of TrxS two-hybrid plasmids, pKSM699 and pKSM741

The signaling domain of M1 GAS TrxS (aa 358-574) was PCR amplified from MGAS5005 (Table 1) using primers T18C-trxStrun-BamHI and T18C-trxS-XmaI (Table

2). The product was digested with BamHI/XmaI and ligated into BamHI/XmaI-digested plasmids pT25C-link and pT18C-link (Table 1) to form pKSM699 and pKSM741, respectively. The resulting plasmids were verified through DNA sequencing to confirm an ORF that would express TrxS in-frame with the adenylate cyclase fragment.

Construction of recombinant GAS TrxS and TrxR expression vectors, pKSM643 and pKSM655

An amino-terminal fusion of 10xHistidine-MBP to the signaling domain of M1 GAS TrxS (aa 358-574) was constructed as described below. A 670 bp region containing the signaling domain was PCR amplified from M1 MGAS5005 (Table 1) gDNA using the primer pair M1 TrxS Nde-L and M1 TrxS Xho-R (Table 2). The resulting product was digested with NdeI/XhoI and ligated into NdeI/XhoI-digested pVL847 (Table 3) to produce pKSM643 (Table 3). Following PCR verification and DNA sequence analysis, pKSM643 was transformed into C41 [DE3] (Table 1) for protein expression.

An amino-terminal fusion of 10xHistidine-MBP to full-length M1 TrxR was constructed by PCR amplifying a 1,497 bp region from M1 MGAS5005 (Table 1) gDNA using the primer pair M1 TrxR Xho-L and M1 TrxR Nde-L (Table 2). The resulting product was digested with XhoI/NdeI and ligated into XhoI/NdeI-digested pVL847 (Table 3) to produce pKSM655 (Table 3). After PCR verification and DNA sequence analysis, pKSM655 was transformed into C41 [DE3] (Table 1) for protein expression.

Construction of expression plasmids containing mutated signaling residues, H383 (TrxS) and D55 (TrxR)

Using pKSM643 (His-MBP-TrxS) and pKSM655 (His-MBP-TrxR) as template DNA (Table 3), point mutations were made in the catalytic residues using the Quikchange II site-directed mutagenesis kit (Stratagene). Briefly, using either pKSM643 or pKSM655 as the template vectors, PAGE-purified oligonucleotides containing the mutated residue, each complementary to opposite strands of the vector, were extended during 16 cycles by PfuUltra HF DNA polymerase. For the extension time, 7.5 and 8.4 minutes were used for His-MBP-TrxS and His-MBP-TrxR, respectively. To create H383A in His-MBP-TrxS, primers TrxS H383A-L and TrxS H383A-R (Table 2) were used. In a similar manner, to create D55A or D55E in His-MBP-TrxR, primers TrxR D55A-L and TrxR D55A-R or TrxR D55E-L and TrxR D55E-R (Table 2) were used. Following temperature cycling, the PCR product was DpnI treated and transformed into ElectroMAX DH5alpha electrocompetent cells. Upon sequence analysis and mutation verification, the plasmid was digested with NdeI/XhoI and the *trxS* or *trxR* fragment was moved into a clean pVL847 (Table 3) plasmid cut with NdeI/XhoI in the DH5α background. The resulting plasmids were named pKSM654, pKSM657, and pKSM662, representing His-MBP-TrxS H383A, His-MBP-TrxR D55A, and His-MBP-TrxR D55E (Table 3), respectively.

Construction of His-MBP-TrxR complementation vectors, pKSM678, pKSM680, pKSM690

To place wild type His-MBP-TrxR under the constitutive promoter, P*rpsL*, His-MBP-TrxR was amplified from pKSM655 (Table 3) using primers His-MBP-TrxR-Hind

and His-MBP-TrxR-Sph (Table 2). After digestion of the PCR product with HindIII and SphI, it was cloned into pKSM324 also cut with HindIII and SphI. The resulting pKSM678 plasmid (Table 3) was confirmed through DNA sequencing.

To make the mutant pKSM680 His-MBP-TrxR D55A (Table 3) under P*rpsL*, His-MBP-TrxR D55A was amplified from pKSM657 (Table 3) using the same strategy as above. pKSM690 (Table 3), P*rpsL*-His-MBP-TrxR D55E, was created in the same manner, amplified from pKSM662 (Table 3).

Construction of TrxR HTH-1/2 mutant vector, pKSM697

To mutate the two amino acids in each putative helix-turn-helix (HTH) domain of TrxR to alanines, a 3-step approach was employed. First, using pKSM678 (Table 3) as the template plasmid, two base pairs within the first amino acid of HTH-1 were mutated to change Tyr (TAT) to Ala (GCT) using the Quikchange II site-directed mutagenesis kit (Stratagene). Briefly, PAGE-purified oligonucleotides containing the mutated residue, each complementary to opposite strands of the vector, were extended using the primers TrxR HTH-1 YL413AL-L/R (Table 2) for 6.45 minutes during 18 cycles by PfuUltra HF DNA polymerase. Following temperature cycling, the PCR product was DpnI treated and transformed into ElectroMAX DH5alpha electrocompetent cells (Invitrogen). Upon sequence analysis and mutation verification, the plasmid was digested with HindIII/SphI and the fragment was moved into a clean pKSM324 (Table 3) plasmid cut with HindIII/SphI in the DH5α background. The resulting plasmid was named pKSM691 (Table 3).

In the second step, four point mutations were made within HTH-2 of pKSM691 to change Asn (AAT) His (CAT) to Ala (GCT) Ala (GCT) in a similar manner as above using primers TrxR HTH-2 NH461AA-L/R (Table 2). The sequence was verified and the fragment was moved into a clean plasmid background, creating pKSM694 (Table 3).

In the final step to make P*rpsL*-His-MBP-TrxR HTH-1/2, two additional point mutations within pKSM694 were made to change the second amino acid of HTH-1 Leu (CTA) to Ala (GCA) with primers TrxR HTH-1 AL413AL-L/R (Table 2) using the Quikchange method. The final P*rpsL*-His-MBP-TrxR HTH-1/2 plasmid was named pKSM697 (Table 3).

Construction of TrxR HTH-1/2 expression plasmid, pKSM733

TrxR HTH-1/2 was PCR amplified from pKSM697 (P*rpsL*-His-MBP-TrxR HTH-1/2) (Table 3) using the primer pair M1 TrxR Xho-L and M1 TrxR Nde-L (Table 2). The resulting product was digested with XhoI/NdeI and ligated into XhoI/NdeI-digested pVL847 (Table 3) to produce pKSM733 (Table 3). After PCR verification and DNA sequence analysis, pKSM733 was transformed into C41 [DE3] (Table 1) for protein expression.

Construction of plasmids containing truncated forms of His-MBP-TrxR

To create truncated His-MBP-TrxR proteins, the designated regions of the protein were first cloned into pVL847 (Table 3) resulting in TrxR in-frame with His-MBP. Briefly, the receiver-linker, Δeffector (bp 1-1167), linker-effector, Δreceiver (bp 351-1485), or effector alone (bp 1167-1485) were PCR amplified from the MGAS5005

(Table 1) chromosome with added NdeI/XhoI sites using the following primer pairs: M1 TrxR-NdeI/M1 TrxR-linker-Xho, M1 TrxR linker-Nde/M1 TrxR effector-Xho, and M1 TrxR effector-Nde/M1 TrxR-effector-Xho (Table 2), respectively. The digested PCR fragments were cloned into NdeI/XhoI-digested pVL847 and the resulting plasmids (pKSM734, pKSM735, and pKSM736 (Table 3) were confirmed through DNA sequencing.

To place the His-MBP-TrxR proteins under P*rpsL*, the entire His-MBP-TrxR regions were PCR amplified from pKSM734-736 (Table 3) using the following sets of primers with added HindIII/SphI sites: His-MBP-TrxR-Hind/His-MBP-TrxR-linker for His-MBP-TrxR Δeffector and His-MBP-TrxR-Hind/His-MBP-TrxR-effector for Δreceiver and effector-alone (Table 2). The digested PCR fragments were cloned into HindIII/SphI-digested pKSM324 (Table 3) and the resulting plasmids pKSM737, pKSM738, and pKSM739 (Table 3) were confirmed through DNA sequencing.

B. Strain constructions

Temperature-sensitive allelic exchange of pKSM636 to create MGAS5005.*trxT*

MGAS5005 (Table 1) was transformed with pKSM636 (Table 3) as previously described (195). Briefly, after electroporation, cells were outgrown for four hours at 30°C prior to plating on plates containing both kanamycin and spectinomycin selection. Plates were incubated at 30°C until isolated colonies appeared. Colonies were inoculated into liquid cultures with kanamycin and spectinomycin selection and passaged twice

overnight at 30°C. Cells were then passaged twice at 37°C with spectinomycin selection only and were serially diluted onto THY spectinomycin agar and incubated at 37°C. Mutants were screened by sensitivity to kanamycin and verified by PCR across the *trxT* gene using primers Spy1307-L/R (Table 2).

Inactivation of *trxR* in GA40634 and NZ131

trxR was inactivated in M4 GA40634 and M49 NZ131 (Table 1) using the temperature-sensitive integration method as previously described (194). Briefly, plasmid p233-10R (Table 3) was electroporated into GA40634 and NZ131, followed by passage twice at 30°C with erythromycin selection. To allow for integration of the plasmid, cells were passaged twice at 37°C under erythromycin selection. Integrants were screened by PCR for junctions and absence of the wild type *trxR* gene using the primers Spt10R-L1 and Spt10R-R1 (Table 2).

Creation of cured GA40634.*trxR* and NZ131.*trxR*

The strains GA40634.*trxR* and NZ131.*trxR* (Table 1) were cured of the plasmid inactivating *trxR* by passage in liquid culture five times at 30°C and one time at 37°C with no drug selection. PCR was used to screen for the intact *trxR* gene and restoration of correct wild type sequence was verified.

RNA ANALYSIS

RNA extraction and DNase treatment

RNA was isolated using a Triton X-100 method as previously described (245). Briefly, 10 ml of THY broth was inoculated 1:20 from an overnight culture and grown to the appropriate Klett unit. Cells were then pelleted by centrifugation at 9,000 x *g* for 10 minutes at 4°C. Cells were then resuspended in TE buffer containing 0.2% Triton X-100 (v/v) and boiled for 10 minutes. Upon cooling, the lysate was extracted with chloroform-isoamyl alcohol twice and ethanol precipitated at -80°C for 25 minutes. The reaction was then pelleted at 10,000 x *g* for 10 minutes and washed with 1 ml of 70% ethanol. The RNA was finally resuspended in DEPC-treated water and quantified using a spectrophotometer. The RNA was assessed for quality on a formaldehyde gel (18% (v/v) formaldehyde, 1% (w/v) agarose, 72% (v/v) DEPC-treated water, and 10% (v/v) 10x MOPS.

RNA for microarray and real-time RT-PCR analysis was treated with Turbo DNase (Applied Biosystems) to remove genomic DNA (gDNA) from the sample. Briefly, approximately 20 µg of RNA was incubated with DNase and RNase inhibitor at 37°C for 40 minutes according to the manufacturer's instructions followed by one extraction with chloroform:isoamyl-alcohol. A PCR reaction was then performed on 0.5 µl of the DNased RNA to verify complete degradation of the gDNA and a RNA integrity gel was run.

RT-PCR

RNA for RT-PCR was treated with DNase to remove residual gDNA. cDNA was then generated using the SuperScript first-strand synthesis kit for RT-PCR (Invitrogen) according to manufacturer's instructions. Briefly, the DNA-free RNA was denatured at 65ºC for 5 minutes, snap cooled on ice, and incubated with dNTPs and the random hexamer primers for 10 minutes at 25ºC. Reactions with and without (control) reverse transcriptase were then incubated at 50ºC for 50 minutes to allow for cDNA synthesis. The reactions were then heated to 85ºC for 5 minutes, stopping the reaction, and the samples were treated with RNase H for 20 minutes at 37ºC to remove original RNA template. PCR reactions were then performed on the RT+ and RT- cDNA samples, as well as on gDNA, using Taq polymerase. The following primer sets were used to amplify intragenic regions within the *trxTSR* operon: *trxT-trxS* (Spt10PE and Spy1589-R); *trxS-trxR* (*trxS* M1 RT-L and *trxR* M1 RT-R); *trxR-bgaA* (*srxR*-Spy1586 RT-L and *srxR*-Spy1586 RT-R); and *trxS-bgaA* (Spt10R-L1 and Bgal-L).

Microarray

Microarray experiments were performed as previously described (207). Briefly, total RNA from 3 biological replicates was isolated from MGAS5005 containing the empty vector pJRS525 and the isogenic *trxR* mutant strain MGAS5005.*trxR* containing the empty vector pJRS525 at late-logarithmic phase (100 Klett units) using the TritonX-100 isolation protocol. Both strains were grown in the presence of spectinomycin for the overnight seed cultures, but not during growth for RNA isolation. DNase I-treated RNA samples were converted to cDNA with an amino-allyl UTP and were Cy3 and Cy5

labeled using the Amino Allyl cDNA Labeling Kit (Ambion) to allow for dye-swap experiments. Yield and incorporation rate of the labeled cDNA was determined using a Nanodrop ND-1000 (Nanodrop Technologies). Equal volumes (35.42 µl) of labeled Cy5 cDNA and Cy3 cDNA were dried under vacuum, resuspended in 23.8 µl of dH_2O and boiled for 5 minutes followed by cooling on ice for 5 minutes. 5x Hybridization Buffer (17 µl) (GE Healthcare) and formamide (27.2 µl) were added to the cDNA and applied to array slides under raised cover slip (Lifterslip, Inc). Microarray slides were hybridized at 50°C overnight in slide chambers (Array It). Slides were washed twice for 10 minutes each in the following buffer concentrations and temperatures: 6X SSPE/0.01% Tween-20 at 50°C, 0.8X SSPE/0.001% Tween-20 at 50°C, and 0.8X SSPE at RT. Slides were scanned using a Genepix 4100A personal array scanner and GenePixPro 6.0 software (Axon Instruments).

Data obtained from the wild type and *trxR* mutant strains were compared for 2-fold changes in expression, ≥ 2.0 or ≤ 0.50, and was analyzed using Acuity 4.0 software (Axon Instruments). Using a ratio-based normalization, data was normalized by the ratio of the means and samples were removed when 4 out of the 6 experiments did not show significance. Validation of array data was carried out by real-time RT-PCR of 12 differentially regulated genes using primers listed in Table 4. Correlation coefficients for the arrays were determined by plotting the log value of the array on the X-axis to the log value of the real-time RT-PCR on the Y-axis. An equation determining the line of best fit was determined, and the resulting R^2 value was calculated, which represented the fitness of the data.

Table 4. Real-time PCR primers

Target	Primer	Sequence (5'-3')	Reference
arp	*arp* M4 RT-L	TAGCTGTTTCGCCTGTTGAC	This study
	arp M4 RT-L	GCTAAAGTAGCCCCACAAGC	This study
atpB	*atpB* M1 RT-L	AATCTGGCTTTTGACCTTGC	(12)
	atpB M1 RT-R	TAGCCAAACGTTTCAAATGG	(12)
clpL	*clpL* M1 RT-L	TGGCTTGAGCTAAACCTTCA	This study
	clpL M1 RT-R	CTTGGCACGACGAACTAAAA	This study
emm	*emm1* RT-L	ACTCCAGCTGTTGCCATAACAG	(20)
	emm1 RT-R	GAGACAGTTACCATCAACAGGTGAA	(20)
	emm M49 RT-L	GCTTTGCAAACCAAACAGAA	This study
	emm M49 RT-R	CTTGCAACGCTAGACACGTT	This study
fasB	*fasB* M1 RT-L	CTGAGCCGTATAGAGCGTTTAGG	(135)
	fasB M1 RT-R	ACCGTTTGGGCATAAATATCTTG	(135)
fba	*fba* M1 RT-L	GTCTACTGAGTCTACTACTCAGCCAGTTG	(135)
	fba M1 RT-R	CCTGTCACCATCGAATCTGAAG	(135)
gyrA	*gyrA* M1 RT-L	CGACTTGTCTGAACGCCAAAGTC	(20)
	gyrA M1 RT-R	ATCACGTTCCAAACCAGTCAAAC	(20)
lacD.2	*lacD.2* M1 RT-L	GCTGCTTGTGGTCCTTCTTC	(135)
	lacD.2 M1 RT-R	TTGGTGTTTGCAGCAGAATC	(135)
lacE	*lacE* M1 RT-L	GGAGCTGGTGTAGTCCAAGG	(135)
	lacE M1 RT-R	CACCGATTGTCAACGTATGG	(135)
lacF	*lacF* M1 RT-L	TTGTCTGAGCATTGTGA	(135)
	lacF M1 RT-R	GCGCAAGAAGGAGATTATGC	(135)
mga	*mga* M1 RT-L	CGCTGAGTTGAGCCTGATTTC	(135)
	mga M1 RT-R	AGACTCACCAACGGGCTGTC	(135)
	mga M6 RT-R	AACCAACGCCTATTTGACG	(4)
	mga M6 RT-R	CGAATCTGGTGTTCATCTCC	(4)
opuAA	*opuAA* M1 RT-L	TGATTTGCAAGACAGCATGA	This study
	opuAA M1 RT-R	CATCAAAGCAATCCGATCAC	This study
sclA	*sclA* M1 RT-L	TGCTGACAAAGAAGCTAACCAAAC	(20)
	sclA M1 RT-R	CGTCTGTGGTTGTTGGCTACAG	(20)
scpA	*scpA* M1 RT-L	TTTCGACACGCATCAAAAGC	This study
	scpA M1 RT-R	TGCTCCATCTGAAACGAAAGAAC	This study
sic	*sic* M1 RT-L	GGTAAAGTAGGCGGACATGCC	(20)
	sic M1 RT-R	CCTCGTGTGCCAGAAAAACC	(20)
slo	*slo* M1 RT-L	AAAACAAACCAGACGCGGTAGT	(12)
	slo M1 RT-R	TTGTCTCCCATACCTGGTAAATCA	(12)
trxR	*srxR* M1 RT-L1	CTCAATTCATCTGTAAGCCAAAGG	This study
	srxR M1 RT-R1	GATGCCCAGCAGGCAGAA	This study
	trxR M1 RT-L3	GCTTTACACCAACCAATCCA	This study
	trxR M1 RT-R3	TTTGGCGATAAACCATTCAA	This study
trxS	*trxS* M1 RT-L	AGATCGGGCAGCTGATCTTA	This study
	trxS M1 RT-R	TGACAGCCACATAAGCCAAG	This study
trxT	*Spy1307* M1 RT-L4	TGAAAAGGGCTGTTCAACTTT	This study
	Spy1307 M1 RT-R4	AAGGAAAGTCAGGGCAAAAA	This study

Real-time RT-PCR

Briefly, 25 ng of DNase I treated total RNA was added to Sybr Green Master Mix (Applied Biosystems) containing 5 µg of each specific real-time primer (Table 4) and combined with 5.75 units of MultiScribe reverse transcriptase (Applied Biosystems) in a 25 µl volume for one-step, real-time RT-PCR. The reactions were run on a Lightcycler 480 (Roche) to detect transcript levels in the relative quantification mode with reaction conditions of 48°C for 30 minutes, 95°C for 10 minutes, and 40 cycles of 95°C for 15 seconds followed by 60°C for 1 minute. Transcript levels presented represent ratios of wild type/experimental relative to the level of *gyrA* transcript. All primers used in real-time RT-PCR were designed using Primer 3: WWW Primer tool (biotools.umassmed.edu/bioapps/primer3_www.cgi).

5' RACE

To identify the promoter upstream of *trxT*, the 5'/3' Race Kit (Roche, 2nd generation) was used following the manufacturer's protocol. Briefly, for 1st strand cDNA synthesis, 2 µg of DNase-treated MGAS5005 total RNA was incubated with buffer, primer Spy1307 SP1, the deoxynucleotide mixture, and Transcriptor Reverse Transcriptase (RT) for 60 minutes at 55°C and then for 5 minutes at 85°C to heat-inactivate the RT. The resulting cDNA was purified using Qiagen's QIAquick PCR purification kit. The addition of a homopolymeric A-tail (dA) to the first-strand cDNA was accomplished through the addition of 2 mM ATP to the purified cDNA sample. This was incubated for 3 minutes at 94°C, and then Terminal Transferase was added to the reaction and it was incubated at 37°C for 20 minutes. The Terminal Transferase was then

heat-inactivated at 70°C for 10 minutes. PCR amplification of the dA-tailed cDNA was achieved by a 2-step reaction procedure. The first PCR reaction included a primer specific to the dA-tail accompanied by a primer for *trxT* (SP2, SP4, or SP6) to amplify the entire piece of cDNA. A second nested PCR reaction was then used to obtain a more specific region within the *trxT* gene using primer Spy1307 SP3, SP5, or SP7. The resulting dsDNA was purified using the QIAquick kit (Qiagen) and sequenced to identify the transcriptional start of *trxT*.

PROTEIN ANALYSIS

Protein expression and purification

GAS His-MBP-TrxR was purified consecutively over amylose and Ni-NTA resins based upon manufacturer's protocols. Briefly, cells were grown in ZYP-5052 auto-induction media for 20 hours at 30°C and the resulting cell pellets stored at -80°C. The frozen pellets were lysed in the presence of 1 mg/ml lysozyme and 1x Complete Protease Inhibitor (Roche) using a Branson sonicator (6 cycles of 45 second pulses at 50% duty cycle, output of 7.5). His-MBP-TrxR was purified from the resulting lysate over the amylose resin under native conditions and directly applied to the Ni-NTA resin. Chosen fractions were then dialyzed into 50 mM Tris-HCl, pH 7.5 overnight and glycerol was added to 10% prior to storage at -80°C. A similar expression and purification scheme was followed for the His-MBP-TrxR D55A and His-MBP-TrxR D55E mutants.

The signaling domain of GAS TrxS tagged with His-MBP was purified consecutively over amylose and Ni-NTA resins based upon manufacturer's protocols. Briefly, cells were grown in ZYP-5052 auto-induction media for 24 hours at 30°C and the resulting cell pellets stored at -80°C. The frozen pellets were lysed in the presence of 1 mg/ml lysozyme and 1x Complete Protease Inhibitor (Roche) using a Branson sonicator (6 cycles of 45 sec pulses at 50% duty cycle, output of 7.5). His-MBP-TrxS was purified from the resulting lysate over the amylose resin under native conditions and directly applied to the Ni-NTA resin. Chosen fractions were then stored as aliquots at -80°C. A similar method was used for purification of His-MBP-TrxS H383A.

GAS protein extracts

Soluble GAS protein extractions were performed using a PlyC (courtesy of Daniel Nelson, IBBR) extraction method. Briefly, GAS cells were inoculated 1:20 into 10 ml THY broth, grown to the appropriate Klett unit, and pelleted by centrifugation for 10 minutes at 8,500 x *g*. Pellets were resuspended in 190 µl TN buffer (10 mM Tris-HCl, pH 8.0, 150 mM NaCl), and 10 µl DNase and 7 µl PlyC were added. The cells were inverted 5-6 times and placed on ice for 20 minutes, followed by centrifugation at 13,000 x *g* for 20 minutes. Supernatants containing the soluble proteins were extracted and protein concentration was assayed using the Bio-Rad protein assay kit, reading the absorbance at 595 nm on a spectrophotometer.

SDS-PAGE gel analysis

SDS-polyacrylamide gels (SDS-PAGE) were made as follows: a 10% resolving gel was mixed and poured followed by a 6% stacking gel using the reagents found in Table 5. Protein samples were mixed with 5x cracking buffer, boiled at 99°C, and loaded into the wells. SDS-PAGE gels were run at 180V for 50 minutes.

Table 5. SDS-PAGE buffer

10- 15% Resolving gel	**6% Stacking gel**
26% (v/v) Lower gel stock 25-37.5% (v/v) 40% Acrylamide/ bis solution 0.5% (v/v) 10% ammonium persulfate 0.1% (v/v) tetramehylethylene diamine Brought up with H_2O	25% (v/v) Upper gel stock 15% (v/v) 40% Acrylamide/ bis solution 0.5% (v/v) 10% ammonium persulfate 0.1% (v/v) tetramehylethylene diamine Brought up with H_2O

Lower gel stock	**Upper gel stock**
1.5M Tris-HCl pH 8.8 0.4% (w/v) SDS Brought up with H_2O	0.5M Tris-HCl pH 8.8 0.4% (w/v) SDS Brought up with H_2O
SDS running buffer	**Coomassie blue stain**
25mM Tris 190mM Glycine 0.1% (w/v) SDS Brought up with H_2O	0.25% (w/v) coomassie blue 45.4% (v/v) methanol 9.2% (v/v) glacial acetic acid Brought up with H_2O

Destain solution	**Gel drying solution**
5% (v/v) methanol 7.5% (v/v) glacial acetic acid Brought up with H_2O	3% (v/v) glycerol 20% (v/v) EtOH Brought up with H_2O

5x Cracking buffer	**Transfer buffer**
0.3M Tris pH 6.8 25% (v/v) 2-mercaptoethanol 51% (v/v) glycerol 10% (w/v) SDS 0.01% (w/v) bromophenol blue Brought up with H_2O Heated at 55ºC	25mM Tris base 0.2M glycine Brought up with 20% methanol
	PBS-Tween
	0.01M PBS pH 7.4 0.5% Tween-20 Brought up with H_2O

Western Blot

Selected protein samples were run on a 10% SDS-PAGE gel with 6% stacking gel for approximately 50 minutes at 180V. The gels were then transferred to nitrocellulose membranes using the Mini-Protean apparatus (Bio-Rad) in 1x transfer buffer (25 mM Tris base, 0.2 M glycine, brought up with 20% methanol). Membranes were blocked overnight at 4°C in blocking solution (5% (w/v) dried milk in PBS-tween). For detection of His-tagged proteins, blots were incubated with a 1:1,000 dilution α-His antibody (Novagen) for two hours, followed by a 10 minute wash in PBS-tween. For detection of TrxS, blots were incubated with a 1:500 dilution α-TrxS polyclonal antibody, followed by the same 10 minute wash. For detection of HSP-60, blots were incubated with a 1:2,500 dilution α-HSP-60 antibody (Stressgen) for two hours, followed by the same 10 minute wash. Blots were then incubated with a 1:20,000 α-mouse-HRP antibody (His-tagged proteins, HSP-60) or 1:20,000 α-rabbit-HRP antibody (TrxS) for one hour, washed 3 times in PBS-tween for 20 minutes, and visualized using SuperSignal West Femto Substrate (Thermo Scientific) and a LAS-3000 CCD camera (FujiFilm).

Co-immunoprecipitation assay

A mouse α-His monoclonal antibody (Roche) was used to precipitate His-MBP-tagged TrxR in GAS lysates. MGAS5005.*trxR* strains were grown in THY under spectinomycin selection to late-logarithmic phase (~ Klett 105). Cells were pelleted and lysed with the cell wall hydrolase PlyC (courtesy of Daniel Nelson, IBBR) (179), to release the soluble proteins, along with 2 units DNase I. The collected lysate fractions

were diluted 1:1 in complete PBS buffer (pH 7.3, supplemented by protease inhibitors) and incubated with constant rocking at 4°C for 15 minutes with Protein A agarose slurry (Calbiochem), 50% equilibrated in 0.5% BSA (Sigma) in dH_20. The samples were centrifuged for 1 minute to pull down non-specific proteins bound to the agarose beads. The supernatant was transferred to fresh tubes containing the α-His antibody, and incubated at 4°C for 2 hours with rocking. Protein A agarose slurry was added to the samples after the first hour of incubation to bind the protein-antibody complex to the beads. After pelleting the beads, the supernatant was removed and the slurry was washed in the PBS buffer. The samples were then heat denatured at 99°C for 10 minutes to dissociate the proteins bound to the beads. The samples were then pelleted once again, collecting the supernatant samples.

Bacterial two-hybrid assay

The selected plasmids for analysis were co-transformed (1 µl each) into BTH101, electroporated, and outgrown for 1 hour at 37°C. The bacteria were plated on MacConkey agar supplemented with 1% maltose and placed at 30°C overnight. Following overnight incubation, colonies were patched onto a fresh MacConkey-maltose plate and placed at 30°C overnight.

TrxS-TrxR *in vitro* phosphorelay

To produce phosphorylated TrxS for transfer to TrxR (TrxS~P), a 50 µl reaction was prepared (50 mM Tris, pH 7.5, 10 mM $MgCl_2$, 50 mM KCl, 1 mM dithiothreitol,

10% glycerol, 63.4 μM TrxS or TrxS:H383A). 20 μCi of [γ-^{32}P]ATP (Perkin Elmer) was added to both labeling reactions, and samples were incubated at room temperature. At 15, 30, 45, and/or 60 minutes after the addition of radiolabeled ATP, 5 μl samples were removed and mixed with 2X SDS loading buffer. At 60 minutes, TrxR was added to TrxS at a concentration of 534 μM. 5 μl samples were taken 0, 0.5, 1, 5, and 10 minutes after the addition of TrxR to TrxS, and 1, 5, and 10 minutes after the addition of TrxR to TrxS:H383A.

To produce phosphorylated TrxS for transfer to TrxR/TrxR:D55A, a 50 μl reaction was prepared containing 67 μM TrxS. TrxR and TrxR:D55A were added to the appropriate reactions at a concentration of 674 μM. 5 μl samples were taken 1, 5, 10, or 20 minutes after the addition of TrxR:D55A to TrxS.

Samples were loaded onto 10% polyacrylamide gels, run at 4°C, and after SDS-PAGE, gels were dried for 30 minutes under no heat and scanned using a FujiFilm FLA7000. The resulting data was analyzed with Multigauge analysis software (FujiFilm, version 3.0).

Electrophoretic mobility shift assay (EMSA)

Promoter probes were generated by PCR amplification with Phusion HF DNA polymerase using MGAS5005 gDNA and the relevant primer pairs (P*mga,* P*emm*) listed in Table 2. PCR fragments were end-labeled with [γ^{32}P]-ATP and purified over a spin-column (Harvard Apparatus) to remove unbound [γ^{32}P]-ATP.

Mobility shift assays were performed with a total volume of 50 μl. Each reaction included 5x binding buffer (100 mM Tris, pH 7.5, 5 mM $CaCl_2$, 5 mM dithiothreitol, 50

µg/ml poly(dI-dC), and 200 µg/ml BSA), a constant amount of labeled promoter probe (2-4 ng), and various concentrations of purified His-MBP-TrxR proteins. DNA and proteins were incubated at either 16°C or 25°C for 20 minutes, after which 10 µl of ficoll loading buffer (1% v/v ficoll and 0.02% w/v bromophenol blue) and 2 µl of 80% glycerol were added, mixed, and immediately loaded onto a 5% polyacrylamide gel at 4°C or 25°C, and run at 180 V. Competition experiments were performed by inclusion of cold probes prior to protein addition. Gels were dried under vacuum at 80°C for 1 hour and exposed overnight to a phosphoimaging screen. Images were scanned using a FujiFilm FLA7000 and the resulting data was analyzed with Multigauge analysis software (version 3.0).

TRANSCRIPTIONAL REPORTER ASSAY

Luciferase Assay

For strains containing the P*mga-luc* construct, luciferase assays were performed as follows: MGAS5005 (WT), MGAS5005.*trxR* (*trxR* mutant), and KSM165-L.5005 (*mga* mutant) transformed with pKSM721 were grown static in 12.5 ml THY medium under spectinomycin selection at 37ºC. Upon reaching Klett 30, 500 µl samples were taken every 30 minutes across growth, encompassing early-logarithmic phase to early stationary phase. The samples were centrifuged and pellets were placed at -20ºC overnight. The luciferase assay was performed using the Luciferase Assay system (Promega). Pellets were resuspended in various amounts of 1x Lysis buffer to normalize

for cell unit according to the equation 4.5= (x ml)((Klett 65)/2). The luciferase assay was read using a Centro XS^3 LB 960 luminometer (Berthold Technologies) where 50 µl of Luciferin-D reagent was directly injected.

For strains containing P*trxT-luc* constructs pKSM637 or pKSM670, luciferase assays were performed as follows: MGAS5005 (WT) and 5448-AN (WT) transformed with either pKSM637 or pKSM670 were grown static in 12.5 ml THY media or C media supplemented with 150 mM NaCl and buffered to 7.5 under spectinomycin selection at 37ºC. Samples were collected every 40 minutes across growth and analyzed in the same manner as the P*mga* luciferase assays.

CHAPTER FOUR:

Characterization of the *trxTSR* operon and its role in the activation of the Mga virulence regulon

INTRODUCTION

TCSs are often used by bacterial pathogens to adapt to changing host conditions during the course of infection and to alter their gene expression profiles. Numerous studies have elucidated the importance of various GAS TCSs. Several of these TCSs have been linked to GAS pathogenesis and virulence gene regulation. Most notably, the CovRS TCS functions as a repressor of many known and putative virulence factors (69, 81). In addition, the Ihk/Irr TCS plays an important role in both detection by, and GAS evasion of, the innate immune system (267). The FasBCAX system controls genes encoding several GAS adhesins and secreted aggressins in a growth-phase dependent manner (124). Lastly, the SptRS TCS has been shown to regulate multiple genes encoding proteins involved in acquisition and processing of complex carbohydrates in human saliva (222).

More recently, mutations in the remaining GAS TCSs were constructed to determine whether they played an important role during infection (206). One of these TCS response regulator mutants, *trxR*, was chosen for further investigation because of its homology to virulence-related TCSs of other Gram-positive pathogens, HK/RR07 of *S. pneumoniae* and HK/RR01 of *E. faecalis*. In addition, the TrxSR TCS has been shown to be repressed by CovRS in two different GAS serotypes (57, 81), providing additional support for further analysis of TrxSR. Using a *trxR* mutant in the M1T1 MGAS5005

strain, a preliminary study using a murine model of GAS soft tissue infection was undertaken. Mice infected with the *trxR* mutant exhibited significantly reduced lesion sizes compared to those infected with wild type MGAS5005 at 48 hours post infection (Fig 4A) (135). Additionally, mice infected with the *trxR* mutant showed a significant increase in survival across a 7-day period compared to those mice infected with the parental wild type strain (Fig 4B) (135).

Given that inactivation of *trxR* leads to attenuation of virulence in a subcutaneous model of GAS soft tissue infection, assessed by both lesion progression and lethality (Fig 4), it was hypothesized that TrxSR positively regulates virulence in the M1 MGAS5005 serotype. In the present study, TrxR is shown to be a conserved activator of the Mga virulence regulon. Based upon the results presented here, in addition to previously published data (135), TrxSR represents a newly identified regulatory pathway employed by GAS for regulation of its virulence genes. Additionally, it adds to the growing virulence regulatory network, which along with other TCSs and stand-alone regulators, help to influence disease progression.

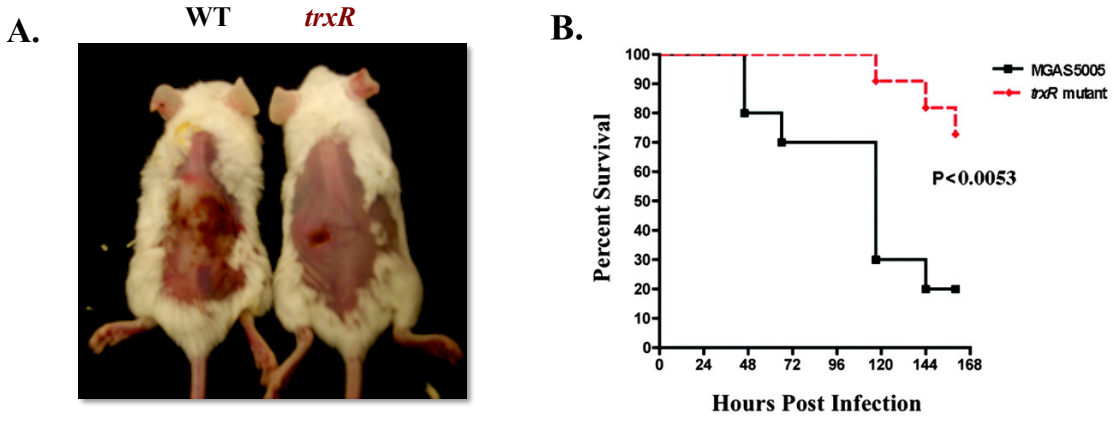

FIGURE 4. ***trxR* mutant in a murine model of streptococcal soft tissue infection.** *A,* Photograph of representative mice infected with WT MGAS5005 (left) or the *trxR* mutant (right) forty-eight hours post infection. *B,* Survival plot comparing mice infected with MGAS5005 (n = 10) or the *trxR* mutant (n = 11) over a 7-day period. A Kaplan-Meier survival analysis and log rank test was used to determine significance.

RESULTS

Genetic organization of the *trxSR* locus

The M5005_*Spy_1307* (*trxT*), *trxS, trxR* and *bgaA* genes are unidirectionally transcribed and the individual open reading frames are separated by no more than 3 bp (Fig 5A). This arrangement suggests that these genes may form a typical prokaryotic operon. Interestingly, both *trxT* and its location next to a TrxSR-like TCS are very well conserved within other Gram-positive pathogenic bacteria (Fig 5B).

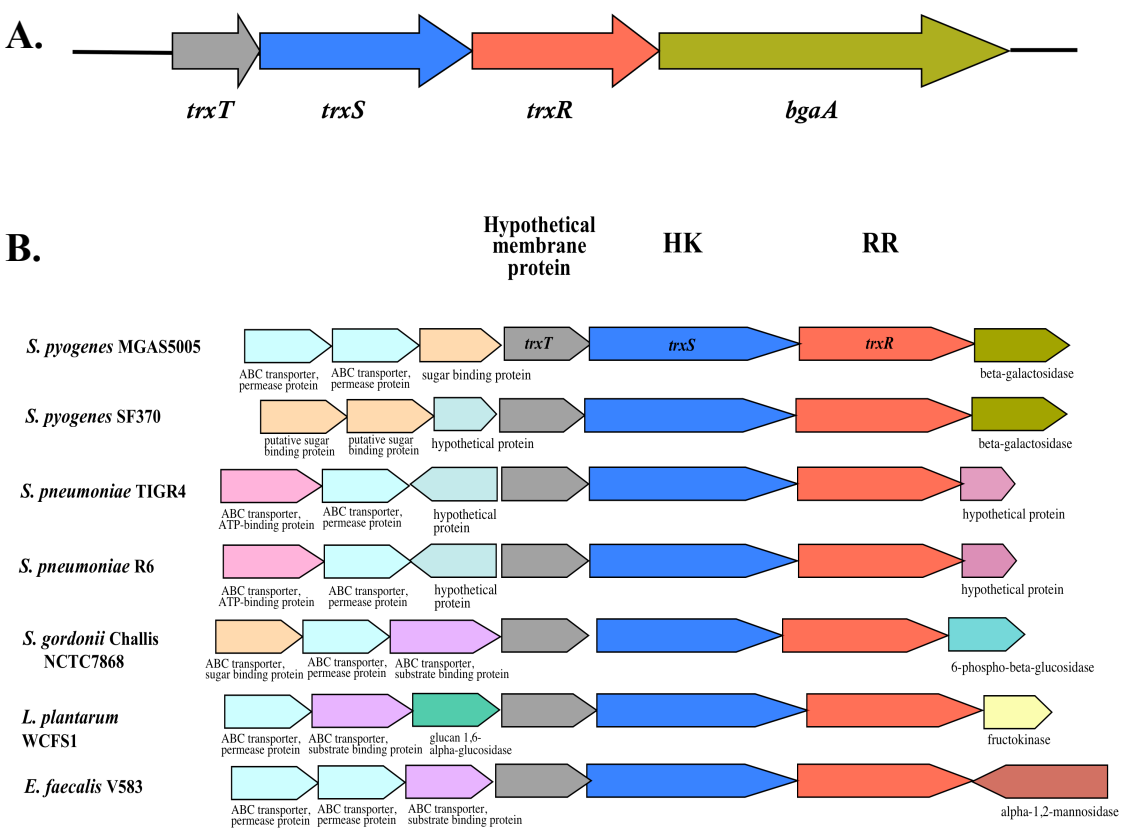

FIGURE 5. **The *trxSR* genomic region**. *A,* operon structure of the *trxSR* region. *B,* alignments of Gram-positive bacteria genome regions containing homology to *trxT, trxS,* and *trxR* genomic region from *S. pyogenes* MGAS5005.

To determine the promoter of the operon, 5' RACE was employed. Initial experiments using a nested primer within *trxT* revealed transcripts that ended around 35-45 bp upstream of the start of TrxT translation (Fig 6A, green line), however, there were no defined sequences that matched a consensus -35 and -10 of *E. coli*. Upon further examination, it appeared that there could be potential secondary structure present with the 5' UTR and this could explain why initial attempts at 5' RACE were identifying this region (Fig 6A, yellow). To determine whether there was a different 5' end to the transcript, a second nested primer was designed to lie directly upstream of the previously

defined region, 35-45 bp upstream of the start of TrxT translation. After sequencing numerous transcripts, it was determined that there was in fact a 5' end that continuously was identified and was located 132 bp upstream of the start of transcription of *trxT*. Additionally, putative sequences that resembled a consensus -35 and -10 of *E. coli* were present, suggesting that this was indeed the true transcriptional start of *trxT* (Fig 6A, pink line).

To learn about transcriptional linkage of these genes, primer pairs were used to amplify their intragenic regions through RT-PCR (Fig 6B). RT-PCR analysis of cDNA clearly demonstrated that some transcripts include *trxT, trxS, and trxR* (Fig 6C). Although a transcript that contains *trxR* and *bgaA* could be detected by RT-PCR, we could not detect a transcript containing *trxS*, *trxR* and *bgaA*. Furthermore, it appears that *bgaA* can be transcribed independently of *trxR* in M1 strain MGAS5005, as a *trxR* mutation did not confer a polar effect on *bgaA* transcription (Table 6). Thus, the operon appears to be composed of *trxT*, *trxS,* and *trxR*.

Expression from P*trxT* varies across growth

In order to assess transcriptional activation of P*trxT* across growth, P*trxT* was fused to the firefly luciferase reporter gene to generate plasmid pKSM637. This plasmid was initially introduced into M1 MGAS5005 and was grown in THY, with samples taken every 40 minutes across growth to assess luciferase activity (Fig 7A). Unfortunately, expressing P*trxT-luc* in MGAS5005 resulted in low levels of relative luciferase units that were equivalent to background (50-70 RLU), making this strain not ideal to use. Therefore, the plasmid was introduced into other M1 strains, SF370 and 5448-AN, to

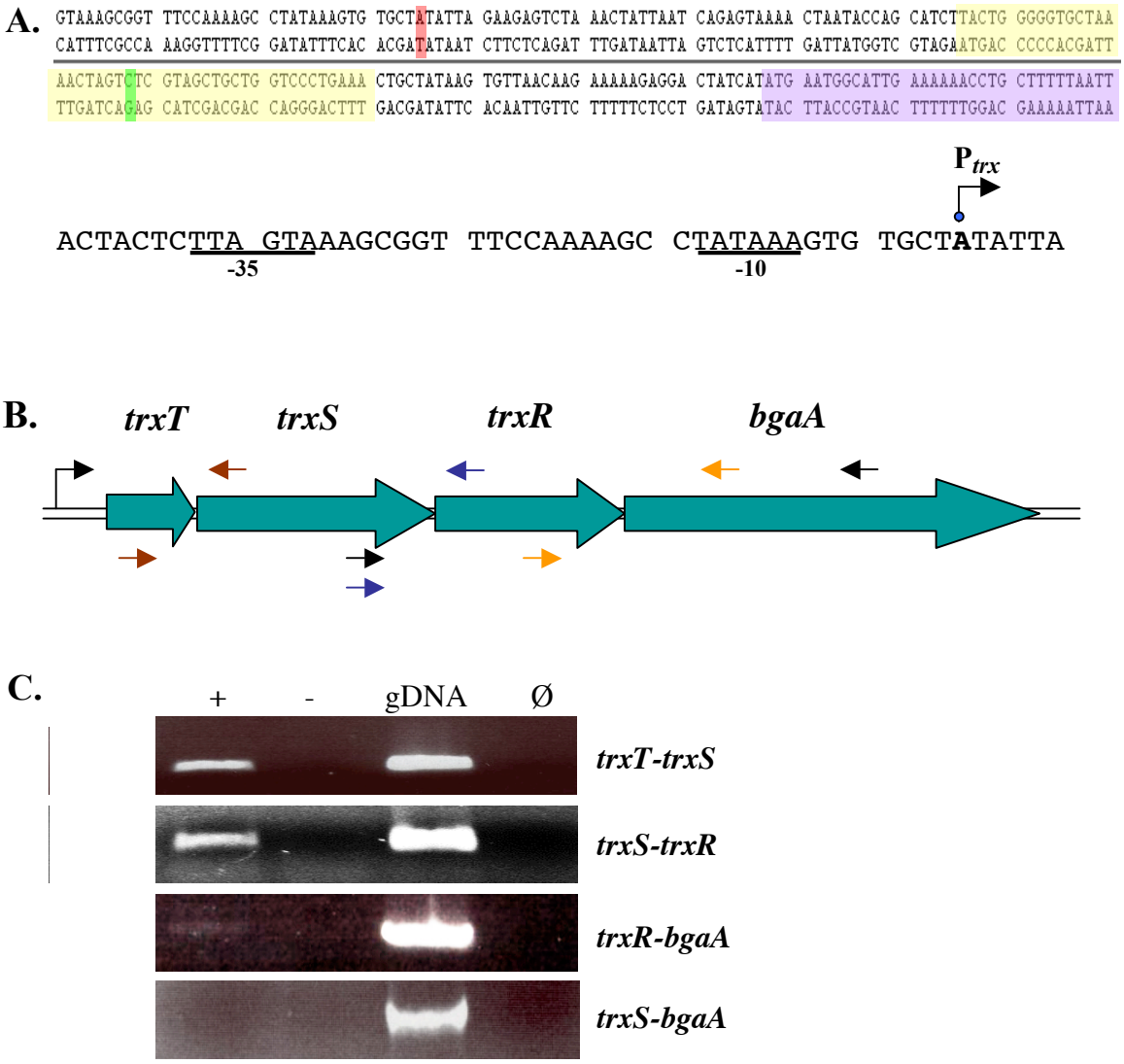

FIGURE 6. **The *trxSR* operon.** *A*, Above, 5' UTR sequence of *trxT*. Shown are the transcriptional start (pink), region of predicted secondary structure (yellow), transcriptional start found from initial 5' RACE (green), and part of the TrxT coding sequence (purple). Below, promoter region of *trxT* with putative -10 and -35 sequences (solid bars) and start of transcription (black arrow) indicated. *B,* Schematic of *trxSR* genomic region in M1 MGAS5005 including putative open reading frames and primer locations used in RT-PCR (B). *C,* Reverse transcriptase PCR reactions for regions indicated in A: red- *trxT-trxS*, blue- *trxS-trxR*, yellow- *trxR-bgaA*, black- *trxS-bgaA*. Shown are reactions with RT (+), without RT (-), a genomic DNA positive control (gDNA), and a no DNA negative control (Ø).

determine if luciferase activity could be monitored within these backgrounds. As luciferase activity appeared to be highest in the 5448-AN, this strain was chosen for further experiments. In addition to growing the strain in THY, the strain was also grown in low glucose C media supplemented with 150 mM NaCl and buffered to a pH of 7.5, as *trxT* has previously been reported to be up-regulated in C media containing 150 mM NaCl (144).

In accordance with this published result, greater expression (~ 4-5 fold increase) was seen in the 5448-AN strain grown in the C media containing 150 mM NaCl and buffered to pH 7.5 than in the THY media alone. This was also seen in MGAS5005 but not to the same RLU levels (Fig 7B, data not shown). Additionally, we compared the wild type P*trxT-luc* construct with a truncated P*trxT* fused to luciferase, to delete the predicted secondary structure in the 5' UTR of the promoter region. Although there appears to be a difference in relative luciferase units between the two constructs, it did not reach statistical difference compared to luciferase produced from the wild type P*trxT-luc* and truncated P*trxT-luc* plasmids in 5448-AN (Fig 7C, data not shown). As expected, expression from P*trxT* was higher at the end of exponential growth at the point of transition from exponential to stationary phases of growth. Moreover, there was a second peak of P*trxT* expression around 90 minutes into stationary phase (Fig 7B), which may represent a second point within growth that TrxSR is expressed within the cell. Thus, this data shows the transcriptional pattern for P*trxT* and suggests that transcriptional activation of P*trxT* is tightly regulated within the cell.

A.

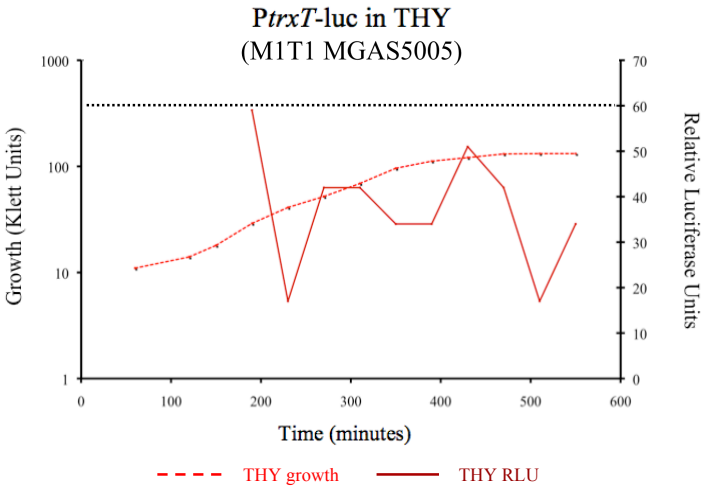
PtrxT-luc in THY
(M1T1 MGAS5005)
Growth (Klett Units)
Relative Luciferase Units
Time (minutes)
THY growth
THY RLU

B.

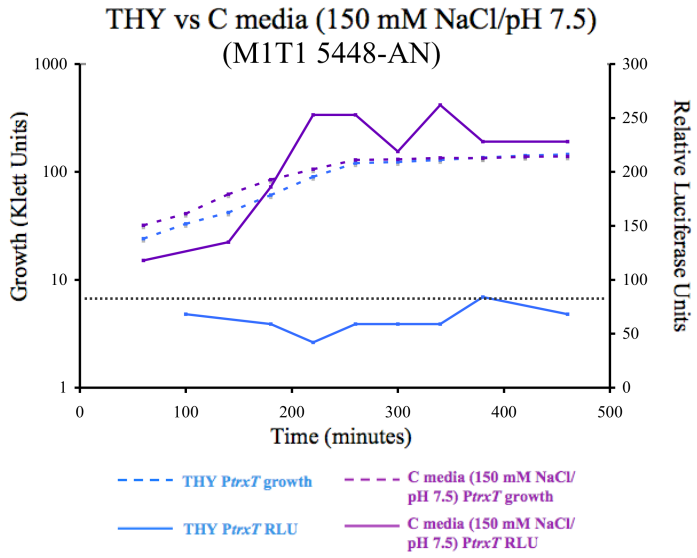
THY vs C media (150 mM NaCl/pH 7.5)
(M1T1 5448-AN)
Growth (Klett Units)
Relative Luciferase Units
Time (minutes)
THY PtrxT growth
C media (150 mM NaCl/ pH 7.5) PtrxT growth
THY PtrxT RLU
C media (150 mM NaCl/ pH 7.5) PtrxT RLU

C.

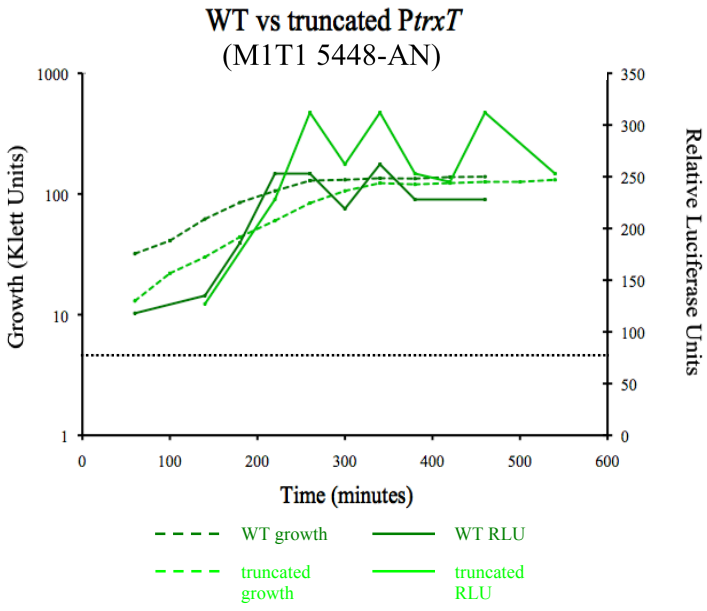
WT vs truncated PtrxT
(M1T1 5448-AN)
Growth (Klett Units)
Relative Luciferase Units
Time (minutes)
WT growth
WT RLU
truncated growth
truncated RLU

FIGURE 7. **P*trxT* expression across growth.** *A,* The growth curve for WT P*trxT-luc* in MGAS5005 grown in THY is shown in Klett Units by a dashed line. The relative luciferase units are shown in a solid bold line. Samples were taken every 40 minutes beginning around Klett 20 and continuing through stationary phase. *B,* The growth curve for WT P*trxT-luc* in 5448-AN grown in THY or C media supplemented with 150 mM NaCl/buffered to pH 7.5 are shown in Klett Units with dashed lines. The relative luciferase unit profiles for each are shown in solid bold lines. *C*, The growth curve for WT P*trxT-luc* or truncated *PtrxT-luc* in 5448-AN grown in C media supplemented with 150 mM NaCl/buffered to pH 7.5 are shown in Klett Units with dashed lines. The relative luciferase unit profiles for each are shown in solid bold lines. For *B* and *C*, samples were taken every 40 minutes beginning around Klett 35 and continuing through stationary phase. Dashed black lines represent background levels of relative luciferase units taken from luciferase resuspension buffer alone. For all graphs, data is representative of three independent experiments.

Definition of the TrxR regulon in GAS

To identify the genes that TrxR regulates, a transcriptome analysis of a MGAS5005.*trxR* mutant was completed. For the global transcriptional profile, the wild type MGAS5005 was compared to the MGAS5005.*trxR* mutant grown to late-logarithmic phase in THY media, a point in growth at which TrxR-mediated regulation would expected to be the strongest based upon the level of *trxR* transcript (Fig 7B). A decrease (TrxR activation) or increase (TrxR repression) in transcript levels in the mutant with a change of twofold or greater was considered significant. A relatively small number of transcripts (29 in total) were affected at late logarithmic phase by inactivation of *trxR* (Table 6, top). Transcripts that were significantly reduced in the mutant (8 in total), suggesting that they are TrxR activated, represent the known members of the core Mga virulence regulon (207). These included *emm* (37-fold), *sic* (26-fold), *fba* (9.3-fold), *scpA* (6.8-fold), *sclA* (4.7-fold), and *grm* (2.9-fold). Although the effect on *mga* itself (1.9-fold) did not reach our 2x threshold of significance, this might be due to low-steady

state levels of the *mga* transcript produced in GAS at late-logarithmic phase. Additionally, when P*mga* was fused to the firefly *luc* gene, there was a significant decrease in luciferase activity at this time point in growth (Chapter 5, Fig 15), confirming low steady-state levels of the *mga* transcript at late-logarithmic phase. There was no evidence from the array analysis that TrxR regulated its own expression in the experimental conditions that we tested.

In addition to activating the virulence genes mentioned above, TrxR also represses transcription of genes in GAS. There were 21 transcripts that showed a significant increase in the mutant, suggesting these genes are repressed by TrxR, either in a direct or indirect manner (Table 6, bottom). The TrxR-repressed genes encode proteins involved in various processes including general metabolism, such as amino acid biosynthesis (*aro)* and DNA replication (*polA)*, as well as in different types of stress response (*dnaI, clpL*, and the transport of the osmo-protectant glycine-betaine *opu*). Thus, TrxR appears to activate the Mga regulon as well as repress other apparently unrelated genes.

Table 6. MGAS5005.*trxR* vs. MGAS5005 Microarray and Real-time RT PCR validation

5005_ Spy#	Annotation (TIGR or NCBI)	Gene	Array Mean ± SD [a]	RT Mean ± SE
Spy2018	M1 protein precursor	*emm1*	**0.027** ± 0.186	**0.013** ± 0.003
Spy2016	Sic1.225	*sic*	**0.038** ± 0.239	**0.025** ± 0.005
Spy2009	Fibronectin- and factor H-binding protein	*fba*	**0.103** ± 0.257	**nt**
	P*scpA* 5' probe		**0.108** ± 0.262	**nt**
Spy2010	c5a peptidase precursor	*scpA*	**0.148** ± 0.233	**nt**
Spy1983	Collagen-like protein Scl1, SclA	*sclA*	**0.215** ± 0.379	**0.190** ± 0.015
Spy0430	Hypothetical protein		**0.224** ± 0.286	**nt**
Spy2036	Gene regulated by Mga	*grm*	**0.347** ± 0.437	**nt**
Spy2019	Trans-acting positive regulator of M protein	*mga*	**0.540** ± 0.275	**0.590** ± 0.077
Spy1586	Beta-galactosidase	*bgaA*	**0.926** ± 0.319	**8.610** ± 2.140
Spy0167	Streptolysin O precursor	*slo*	**1.004** ± 0.189	**0.587** ± 0.092
Spy0242	Two-component histidine kinase; TCS1S	*fasB*	**1.020** ± 0.176	**1.457** ± 0.183
Spy0755	ATP synthase subunit 6	*atpB*	**1.222** ± 0.231	**2.333** ± 0.207
Spy1919	Tagatose 1,6-diphosphate aldolase	*lacD.2*	**1.953** ± 0.254	**1.105** ± 0.295
Spy1918	PTS system, cellobiose-specific IIA component	*lacF*	**1.972** ± 0.247	**6.733** ± 0.653
Spy1719	Ribosome-binding factor A, putative	*rbfA*	**2.020** ± 0.321	**nt**
Spy1724	N utilization substance protein A	*nusA*	**2.020** ± 0.245	**nt**
Spy1577	3-dehydroquinate synthase	*aroB*	**2.030** ± 0.267	**nt**
Spy1805	Preprotein translocase, SecA subunit	*secA*	**2.069** ± 0.212	**nt**
Spy1759	DnaJ protein	*dnaJ*	**2.086** ± 0.263	**nt**
Spy0921	tRNA delta(2)-isopentenylpyrophosphate transferase	*miaA*	**2.145** ± 0.248	**nt**
Spy1399	Glucosamine-6-phosphate isomerase	*nagB*	**2.235** ± 0.319	**nt**
Spy1725	Unknown conserved protein		**2.249** ± 0.344	**nt**
Spy0726	CbbY family protein, putative		**2.260** ± 0.199	**nt**
Spy0806	Ribosomal protein L20	*rplT*	**2.283** ± 0.360	**nt**
Spy0185	DNA polymerase I	*polA*	**2.314** ± 0.228	**nt**
Spy1917	PTS system, cellobiose-specific IIC component	*lacE*	**2.316** ± 0.299	**1.700** ± 0.270
Spy1196	integrase/recombinase XerC, putative	*xerC*	**2.353** ± 0.382	**nt**
Spy0808	conserved hypothetical protein		**2.430** ± 0.262	**nt**
Spy1995	FlaR	*flaR*	**2.458** ± 0.247	**nt**
Spy0809	3-dehydroquinate dehydratase, type I	*aroD*	**2.519** ± 0.265	**nt**
Spy1277	phnA protein	*phnA*	**2.642** ± 0.405	**nt**
Spy2066	Conserved hypothetical protein		**2.735** ± 0.303	**nt**
Spy0888	ClpE	*clpL*	**3.044** ± 0.173	**nt**
Spy0183	Glycine betaine transport ATP-binding protein	*opuAA*	**3.047** ± 0.337	**nt**
Spy0184	Glycine betaine-binding protein/ transport system	*opuABc*	**3.209** ± 0.343	**nt**

Data are sorted by Array mean value and shading indicates TrxR regulation; activation (Top), repression (Bottom); unshaded indicates neutral (Middle).

The microarray analysis was validated by real-time RT-PCR on 12 differentially regulated genes (Table 6), resulting in a strong correlation with an R^2 value of 0.892 (Fig 8).

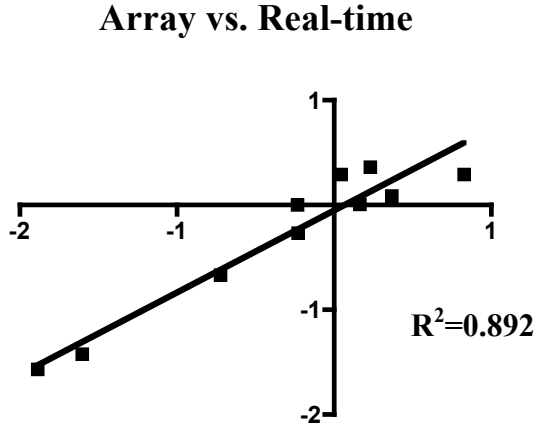

FIGURE 8. **Validation of microarray studies.** The log of the mean value for both WT vs. *trxR*$^-$ microarray and real-time RT-PCR data was plotted. A line of linear regression was calculated to determine the correlation coefficient.

Complementation with *trxR* on a plasmid restores expression of the Mga regulon

To assess the role of *trxR* in the reduced expression of the Mga-regulated genes, a complementation assay was performed. The wild type *trxR* gene was cloned under the control of the constitutive GAS *rpsL* promoter (P*rpsL*) on the multi-copy, replicating plasmid pKSM612. Real-time RT-PCR was performed on total RNA isolated at late-exponential phase from MGAS5005 with an empty vector and compared to the MGAS5005.*trxR* mutant containing either an empty vector or the complementing pKSM612 plasmid. The level of *trxR* transcript was significantly higher in the complemented strain (MGAS5005.*trxR*/pKSM612) than in the wild type MGAS5005 (Fig 9), suggesting that multiple copies of P*rpsL* are likely to be stronger than a single

copy of the *trxR* promoter. For each Mga-regulated gene tested, the complementing plasmid restored the transcript level of the *trxR* mutant to wild type levels (*emm, sic, fba, scpA,* and *sclA*) (Fig 9). This demonstrates that *trxR* alone is capable of complementing the defect in Mga regulon expression caused by inactivation of *trxR* in MGAS5005.

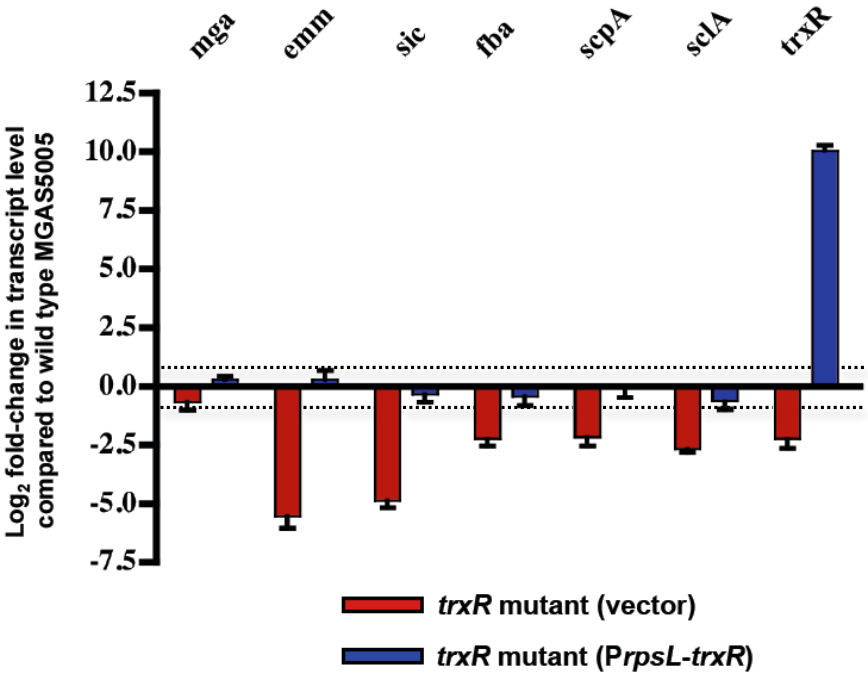

FIGURE 9. **Complementation with *trxR* restores expression of the Mga regulon.** A complementation assay on RNA used in the MGAS5005.*trxR* microarray was performed, on Mga-regulated genes activated by TrxR in the microarray (*mga, emm, sic, fba, scpA,* and *sclA)*. Gene transcript levels were measured by real-time RT-PCR at late-logarithmic growth phase in MGAS5005.*trxR* mutant containing empty vector and MGAS5005.*trxR* containing the P*rpsL-trxR* complementing plasmid pKSM612 compared to WT MGAS5005 containing empty vector. Bars indicate $\log_2$ mean relative changes in gene transcript levels between the two strains with error bars indicating $\log_2$ standard deviations. Values above the x-axis indicate an increase in a mean change in transcript levels, and values below the x-axis indicate a reduction in the change in transcript levels relative to the WT strain MGAS5005. Dotted lines at 0.5 and 2 represent cut-offs for the level of significance.

TrxR activates the Mga regulon in both throat and generalist strains

A *trxR* deletion in two different M1 strains, SF370 and MGAS5005, has different effects on *mga* in late exponential phase (206) (Table 6). Interestingly, SF370 is genetically distinct from serotype M1 strains associated with severe human infections, and thus, the differences in their genetic backgrounds may play a role in the observed effects of TrxR on the Mga-regulated genes. To determine whether there is a functional conservation of TrxR's involvement in virulence regulation, *trxR* was inactivated in the M4 clinical strain GA40634 and in a representative M49 strain, NZ131. Upon inactivation of *trxR*, the strains were also cured to relieve *trxR* of the inactivating plasmid to generate a negative control strain. Real-time RT-PCR was performed on total RNA isolated at late exponential phase under erythromycin selection from the wild type strain (with an empty vector) and was compared to the *trxR*$^-$ mutant strain and its respective cured strain (with an empty vector). Real-time RT-PCR was performed on *trxR* and *emm* (M49) or *arp* (M4), *mga,* and *opuAA*, three genes representing the *trxR*$^-$ phenotype in M1T1. The qPCR results show that in both GA40634 (Fig 10A) and NZ131 (Fig 10B), TrxR has a significant effect on *mga* and *emm/arp*. Additionally, there did not appear to be any affect on *opuAA* transcripts within either of these strains, suggesting that TrxR's regulation of *opuAA* in MGAS5005 might be strain specific. Thus, these results suggest that the influence of TrxR on *mga* and the Mga-regulated genes is not strain or serotype specific, and that its role in virulence regulation is conserved among other major serotypes currently involved in streptococcal disease.

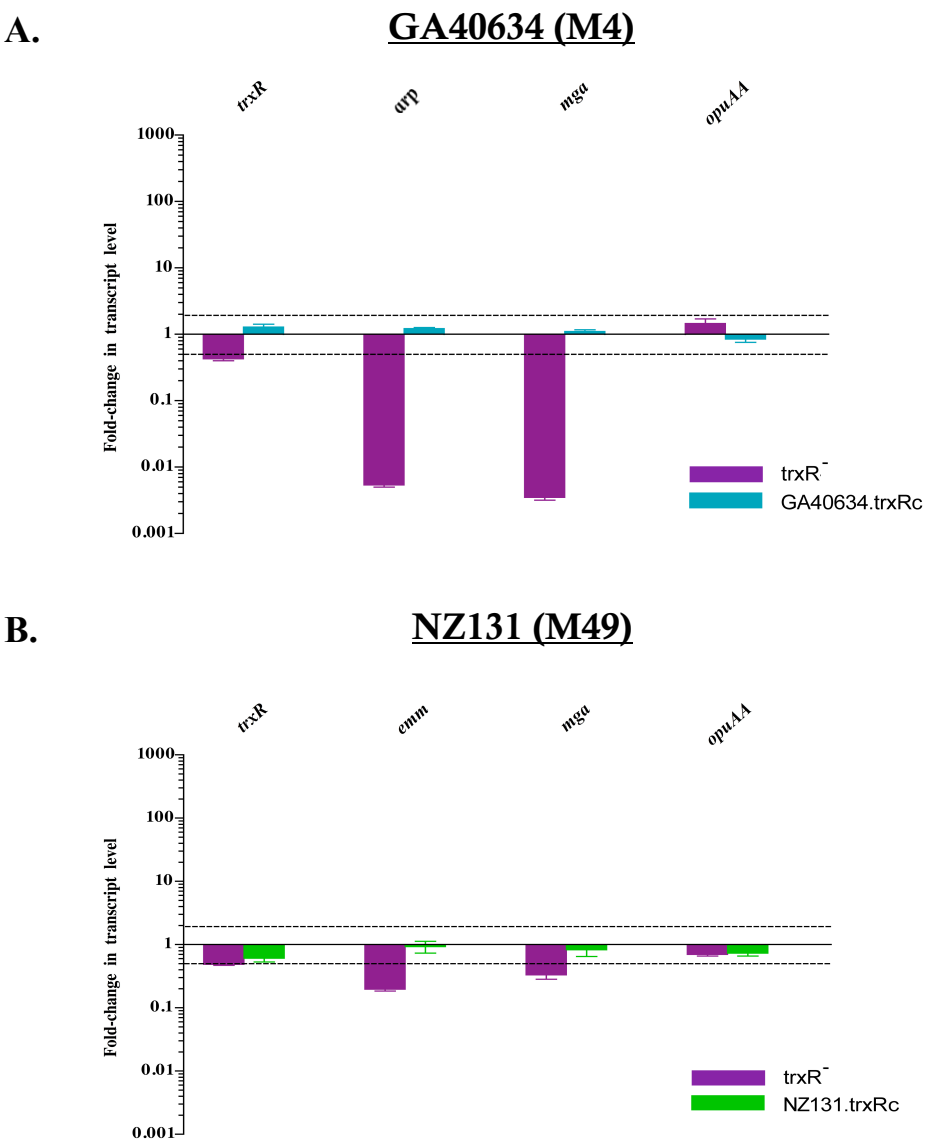

FIGURE 10. **Real-time RT-PCR analysis of *trxR*- and cured strains.** Gene transcript levels of *trxR, emm* (*arp), mga,* and *opuAA* were assessed through qPCR from the *trxR*- (purple) and cured strains (blue- GA40634.*trxR*c, green- NZ131.*trxR*c). Results are shown as transcript fold-change relative to their corresponding WT transcript levels and normalized to the *gyrA* control. Dotted lines at 0.5 and 2 represent cut-offs for significance.

Deletion of *trxT* resembles a *trxR*$^-$ phenotype, however complementation does not restore phenotype

Because *trxT* was found to be co-transcribed with *trxSR* (Fig 6C), it was important to investigate the relationship between TrxT and the TrxSR TCS. To determine whether TrxT is involved in the TCS, a non-polar deletion of the *trxT* gene was made in MGAS5005. This deletion strain, MGAS5005.*trxT*, was then used for real-time RT-PCR analysis to determine a *trxT*$^-$ profile. Total RNA was isolated at late exponential phase (as was the RNA for the *trxR*$^-$ studies) from MGAS5005 with an empty vector and was compared to the MGAS5005.*trxT* mutant containing an empty vector under spectinomycin selection. Transcript levels of several TrxR-regulated genes were assessed in both the wild type and mutant *trxT*$^-$ strains. qPCR results from the *trxT* mutant compared to the wild type strain followed some of the regulatory patterns that were seen in the *trxR*$^-$ strain (e.g. the Mga-regulated gene *sic* was significantly down, *opuAA* levels were up) (Fig 11). This suggests, however, only a potential involvement of TrxT in the TCS if any, as the absence of *trxT* does not completely resemble that of the absence of *trxR* in MGAS5005. Additionally, qPCR demonstrated that in the absence of *trxT*, transcript levels of *trxS* and *trxR* significantly increase, albeit only minimally. This suggests that TrxT may have some sort of auto-regulatory role for this operon.

To confirm that the effect that was seen in the qPCR was due to TrxT, a complementing plasmid expressing TrxT under its native promoter was introduced into MGAS5005.*trxT* to provide TrxT *in trans*. qPCR was performed on RNA isolated from the MGAS5005.*trxT* strain containing the TrxT complementing plasmid and was compared to wild type MGAS5005 RNA as before. Unexpectedly, the expression of the

tested genes did not return to wild type levels, as we would expect, even though *trxT* expression was more than 50-fold higher than the wild type strain (Fig 11). Thus, a role for TrxT in the TrxSR TCS cannot be determined at this time.

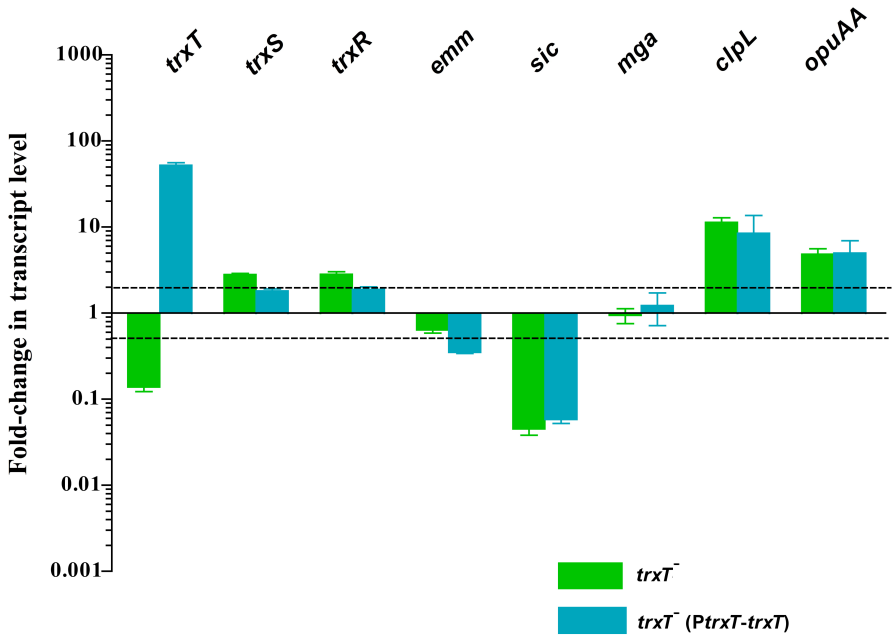

FIGURE 11. **Role of TrxT in the TrxSR TCS assessed through qPCR.** Gene transcript levels of *trxT, trxS, trxR, emm, sic, mga, clpL,* and *opuAA* were assessed through qPCR from the MGAS5005.*trxT*- (green) and complemented MGAS5005.*trxT*- (P*trxT-trxT*) strains (blue). Fold-change was determined relative to the corresponding WT MGAS5005 containing an empty vector with transcript levels normalized to the *gyrA* control. Dotted lines at 0.5 and 2 represent cut-offs for significance.

DISCUSSION

This study was initiated to assess the importance of the uncharacterized TrxSR TCS to streptococcal disease. The evidence presented in this study shows that the TrxSR TCS does influence virulence, likely through regulation of the core Mga virulence

regulon. Furthermore, this work aids in modeling the complex interactions that occur within GAS between different regulatory pathways to influence disease progression.

***trxSR* is part of a tightly regulated operon**

Inspection of the MGAS5005 genome showed four tightly linked open reading frames (*trxT, trxS, trxR,* and *bgaA*) separated by very little intergenic space, suggesting that they may be part of an operon. RT-PCR analysis of MGAS5005 cDNA clearly demonstrated that some transcripts contained *trxT, trxS,* and *trxR*. Additionally, we found that although a transcript that contained *trxR* and *bgaA* could be detected by RT-PCR, the *trxR* mutation did not confer a polar effect on *bgaA* transcription (Table 6), suggesting that *bgaA* can be transcribed independently of *trxR* in the M1 strain MGAS5005.

To learn about transcriptional regulation of the *trxTSR* operon, we first sought to determine why there appeared to be such a large distance between the promoter and the first codon of TrxT. The promoter of the operon, P*trxT*, was previously identified by *in vitro* transcription experiments to be 132 bp upstream of the initiation codon of TrxT (135). In order to verify this location, we employed 5'RACE. Interestingly, when an antisense primer was used that hybridized within *trxT*, the amplified transcripts all ended in a region roughly 50-70 bp upstream of the TrxT initiation codon. None of these transcripts contained a potential promoter that was located anywhere near the identified start site. However, when the nested primer was used that hybridized directly downstream of the previously published promoter region, the promoter was confirmed. Therefore, based on these experiments, we believe that there may exist some sort of RNA

secondary structure within the 5' UTR, which is involved in transcriptional regulation of the *trxTSR* operon. However, we could find no evidence for this, as secondary structure prediction programs such as Mfold or MacVector could not predict any obvious stem-loop structures or rho-independent terminators within this region. As a result, it is also possible that this region may contain a binding site for an unknown regulator of the operon, such as a regulatory RNA, which has yet to be discovered. Nevertheless, the role of this defined region in transcriptional regulation of *trxTSR* still remains unknown, as the data from the P*trxT-luc* experiments (Fig 7C) shows that deletion of this area does not significantly alter or affect expression of luciferase when fused to the truncated P*trxT* promoter region.

As mentioned previously, published data from two different microarray studies using the CovR response regulator showed that CovR could repress *trxSR* transcription (57, 81). Additionally, our *in vitro* transcription studies have shown that increasing concentrations of either CovR or phosphorylated CovR resulted in a reduction in P*trxT*-specific transcript levels (135). These results demonstrate that CovR directly represses transcription initiation or elongation at P*trxT* to regulate the *trxTSR* operon. This CovR repression, along with the aforementioned predicted RNA secondary structure in the 5' UTR of the promoter region, provides tight transcriptional regulation of the TrxSR TCS. Moreover, the luciferase data from the P*trxT-luc* experiments suggest a very weak and/or tightly regulated promoter, as relatively low levels of RLU are produced. Such complex regulation of the *trxTSR* operon, and the TCS in general, is consistent with other members of the AraC family (of which TrxR belongs), as one of the most prominent

features of this family is that their synthesis is tightly and often intricately regulated (160).

Defining the TrxR regulon in GAS

Several GAS TCSs have functional roles in coordinating the regulation of virulence genes within the pathogen. Unlike many prokaryotes, GAS does not appear to rely on alternative sigma factors to control gene expression, as only one has been identified to date (SigX), and it is not expressed under laboratory growth conditions (177, 188). As only four of thirteen TCSs have previously been linked to virulence (as discussed in detail in the Literature Review), several GAS TCSs remain uncharacterized and may play an important role in infection as well.

An insertional inactivation mutant of *trxR* was used in a subcutaneous model of GAS soft tissue infection to determine whether the TrxSR TCS was involved in regulation of virulence. The *trxR*$^-$ mutant exhibited significantly reduced lesion sizes at forty-eight hours post infection and increased survival over a seven day period, when compared to the wild type strain, suggesting a role for TrxR in virulence regulation. Next, to confirm this role, a DNA microarray was performed to determine the TrxR regulon. A relatively small number of transcripts were affected by TrxR in late exponential phase by inactivation of *trxR*, and interestingly, those transcripts that were found to be activated represented known members of the Mga virulence regulon. This result provided an explanation for why the MGAS5005.*trxR* mutant in the murine skin infection model had an attenuation of virulence (135). Other genes in the TrxR regulon exhibit a range of different functions in GAS, including translation (*rbfA* and *rplT*),

transcription (*nusA*), replication (*polA*), transport (*lacE, secA,* and *opuAA-opuABc*), and stress *(clpL*). Although the *trxR* mutant did not show an altered growth phenotype in rich THY medium *in vitro*, it is possible that growth *in vivo* would reveal an effect.

Interestingly, in a previous study using the M1 SF370.*trxR* strain, *trxR* was not identified as necessary for expression of the Mga-regulated gene *emm* (206). Additional real-time RT-PCR and Northern studies of the SF370.*trxR* mutant confirmed these results for several other Mga-regulated genes. Although the two strains belong to the same M1 serotype, SF370 is genetically distinct from other M1 strains associated with GAS infections. SF370, representing a pre-1988 M1 strain, differs from MGAS5005 and other post-1988 serotype M1 strains in a 36-kb region located between genes *purA* and *nadC* in the genome (242). Because two prominent extracellular toxins (SLO and NADase) are encoded by genes in this chromosomal segment, it has been postulated that the pre-1988 M1 strains did not produce any NADase, although they contained an intact *nga* gene. As a result, the post-1988 M1 serotype strains are thought to have a more invasive, virulent phenotype than the contemporary M1 strains due to the presence of NADase production. Therefore, the differences in the genetic backgrounds of SF370 and MGAS5005 may play a role in the observed effects of TrxR on the Mga-regulated genes. However, our qPCR results on the M4 GA40634.*trxR* and M49 NZ131.*trxR* demonstrate that TrxSR has a conserved role in regulation of *mga* and virulence in a broader range of GAS strains currently involved in streptococcal disease. This work, thus, adds TrxSR to the list of regulators that interact with the Mga regulon. The mechanism TrxR uses to interact with *mga* will be investigated in the next chapter (Chapter 5).

Involvement of TrxT in the TrxSR TCS

The arrangement of the *trxTSR* operon in GAS suggests that these genes may encode for proteins that are functionally linked. Although it is common for a HK and RR to be co-transcribed, it is less common for other genes to be co-transcribed with them. Typically, when an additional gene is co-transcribed with those of the TCS, they are often required for proper function of the TCS as an accessory protein (e.g. Agr system of *S. aureus* (183)). Therefore, TrxT, a conserved hypothetical membrane protein of unknown function, may be involved in the TCS. Potential roles for TrxT include aiding in signal reception with the TrxS HK and support to stabilize the TrxSR interaction during phosphate transfer.

From our results, whether the TrxSR TCS and TrxT are functionally linked is unclear at this time. Although it appeared that a mutation in *trxT* followed some of the same regulatory patterns of the *trxR*$^-$ mutant, when TrxT was over-expressed in the *trxT*$^-$ background, it did not rescue its phenotype. There are numerous possibilities as to why over-expressing TrxT in our experiments may not have restored the *trxT*$^-$ phenotype. One possible reason for this result is that the TrxT protein is not functional when expressed off the complementing plasmid. Additionally, *trxT* may need to be co-transcribed along with *trxSR* in a complex, in order to make a functional protein. In *B. subtilis*, activation of its σ^B transcription factor in response to stress requires three proteins, RsbSTU, transcribed from the same operon (273). For RsbT, a positive regulator of the σ^B transcription factor, its ability to function is strongly influenced by coexpression with its adjoining genes (273). Perhaps a similar coexpression with *trxSR,* is essential for *trxT* to allow for its proper function. Also, over-expressing *trxT*, because it is a predicted

membrane protein, may provide stress to the cell, leading to aberrant function of TrxT due to higher than normal levels of the protein. Whether any of these possible explanations are correct is unknown at this time, and further studies investigating TrxT with TrxSR need to be completed in order to provide solid evidence for or against its involvement in the TCS.

CHAPTER FIVE:

TrxR interacts directly with P*mga*

INTRODUCTION

Two-component systems function as information processing pathways to link an outside stimulus to an internal response. Typically, both an HK and RR are needed to relay this response from the outside of the cell to within. Upon a series of phosphorylation steps, the 'signal' is passed from one protein to another, generally resulting in changes to the transcriptional profile of the cell. Much of this transcriptional regulation involves proteins that either activate or repress expression of particular genes. As the majority of RRs have DNA-binding effector domains (77), numerous subfamilies of RR proteins exist, identified based upon their homology to one another.

The AraC family represents one of the smaller subfamilies of RRs containing DNA-binding effector domains, as it exists in approximately 1% of all RRs (76). Although functional activities have not been assigned to all AraC-like members, based upon *in silico* searches, these proteins primarily represent transcriptional activators that regulate diverse bacterial functions including sugar catabolism, responses to stress, and virulence (160). Members of the AraC family span across diverse prokaryotic genera, although most members are γ-proteobacteria (75). The AraC family is characterized by significant amino acid sequence homology extending over a 100-residue stretch at the C-terminal end of the proteins, constituting the DNA binding domain (75). This conserved region has been shown to contain seven α-helices, including two helix-turn-helix (HTH)

binding motifs (α_2-T-α_3 and α_5-T-α_6), connected by a linker α-helix (α_4), and two flanking α-helices (α_1 and α_7) (213).

The first, well-characterized member of the AraC family is MarA, a transcriptional activator of more than a dozen genes in the multiple antibiotic resistance (*mar*) regulon of *E. coli*. The crystal structure of MarA has served as a reference for how members of the AraC family bind DNA. Containing two HTH domains per subunit, MarA inserts into two adjacent segments of the major groove (205). These adjacent major groove segments are located on the same face of the DNA, but are separated by only 27 Å, and MarA thereby bends the DNA by approximately 35° (205). Additionally, the most important determinants of MarA's binding appear to be hydrogen bonds made by both HTH motifs with several bases of the DNA.

Another well-characterized member of the AraC family is XylS of *Pseudomonas putida*. Extensive mutational analysis of the 100 conserved C-terminal amino acids of XylS has revealed defined structural requirements for how the protein interacts with the DNA. Although mutations in conserved residues within the α_5-helix had little effect on XylS transcriptional activity, it was found that the distribution of polarity in the α_6-helix was important for its activity (158). Surprisingly, the strongest effect of the mutations was not observed in the HTH binding motifs, but in the conserved residues located outside the DNA-binding domain. These residues in XylS included Gly-290 located in the turn between the two helices α_5 and α_6, Pro-309 located downstream of α_6, and Leu-313 located in the small last helix α_7 (158). It is thought that these three residues play an important role in the activation of RNA polymerase to initiate transcription.

NCBI PSI-BLAST and Pfam database searches have identified a putative AraC-like DNA binding domain at the C-terminus of TrxR. Since none of TrxR's homologs have been studied in detail biochemically, a mode of interaction for how TrxR might interact with its target genes was assessed. In this study, we first demonstrate that TrxSR is a functional phosphorelay system, capable of interacting to pass a signal from one protein to another. Additionally, TrxR's mechanism of action is explored, in reference to P*mga,* and details of this interaction are determined.

RESULTS

TrxS can dimerize *in vivo*

The first step in a TCS pathway upon signal recognition is autophosphorylation of the HK, followed by its own dimerization with another HK monomer. In order to determine if TrxS can interact with itself and dimerize *in vivo*, the soluble, signaling domain of TrxS was fused in-frame to the C-terminal side of both the T18 and T25 catalytic domains of *Bordetella pertussis* adenylate cyclase (CyaA) for use in a bacterial two-hybrid system (113). Initial attempts at using the full-length TrxS protein for these experiments failed due to solubility issues, therefore only the signaling domain was expressed (134). Within this system, functional complementation of adenylate cyclase occurs only when the two halves of the CyaA are brought within close proximity to one another, as CyaA is not functional when its catalytic subunits are physically separate.

To determine whether TrxS can dimerize, pT18C-TrxS and pT25C-TrxS were co-transformed into BTH101, a *cya*$^{-}$ *E. coli* strain. Additionally, the empty vectors and pT18C-TrxS/pT25C-TrxS were co-transformed to serve as negative controls

(pT18C/pT25C; pT18C-TrxS/pT25C; pT18C/pT25C-TrxS). The transformation plating and patching were performed on MacConkey media supplemented with maltose. MacConkey media is a defined media that contains bile salts and a neutral red dye, which is a pH indicator that is yellow above a pH of 8.0, and red below a pH of 6.8. When the two halves of CyaA are brought within close proximity of one another, cAMP synthesis occurs. cAMP binds to CAP, and the cAMP/CAP complex bind to the *malT* promoter, activating the transcription of *malT* and *malEFG* (115). These proteins aid in maltose uptake and degradation and create a byproduct of H^+ ions. The increase of H^+ ions causes an acidic pH, and color change from yellow to magenta. Upon plating and patching of the co-transformants, the three negative controls exhibited no color change (yellow), while the pT18C-TrxS/pT25C-TrxS turned magenta. This result suggested that TrxS could dimerize, as it interacted with itself *in vivo* (Fig 12), to functionally complement CyaA.

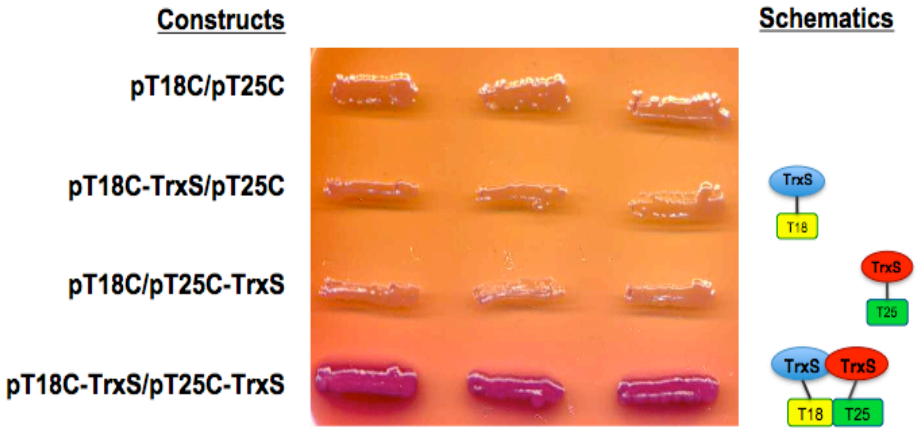

FIGURE 12. **TrxS dimerizes *in vivo*.** Bacterial two-hybrid assay plated on MacConkey agar plus 1% maltose. Shown are panels with patches from plasmid co-transformants in BTH101, a *cya*$^-$ *E. coli* strain: negative controls pT18C/pT25C, pT18C-TrxS/pT25C, pT18C/pT25C-TrxS, and experimental pT18C-TrxS/pT25C-TrxS. Yellow color indicates negative reaction and magenta color indicates positive reaction.

TrxS exhibits autophosphorylation activity and phosphorelay to TrxR *in vitro*

Upon receiving stimulation in the form of a signal, the histidine kinase undergoes *trans* autophosphorylation at a specific histidine residue and dimerization, to transfer this phosphoryl group to an aspartate residue within the receiver domain of their cognate response regulator, to propagate the signal. To identify the residues involved in this phosphorelay, we first aligned TrxS with characterized bacterial TCS histidine kinases such as EnvZ. However, because TrxS belongs to a rather unusual histidine kinase subclass that has an atypical H-box (32), alignment of TrxS with the characterized HKs was very difficult. Within the H-box, a proline precedes the conserved histidine, while the proline found in most kinases located five residues downstream from the histidine, is missing (84). Additionally, the H-box histidine is followed by a phenylalanine instead of the usual acidic residue. Once TrxS was aligned with three other members of the HPK_8 subclass (84), LytS, YehU, and HK07 (*S. pneumoniae*), a conserved histidine residue (His-383) was readily identified in the predicted dimerization/phosphorylation domain of TrxS (Fig 13A). TrxR could be aligned with known bacterial response regulators, such as CheY and OmpR, and a conserved aspartate residue (Asp-55) was identified in the predicted phosphoacceptor domain of TrxR (Fig 13B).

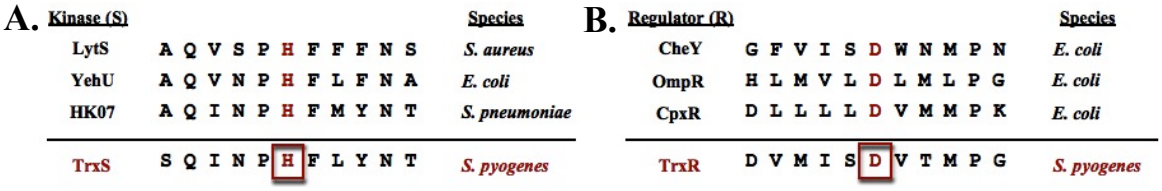

FIGURE 13. **Predicted catalytic residues of TrxS and TrxR**. *A*, alignment of residues within the dimerization/autophosphorylation domain from several histidine kinases. Phosphorelay histidine residues are in red; the predicted phosphorelay histidine of TrxS (His-383) is boxed. *B*, alignment of residues within the phosphoacceptor domains of several well-characterized response regulators. Phosphoacceptor aspartate residues are in red, the predicted phosphorelay aspartate of TrxR (Asp-55) is boxed.

To determine whether TrxS undergoes autophosphorylation and catalyzes phosphorylation of TrxR, and to determine whether His-383 of TrxS and Asp-55 of TrxR are the signaling residues of TrxSR, *in vitro* phosphorelay experiments were performed. The signaling domain from both the wild type and mutant TrxS (TrxS and TrxS:H383A) along with the full-length wild type and mutant TrxR (TrxR and TrxR:D55A) proteins were expressed as 10xhistidine-MBP-tagged fusion proteins and were purified by affinity chromatography over both amylose and Ni-NTA resins (Fig 14A). To demonstrate *in vitro* autophosphorylation of the signaling domain of TrxS, radiolabeled [γ-^{32}P]ATP was added to TrxS and autophosphorylation was observed by SDS-PAGE followed by exposure to a phosphoimaging cassette. Exposure of TrxS to [γ^{32}P]-ATP resulted in autophosphorylation that was not observed in TrxS:H383A (Fig 14B, D), and a maximal level of phosphorylation was observed within 60 minutes (Fig 14B). Addition of TrxR to phosphorylated TrxS resulted in rapid dephosphorylation of TrxS and phosphorylation of TrxR (Fig 14C, F), whereas TrxS dephosphorylation and TrxR phosphorylation were not observed when TrxR:D55A was added (Fig 14E). These results suggest that TrxS and TrxR can form an *in vitro* phosphorelay in which TrxS undergoes autophosphorylation at His-383 and subsequently transfers its phosphate group to Asp-55 of TrxR.

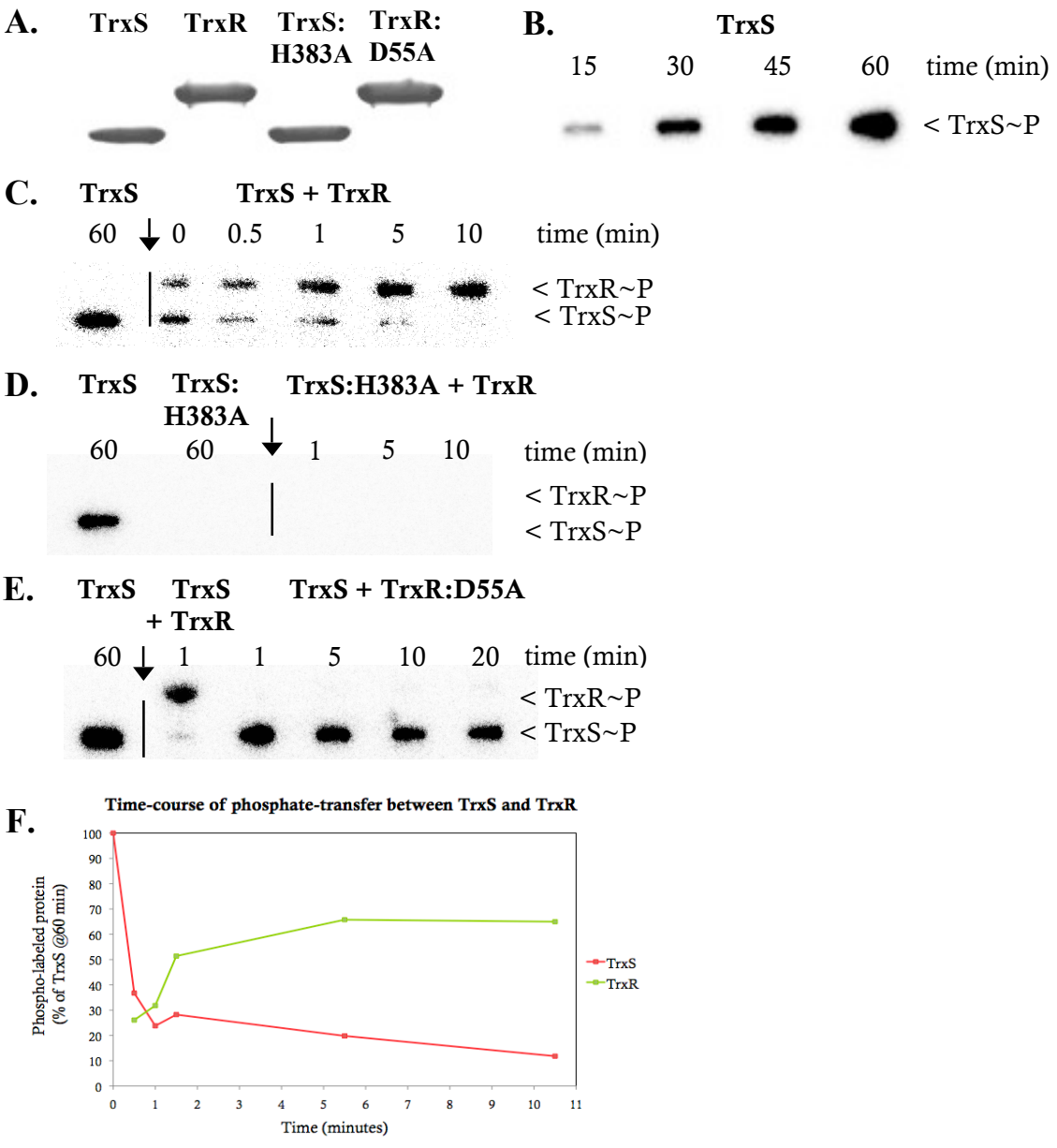

FIGURE 14. **Histidine 383 of TrxS and aspartate 55 of TrxR are essential for TrxSR phosphorelay**. *A*, Coomassie blue stain of SDS-PAGE with purified His-MBP tagged TrxS, TrxR, TrxS:H383A, and TrxR:D55A proteins. *B,* incubation of 63.4 µM TrxS with [γ^{32}P]-ATP over time. *C, in vitro* phosphorelay between TrxS and TrxR. 63.4 µM TrxS was incubated with [γ^{32}P]-ATP for 60 minutes and following labeling, 534 µM TrxR was added to the reaction (vertical arrow) and samples were taken. Proteins were separated by SDS-PAGE, and gels were exposed to autoradiography. *D,* incubation of 63.4 µM TrxS:H383A and transfer to 534 µM TrxR over time. *E*, incubation of 67 µM TrxS and transfer to 674 µM TrxR:D55A over time. *F*, quantification of phosphotransfer in *C*. Amount of radiolabeled protein is shown as a percentage of TrxS at 60 minutes. The x-axis represents time after the addition of TrxR to the reaction. Phosphotransfer pattern is representative of three independent experiments.

TrxS can interact with TrxR *in vivo*

After establishing that TrxS could *trans*phosphorylate TrxR *in vitro*, we next wanted to determine whether the two proteins could physically interact. Initial attempts utilized the bacterial two-hybrid assay to look at this interaction *in vivo*. The previous pT25C-TrxS construct was used to express soluble TrxS fused to pT25C while TrxR was fused to pT18C to create pT18C-TrxR. Although we could verify expression of the full-length TrxS fusion construct, we could not confirm that a functional full-length TrxR fusion product was made from the pT18C-TrxR plasmid (data not shown), preventing our use of the bacterial two-hybrid assay to look at the TrxS-TrxR interaction.

Thus, we utilized a different *in vivo* environment, that of a native GAS cell, to look at this interaction. In order to do so, His-MBP-TrxR was expressed on a plasmid under the P*rpsL* promoter in the *trxR*$^-$ strain, MGAS5005.*trxR*. Additionally, two aspartate mutants, D55A and the phosphomimetic D55E, also expressed under P*rpsL*, along with an empty replicating vector pJRS525, were expressed in the same MGAS5005.*trxR* background. These strains were grown to late-logarithmic phase and used in a co-immunoprecipitation (co-IP) assay with an α-His antibody to pull down soluble proteins that His-MBP-TrxR, or its mutants, interacted with. The collected co-IP samples were run in duplicate on SDS-PAGE gels and analyzed via Western blots using either α-His or α-TrxS antibodies.

Western blot analysis using the α-His antibody confirmed the presence of the His-tagged TrxR proteins, along with equal loading of the co-IP lysates, as all three His-MBP-TrxR proteins had comparable intensities for this TrxR band (Fig 15A). When the α-TrxS antibody was used on the same co-IP lysates, there seemed to be a TrxS band

present in all lanes including the control, suggesting that the antibody was not clean (Fig 15B). However, wild type His-MBP-TrxR appeared to pull down the cytosolic portion of TrxS more efficiently than the other proteins, as it had a very intense, dark band. Additionally, the D55E phosphomimetic mutant of TrxR appeared to minimally pull down cytosolic TrxS (58% increase over the control), compared to the wild type lane, while the D55A mutant had a band comparable to that of the control lane, suggesting that it could not interact with TrxS at all (Fig 15C). Thus, TrxR is capable of interacting with TrxS within a GAS cell, and this interaction appears to be phosphorylation dependent.

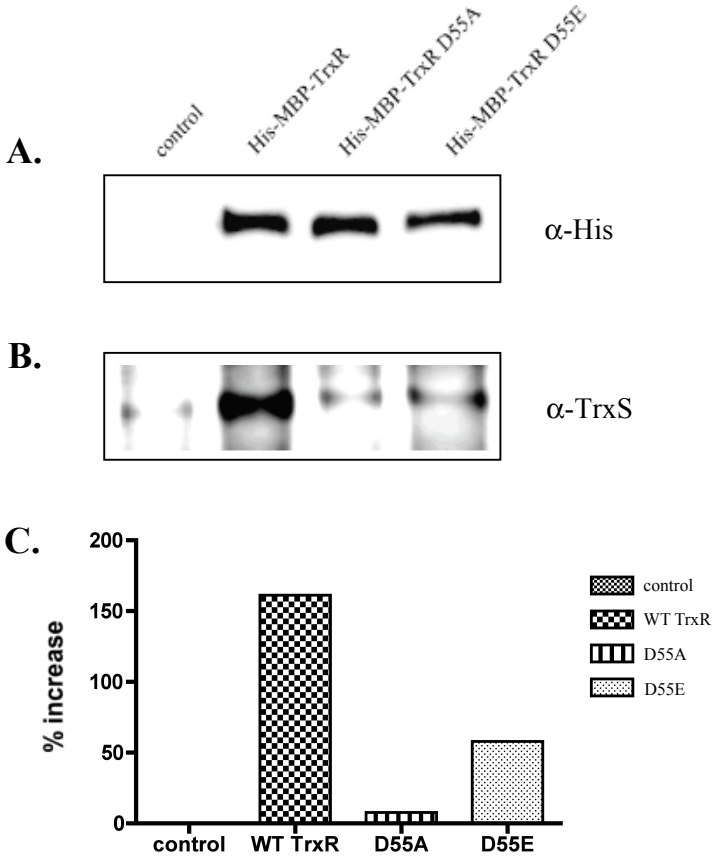

FIGURE 15. **Native TrxS is pulled down by His-MBP-TrxR.** Western blot analyses of control (pJRS525 empty vector), His-MBP-TrxR, His-MBP-TrxR D55A, and His-MBP-TrxR D55E co-immunoprecipitation samples run on a 10% SDS-PAGE gel. Immunoblot using *A,* α-His monoclonal antibody and *B*, α-TrxS polyclonal antibody. *C*, Quantification of α-TrxS Western in *B*. Data is shown as a percentage increase over the control and is representative of three independent experiments.

TrxR activates P*mga*

As an initial step to determine how TrxR regulates *mga* expression, the firefly luciferase reporter gene was fused to the *mga* promoter to generate the P*mga-luc* allele. Luciferase activity was assayed from early logarithmic growth to early stationary phase in MGAS5005 (WT), KSM165-L.5005 (*mga* mutant), and MGAS5005.*trxR* containing the P*mga-luc* plasmid (Fig 16). At several different points in the growth cycle in the wild type (MGAS5005) and the *trxR* mutant containing P*mga-luc*, the *trxR* mutant exhibited significantly reduced P*mga-luc* activity compared to wild type MGAS5005, including mid-logarithmic (3.1 fold) and early stationary (3.4 fold) phases of growth. Relative to the wild type strain, the levels of P*mga-luc* activity were similar for the *trxR* and *mga* mutants. Interestingly, P*mga* activity dropped in the wild type strain at late logarithmic point, the same time point used for the microarray (Table 6 and Fig 16). These data suggest that TrxR activates the Mga regulon through regulation of P*mga*.

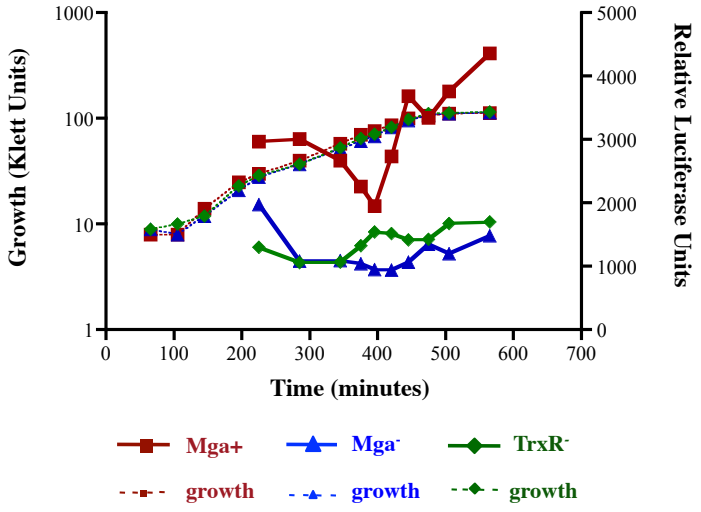

FIGURE 16. **P*mga* activity is regulated by TrxR.** MGAS5005 (WT), KSM165-L.5005 (*mga* mutant), and MGAS5005.*trxR* strains containing the P*mga-luc* reporter plasmid were grown in THY medium under spectinomycin selection. Upon reaching 30 Klett units, 500 µl samples were taken every 30 minutes across growth (dashed lines) and assayed for luciferase production (solid lines).

TrxR specifically binds to P*mga in vitro*

To determine if TrxR directly interacts with the promoter region of the *mga* gene, electrophoretic mobility shift assays (EMSAs) were performed on P*mga*. A P*mga* probe was amplified from MGAS5005 that included a 301 bp fragment encompassing both Mga binding sites 1 and 2, and was centered between the P1 and P2 promoters of *mga*. To address specificity of TrxR binding, a probe consisting of the promoter region of *emm* was generated. Assays were performed using purified His-MBP-TrxR at 25°C (see Materials and Methods).

Increasing amounts of His-MBP-TrxR (0.9-2.8 μM) resulted in a mobility shift of labeled P*mga*, indicating DNA binding by TrxR (Fig 17A, lanes 1-4, B). This shift of the TrxR-P*mga* interaction appeared smeary, however, and did not resolve into a distinct single band, remaining rather diffuse. The addition of 500 ng of cold P*mga* was able to compete for the interaction, nonetheless, whereas the addition of the same amount of cold P*emm* had no effect (Fig 17, lanes 5 and 6). Thus, His-MBP-TrxR is able to bind directly, and specifically, to P*mga in vitro*.

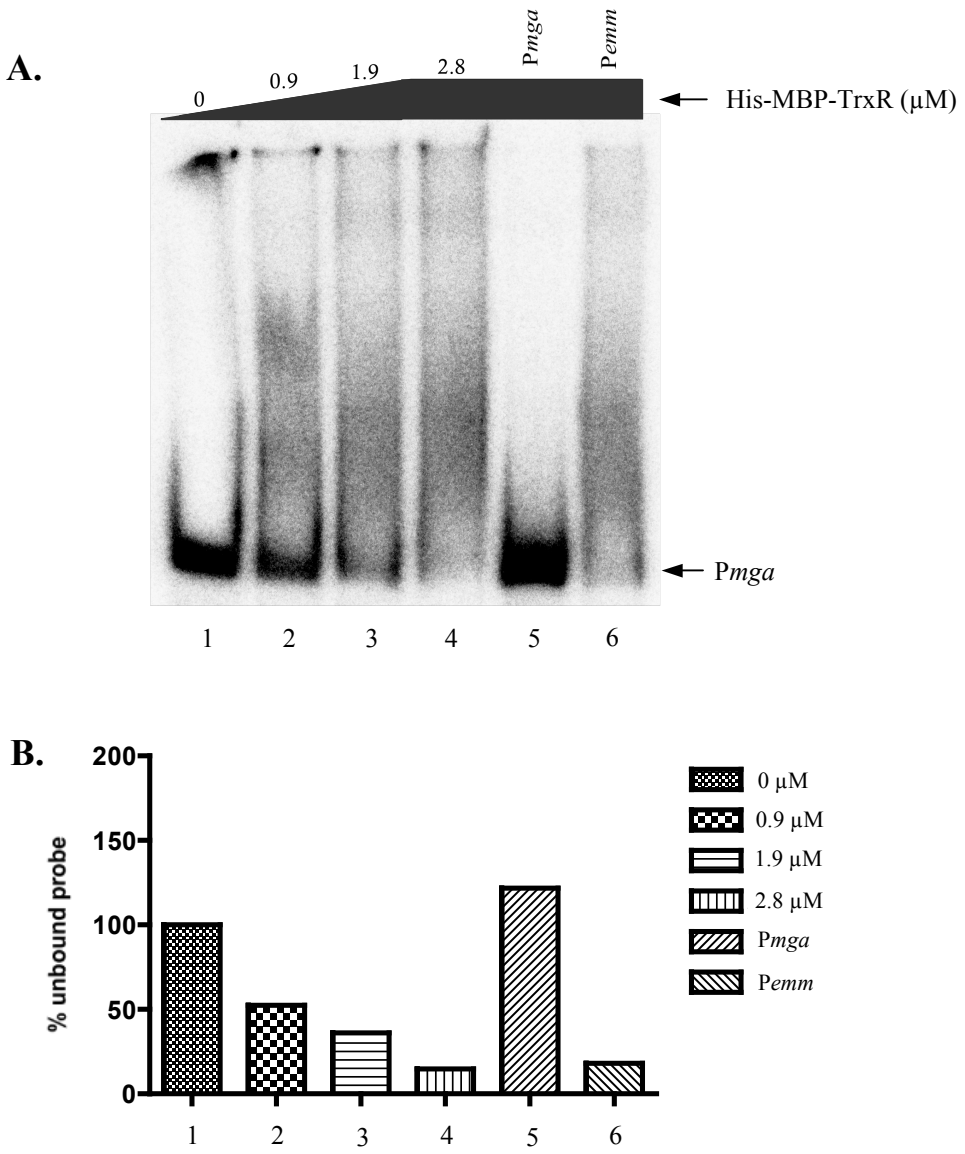

FIGURE 17. **TrxR binds specifically to P*mga*.** *A,* EMSA using a 301 bp P*mga* probe with His-MBP-TrxR. A constant amount (2.75 ng) of labeled probe was incubated with increasing amounts (0-2.8 μM) of purified His-MBP-TrxR (lanes 1-4). Unlabeled competitor P*mga* (500ng, lane 5) and P*emm* (500ng, lane 6) were used to assess specificity of protein binding to P*mga*. *B,* Quantification of EMSA in *A*. Data is shown as the percent of the unbound, radiolabeled P*mga* probe with matching lanes to the EMSA, and the trend is representative of three independent experiments.

The effect of phosphorylation on TrxR's ability to bind to DNA and regulate gene activation

In the prototypical TCS, the protein's effector domain is typically blocked from access and activity until the phosphate group has been transferred from the HK. When this transfer occurs, the conformation of the RR changes, and relieves the effector domain from obstruction. This conformational change generally causes relaxation of the protein and allows the RR to continue the signal propagation to elicit its cellular response.

In order to determine whether a phosphorylated TrxR is necessary for its ability to activate the Mga regulon, His-MBP-TrxR and the D55A or D55E mutants were expressed in a *trxR*$^-$ background under P*rpsL*. Western blot analysis shows approximately equal TrxR protein levels for the three proteins, suggesting that the phosphorylation state of the catalytic aspartate has no affect on expression of the protein (Fig 18A). The protein's ability to complement a *trxR*$^-$ phenotype was then determined. Real-time RT-PCR was used to measure levels of TrxR-regulated genes in a *trxR*$^-$ strain containing an empty vector, wild type His-MBP-TrxR, His-MBP-TrxR D55A, or His-MBP-TrxR D55E. The results from these experiments show that, as predicted, the wild type protein can complement a *trxR*$^-$ phenotype. However, unexpectedly, both the D55A and D55E TrxR mutants can as well (Fig 18B). Since it can be interpreted that both of these proteins are active because they could both bind to P*mga in vitro* (Fig 18C), the phosphoacceptor residue within the receiver domain does not appear to affect TrxR's activity for the genes tested. This suggests that the phosphorylation state of TrxR has little significance on the protein's function in relation to activating the Mga regulon or repressing *opuAA*.

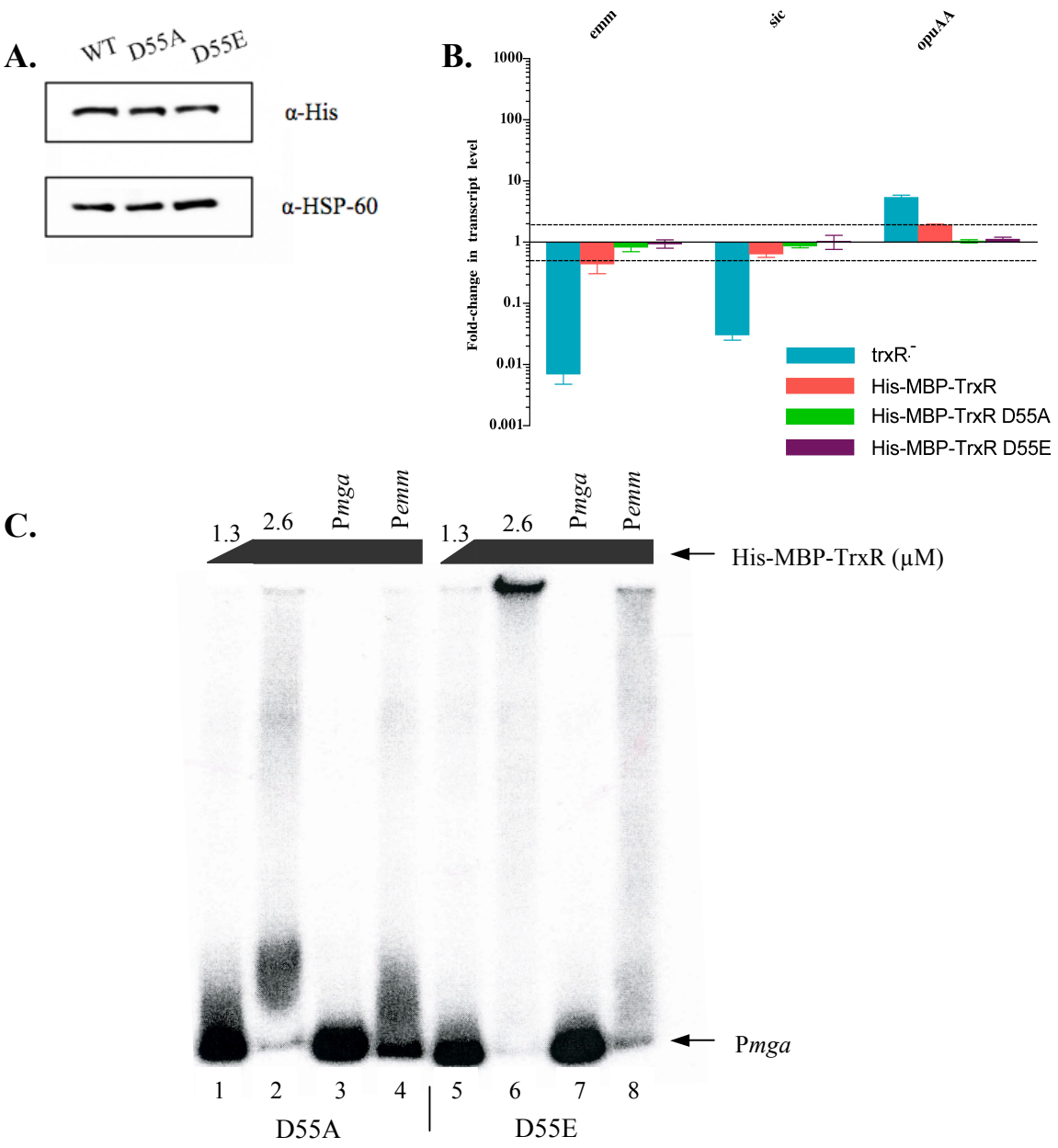

FIGURE 18. **Effect of TrxR's phosphorylation state on gene transcription and DNA binding.** *A,* Western blot analysis to determine the amount of His-MBP-tagged TrxR under P*rpsL* for the WT, D55A, and D55E proteins in the MGAS5005.*trxR* background. Shown are blots to detect His and HSP-60 (loading control). *B,* Transcript levels of *emm, sic,* and *opuAA* from the *trxR*- (blue), WT TrxR (orange), TrxR D55A (green), and TrxR D55E (purple) in the MGAS5005.*trxR*- background. Shown as transcript fold-change relative to their corresponding WT transcript levels and normalized to the *gyrA* control. Dotted lines at 0.5 and 2 represent cut-offs for the level of significance. *C*, EMSA using a 301 bp P*mga* probe with His-MBP-TrxR D55 mutants. A constant amount (3.26 ng) of labeled probe was incubated with increasing amounts (1.3-2.6 μM) of purified His-MBP-TrxR D55A (lanes 1-4) or D55E protein (lanes 5-8). Unlabeled competitor P*mga* (400ng, lanes 3, 7) and P*emm* (400ng, lanes 4, 8) were used to assess specificity of protein binding to P*mga.*

TrxR requires its HTH domains to bind to P*mga*

To further investigate the nature of His-MBP-TrxR binding to P*mga*, we focused on TrxR's two predicted HTH motifs to assess their functionality in DNA binding. The two HTH DNA-binding motifs were identified based upon their amino acid homology to AraC and numbered according to their physical position (Fig 19A, B). Alanine substitutions were made in two amino acids within the 'recognition' helices that were predicted to make contact with the DNA, α_3 and α_6-helices (205) (Fig 19B). To allow analysis of DNA-binding activity *in vitro*, the HTH mutations were introduced directly into the *trxR* allele within a His-MBP-TrxR fusion protein contained on the plasmid pKSM697. The resulting mutant fusion protein was purified from soluble *E. coli* lysates, with no significant degradation caused by the presence of the HTH mutations (data not shown).

To assay the effect of the HTH mutations on DNA binding, the ability of the TrxR HTH-1/2 mutant to interact with P*mga* was determined *in vitro* by EMSA analysis. Using the same P*mga* probe as the previous EMSA experiment (Fig 17), increasing amounts of His-MBP-TrxR and the HTH-1/2 mutant (1.7-2.5 μM) were added to a labeled P*mga* probe. Using the wild type His-MBP-TrxR protein as a control for DNA binding (Fig 19C, lanes 2-5), no detectable binding of the HTH-1/2 mutant protein to the P*mga* probe was observed (Fig 19C, lanes 6-9). Thus, the two HTH motifs within the AraC-like DNA binding domain of TrxR are involved in binding to the *mga* promoter *in vitro*.

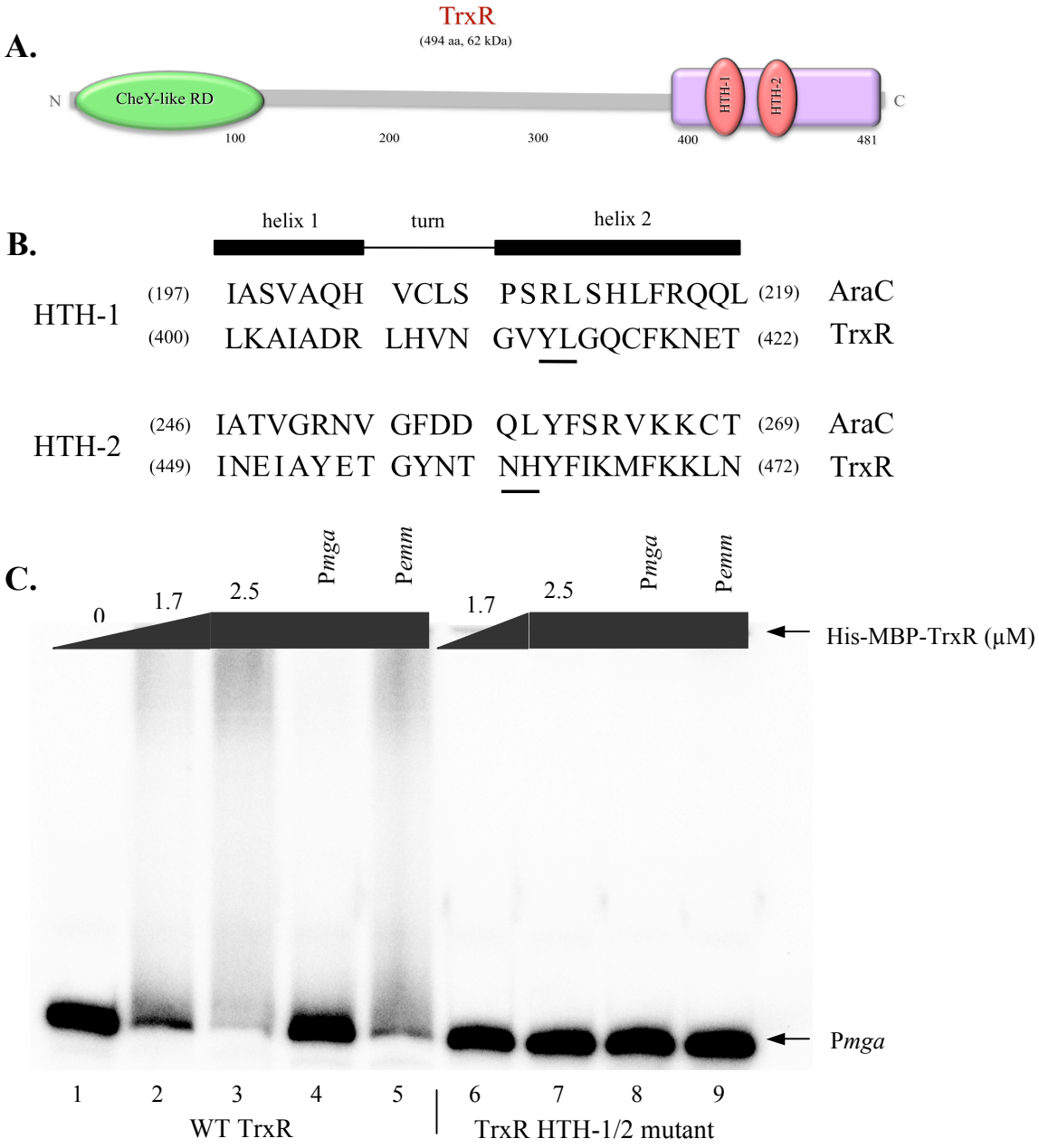

FIGURE 19. **TrxR requires its HTH domains to bind to P*mga*.** *A,* schematic of the TrxR protein showing potential helix–turn–helix (HTH) DNA-binding motifs (red ovals) based on amino acid sequence homology to AraC. *B,* amino acid residues composing the two putative HTH domains of AraC and TrxR are shown with numbers in parentheses referring to the corresponding amino acid location. The expected HTH secondary structures and their residue positions within the motif are illustrated. Amino acids within each 'recognition' helix of TrxR that were mutated to alanine residues are underlined. *C,* EMSA using a 301 bp P*mga* probe with His-MBP-TrxR and His-MBP-TrxR HTH-1/2 mutant. A constant amount (2-4 ng) of labeled probe was incubated with increasing amounts (0-2.5 μM) of purified His-MBP-TrxR (lanes 1-5) or HTH-1/2 mutant (lanes 6-9). Unlabeled competitor P*mga* (400ng, lanes 4, 8) and P*emm* (400ng, lanes 5, 9) were used to assess specificity of protein binding to P*mga.*

TrxR's HTH domains are not needed for *in vivo* activation of P*mga*

As the HTH domains were shown to be required for TrxR to bind to P*mga in vitro*, the requirement of the HTH domains for activation of the Mga regulon *in vivo* was next investigated. The His-MBP-TrxR HTH-1/2 mutant was placed under P*rpsL* and was introduced into the MGAS5005.*trxR* mutant. Real-time RT-PCR was performed on total RNA isolated at late-exponential phase from MGAS5005 with an empty vector and compared to the MGAS5005.*trxR* mutant containing either an empty vector or the P*rpsL*-His-MBP-TrxR HTH-1/2 plasmid. Surprisingly, transcript levels of all three TrxR-regulated genes in the HTH-1/2 mutant returned to wild type levels (Fig 20), suggesting that the HTH domains of TrxR are not needed *in vivo* for its activation of the Mga-regulated genes *emm* and *sic*, or *opuAA*.

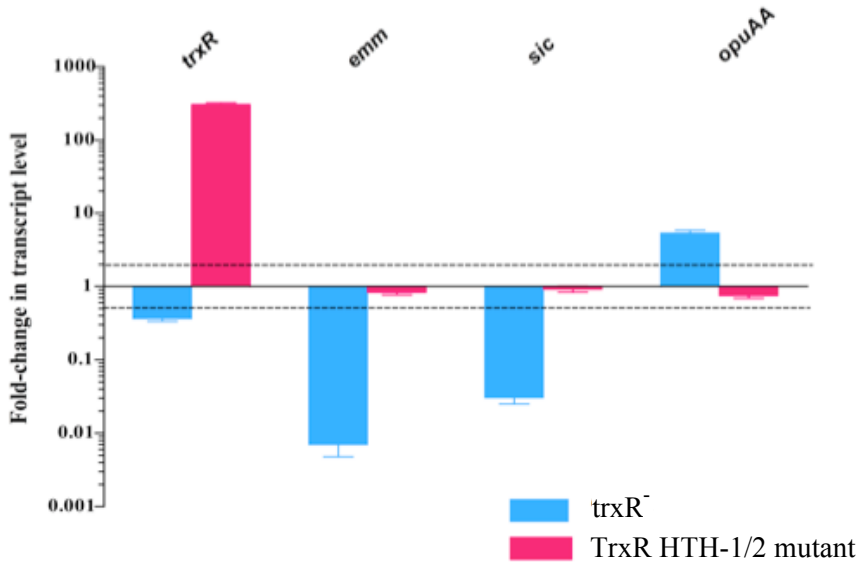

FIGURE 20. **TrxR does not require its HTH domains to affect gene transcription of the Mga regulon**. Transcript levels of *trxR, emm, sic,* and *opuAA* from the *trxR*$^-$ (blue) and TrxR HTH-1/2 mutant in MGAS5005.*trxR* (magenta) are shown as transcript fold-change relative to their corresponding WT (MGAS5005) transcript levels and normalized to the *gyrA* control. Dotted lines at 0.5 and 2 represent cut-offs for the level of significance.

Truncating TrxR does not affect its ability to rescue a *trxR*$^-$ phenotype

Since the HTH mutations did not appear to abrogate TrxR's ability to activate the Mga regulon *in vivo*, it was therefore important to determine if the activity of TrxR was due to another region of the protein. Pfam searches of TrxR reveal that TrxR has a CheY like receiver domain at its N-terminus and an AraC-like DNA binding effector domain at its C-terminus (Fig 21A). Between these two domains, there are roughly 300 amino acids with no ascribed function. Presumably there is a flexible linker within this region, however its location and size currently remain unknown. In order to ascertain whether this "linker" region has a separate function for the TrxR protein, three truncations of TrxR were made: a Δeffector consisting of the entire protein minus the predicted effector region (aa 1-389), a Δreceiver which removed the predicted receiver domain from TrxR (aa 118-494), and the effector alone (aa 390-494) (Fig 21A). These regions were first cloned in-frame with His-MBP, and subsequently placed under P*rpsL* in the same manner as the other TrxR complementation constructs as previously discussed. Each protein's ability to complement a *trxR*$^-$ phenotype was then determined. Real-time RT-PCR was performed on total RNA isolated at late-exponential phase and was used to measure levels of TrxR-regulated genes in a *trxR*$^-$ strain containing an empty vector, wild type His-MBP-TrxR, His-MBP-TrxR Δeffector, His-MBP-TrxR Δreceiver, and His-MBP-TrxR effector alone. From these experiments, the results indicate any portion of the TrxR protein is capable of rescuing a *trxR*$^-$ phenotype (Fig 21B), even only the last 104 C-terminal residues.

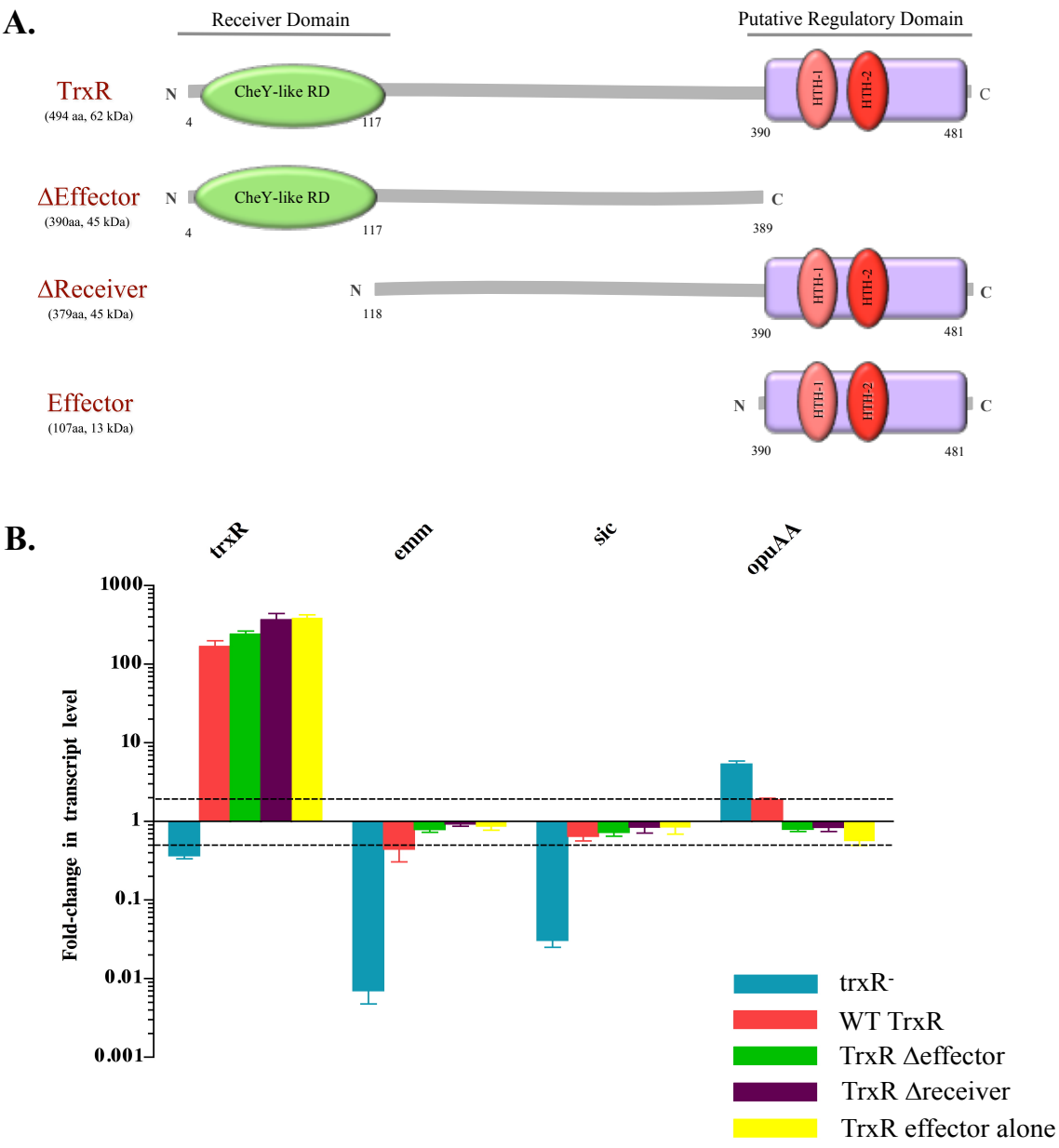

FIGURE 21. **Effect of TrxR truncations on the activity of the protein *in vivo*.** *A,* schematic of the WT TrxR protein showing CheY-like receiver domain and putative regulatory effector domain based on a Pfam domain search. Also shown are schematics of the Δeffector, Δreceiver, and effector TrxR truncation proteins. *B*, Transcript levels of *emm, sic* and *opuAA* from the *trxR*$^-$ (blue), WT TrxR (orange), Δeffector (green), Δreceiver (purple), and effector alone (yellow) in the MGAS5005.*trxR* background. To quantify the level of *trxR* transcript in the TrxR effector alone protein, separate primers were used in the 3' end of the gene, as the main *trxR* primer set sits down closer to the 5' end. Shown as transcript fold-change relative to their corresponding WT transcript levels and normalized to the *gyrA* control. Dotted lines at 0.5 and 2 represent cut-offs for the level of significance.

DISCUSSION

While the interaction between TCS proteins and their mechanisms of action have been well studied, within GAS, the majority of this work has focused on the CovRS system. This study focuses on TrxSR, the newly discovered TCS that activates virulence in *S. pyogenes*. The evidence presented here shows that *in vitro,* TrxSR TCS is a functional phosphorelay, which requires the HTH domains of TrxR for binding to P*mga*. However, our *in vivo* results suggest that neither the HTH domains of TrxR, or phosphorylation of the protein are necessary for activation of the Mga regulon. While the exact mechanism of this interaction is not entirely fully understood, this work lays the groundwork for understanding how TrxR, and potentially other YesN homologs, interact with their target DNA to control gene expression.

TrxSR is a functional phosphorelay, yet it may not be needed for TrxR's Mga-specific activity

In order for a TCS to sense a signal and create a specific internal response, a HK must be able to dimerize and bind ATP. Once this has occurred, a phosphate is transferred from ATP to a conserved histidine residue in the catalytic domain of the HK. This phosphate is then subsequently transferred to a conserved aspartate residue within the receiver domain of the RR. Typically, this transfer causes conformational changes to the protein that unblocks its effector domain, allowing the protein to perform its necessary effector function within the cell. If dimerization of the HK and phosphate transfer between the two proteins does not occur, there usually cannot be a successful response created by the TCS.

To ascertain whether TrxS can undergo dimerization/autophosphorylation and catalyze phosphorylation of TrxR, bacterial two-hybrid and phosphotransfer experiments were performed. Using the soluble, signaling domain of TrxS, the experiments confirmed the catalytic histidine, H383, and verified that TrxS can dimerize and autophosphorylate within its predicted signaling domain. Upon establishing functionality of the TrxS protein, it was next important to confirm that phosphotransfer from TrxS to TrxR could take place. Here, we show that Asp-55 may indeed be the catalytic phospho-accepting residue within this domain, as TrxS was capable of successfully transferring a radiolabeled phosphate to TrxR. Additionally, when the aspartate was mutated to an uncharged alanine, this abrogated phosphotransfer, thus supporting the role of this aspartate in the transfer. Although TrxS rapidly dephosphorylated upon addition of TrxR, there appears to be some loss of the radiolabeled ATP as only roughly 65% of the initial ATP from phospho-TrxS was transferred to TrxR. Since TrxS may possess phosphatase activity, either against itself or TrxR, this could account for the missing radiolabel on either of the proteins. Nevertheless, we have successfully reconstituted *in vitro* the TrxSR phosphorelay system.

Given this result, the question became whether this interaction occurred within the GAS cell. A co-immunoprecipitation assay using TrxR expressed *in trans* in the MGAS5005.*trxR* strain demonstrated that the native cytosolic portion of TrxS could be pulled down with the His-MBP-tagged TrxR. In order to achieve this result, sustained protein-protein interactions between TrxS and TrxR must have occurred to withstand the centrifugation and washing steps of the procedure. Since TrxS appears to physically

interact with TrxR within the GAS cell, albeit with one protein expressed off a plasmid, it strongly suggests that these two proteins do act like a canonical TCS *in vivo*.

Interestingly, when *in vivo* experiments were performed to determine whether phosphorylation of TrxR was necessary for gene activation of *mga*, TrxR did not appear to need a phosphorylated aspartate within its active site to regulate gene expression. Both the aspartate:alanine and aspartate:glutamate mutations appeared to complement and return gene transcript levels back to that of the wild type, suggesting that either form of TrxR, unphosphorylated or phosphorylated, appear to be used in regulation of gene expression. Why, then, does TrxR participate in a phosphorelay with TrxS if phosphorylation of TrxR does not appear to correlate with its primary activity? Phosphorylation of TrxR must serve some purpose for the protein, as it is unlikely that it participates in a phosphorelay with TrxS for no additional gain. The co-immunoprecipitation assay also suggested that the TrxS-TrxR interaction depended on the phosphorylation state of TrxR, as a D55A mutant did not appear to pull-down any TrxS. Therefore, it is plausible that TrxR may have one set of genes that it regulates in the absence of phosphorylation, and a second, potentially overlapping set that it regulates when phosphorylated. Such is the case for CovR, as GAS uses both unphosphorylated and phosphorylated forms of the RR to regulate gene transcription (58). In support for this hypothesis, our EMSA data showed that both the D55A and D55E proteins could bind to P*mga in vitro*. This would suggest that both forms of the protein are indeed, active, and may both be used in regulating gene expression. However, what remains to be determined is how the roles of the two forms of the protein are actually different in reference to their activity.

One caveat of the *in vivo* complementation experiments, however, lies in the design of the plasmid from which His-MBP-TrxR is expressed. The protein is expressed under P*rpsL*, which is a constitutive promoter that appears to be stronger than TrxR's native P*trxT*. Additionally, this construct is expressed within GAS on a multi-copy plasmid. Taken together, the amount of *trxR* transcript expressed from this plasmid is likely higher than native levels within the cell, when expressed from P*trxT*. As stated previously in Chapter 4, it appears that transcription from the P*trxT* promoter is very tightly regulated. This increase of *trxR* transcript, expressed off the plasmid from P*rpsL*, may translate into more total TrxR protein within the cell, allowing the *trxR*$^-$ phenotype to be overcome simply due to more TrxR protein around. In order to test this explanation, TrxR would need to be expressed either under a weaker promoter and/or in single copy to reduce the amount of TrxR expressed from the plasmid.

TrxR interacts with the promoter of *mga*

The results of the TrxR transcriptome analysis in MGAS5005 began our interest in TrxR's relationship with Mga in GAS. Since TrxR not only activates the Mga virulence regulon in MGAS5005, but in other serotypes as well, it became important to determine how TrxR was interacting with *mga* to cause this effect. Due to the fact that TrxR activated the Mga regulon, our initial studies focused on using the firefly luciferase reporter gene fused to the promoter of *mga*, in order to monitor TrxR's regulation of P*mga* across growth. Luciferase activity from P*mga-luc* was assayed in the MGAS5005.*trxR* mutant and compared to that of the wild type and *mga* mutant. Our results show that the *trxR* mutant exhibited significantly reduced P*mga-luc* activity

compared to wild type at most time points. Relative to the wild type strain, the levels of P*mga* activity were similar for both the *trxR* and *mga* mutants. Thus, from these data, it appeared that TrxR was activating the Mga regulon through regulation of P*mga*.

As TrxR has a predicted AraC-like DNA binding domain at its C-terminus, our next investigation involved direct binding of TrxR to the promoter of *mga*. In order to determine whether TrxR was capable of this binding, EMSAs were performed with purified His-MBP-TrxR and a P*mga* probe that contained a large region of the 5' UTR of *mga*. Our results indicate that purified TrxR is able to bind specifically to the promoter of *mga in vitro*. However, this interaction appears to be somewhat modest, resulting in a smear shift wherein the resulting protein-DNA interaction does not stay associated throughout the length of the gel. The addition of greater amounts of TrxR protein does not appear to prolong or improve this interaction. Nevertheless, TrxR does not bind to the promoter of *emm,* confirming that TrxR's regulation of *emm* is not direct, and likely through P*mga*.

In an effort to determine whether the binding of TrxR to P*mga* could be enhanced, experiments were run at 4°C to observe whether slowing down the interaction at a colder temperature could enable TrxR to bind to the DNA more tightly. Unfortunately, it did not appear that we could enhance TrxR-P*mga* binding in this manner. Consequently, other factors within our EMSA reactions (i.e. length of probe, gel percentage, reaction component) could potentially be the cause of our smear, or it is possible that TrxR's interaction with P*mga* really may be very rapid and highly transient. Thus the interaction of TrxR with the promoter of *mga* appears to be direct and the specificity of the interaction indicates that TrxR is capable of binding to the *mga* promoter.

Role of TrxR's HTH domains

The HTH domains of AraC-like proteins allow the proteins to interact with the DNA of their respective regulated genes by inserting into two adjacent segments of the major groove of the DNA to bind. These domains have been shown to be necessary for DNA binding for many well-characterized AraC-like proteins, such as MarA (205) and XylS (158). In order to determine their importance in TrxR, two amino acids of each recognition helix in TrxR's two putative HTH motifs were mutated to alanines to disrupt potential interactions with DNA.

DNA binding through TrxR's HTH domains was assayed *in vitro* through EMSAs using a probe containing the promoter region of *mga*. Using a His-MBP-tagged TrxR, DNA binding was assessed in both wild type and the HTH-1/2 versions of the protein. Although the shift created by wild type TrxR binding to P*mga* was smeary and small for the highest amount of protein tested, almost the entirety of the unlabeled radiolabeled probe had shifted. In contrast, the HTH-1/2 mutant had no visible shift when the protein was added, with the highest mutant TrxR concentration resembling the no protein lane. Since a double HTH mutant was used, whether this lack of binding is due to the mutations made in HTH-1 or HTH-2 cannot be determined at this time. For other AraC-like DNA binding proteins such as XylS, HTH-1 appears to be necessary for binding to the target DNA while HTH-2 is structurally, rather than functionally, required for specific DNA interactions (158). Additional band-shift experiments would need to be completed with either single HTH mutant in order to determine whether the HTH domains of TrxR act in concert like those of XylS. Nevertheless, the data presented here suggests that TrxR requires its HTH domains *in vitro* to bind to the promoter region of *mga*.

Surprisingly, when complementation experiments were performed to determine whether TrxR's HTH domains were required for gene activation of *mga*, the HTH-1/2 mutant was able to rescue the transcript levels of the TrxR regulated genes. This suggests, potentially, that the HTH domains of TrxR are not necessary for *in vivo* binding to the *mga* promoter, which contradicts the *in vitro* data showing that the HTH mutant could not bind. Although this may be a result of gene dosage as mentioned previously, there could also be another explanation. For XylS of *P. putida*, the most important residues for DNA binding were not the residues within the HTH domains that were shown to make contact with the DNA, but rather residues that laid directly outside those domains that aided in its interaction with RNA polymerase (158). Potentially, if these same key residues were mutated in TrxR and expressed *in vivo*, we might see *trxR*$^-$ like transcript levels for the HTH-1/2 mutant, as mutations of these residues may prevent TrxR's interaction with RNA polymerase. Additionally, it is plausible that TrxR may require interaction with RNA polymerase, and/or additional proteins at P*mga,* for binding of TrxR to occur.

Alternatively, TrxR may use an additional, alternative method of protein-DNA interaction outside of its AraC-like DNA binding domain. While Pfam searches show only one putative DNA binding domain at the C-terminal end of the protein, there is a large region of the protein (~270 aa), assumed to be the 'linker' for the receiver and effector domains, that exhibits no functional homology to known characterized proteins (Fig 21A). It is possible, then, that TrxR may have a second uncharacterized DNA binding domain that is not recognized or found by such programs as Pfam or Phyre2. At this time, our results are not conclusive as to whether this region plays a significant role

in TrxR's function. As we attempted to make different truncations of the TrxR protein, in an effort to elucidate and tease out the role of this region, even the smallest truncated TrxR product tested was able to complement the *trxR*$^-$ phenotype. We believed this protein, which only contains the last 104 aa of TrxR, and no receiver domain, was unable to complement the *trxR*$^-$ phenotype due to the fact that it lacked the majority of the protein.

Ultimately, there are three likely explanations as to our results surrounding the mode of action TrxR uses. As discussed previously, there is the issue of gene dosage, as all of our TrxR proteins are expressed under a constitutive promoter on a multi-copy plasmid. Not until these proteins are expressed under their native promoter, in the chromosome, will this issue be resolved. Additionally, TrxR may be regulated by an unidentified factor (e.g. protein-protein interactions) present in our *in vivo*, but not *in vitro* experiments. This would allow TrxR binding to P*mga* in our *in vitro* experiments, but be overlooked in our complementation experiments within GAS. Therefore further experimentation is needed to elucidate if and what this additional factor may be. And lastly, TrxR may participate in DNA binding through use of a second uncharacterized domain, in addition to the previously identified AraC-like DNA binding domain. Despite not knowing which explanation(s) are correct at this time, we have mounting evidence surrounding the TrxR-P*mga* interaction that enables us to begin to model how TrxR interacts with its target DNA to control gene expression.

CHAPTER SIX:

Conclusions and Recommendations

The Group A streptococcus (GAS) is a strict human-restricted pathogen that is able to cause a wide range of diseases in diverse niches within the human body. In order adapt to these locations, GAS utilizes several two-component systems to regulate transcription of genes necessary for their survival in these environments. In this study, TrxR, one of the previously uncharacterized TCSs, was chosen for further examination based upon its homology to known virulence TCSs. The experiments presented aimed to identify the role of TrxSR to the GAS cell, as well as determine the mechanism by which TrxR interacts with, and regulates, its target genes. Overall, these studies sought to shed light on the complex regulation networks used by this pathogen to adapt to host niches.

Complex nature of the TrxR protein

The AraC protein family of transcriptional regulators encompasses a large breadth of diverse functional activities, ranging from proteins that are involved in sugar metabolism and the stress response, to those that are involved in the regulation of virulence. TrxR represents a newly characterized AraC-like virulence regulator and joins previously described regulators of virulence such as AggR (178) and Rns (37) of *E. coli,* and VirF (62) of *Shigella flexneri*.

Beyond its characterization as an AraC-like DNA-binding protein, TrxR also belongs to the YesN protein family, based upon its homology to the YesN response regulator of *B. subtilis*. Interestingly, there is very little known about this family of regulators. Previous characterizations of two-component systems found in the genomes

of both *S. pneumoniae* and *E. faecalis* have identified several YesN homologs. RR07 of *S. pneumoniae* has been shown to be essential for full virulence in a pneumococcal mouse respiratory tract infection model (252), however no further characterization of its involvement in pneumococcal infection has been elucidated. In *E. faecalis*, an RR01 mutant had increased sensitivity to bacitracin, suggesting an involvement in the bacteria's defense against antibiotics that target the cell-wall (92).

Outside of these initial findings in *S. pneumoniae and E. faecalis*, no other published information exists for YesN homologs. Intriguingly, each of the studies' authors note the respective protein's unusual domain organization, one that includes a predicted linker domain that is very large in comparison to other response regulators. Because of the length of this predicted linker, it has been postulated that this region of the protein might form its own entirely separate domain, apart from just serving as a flexible linker between the receiver and effector domains. However, since there is no obvious similarity of this 'linker' to other protein sequences deposited in public databases, extrapolation of any further information becomes difficult. Lange *et al.* has postulated that because of the large nature of this region, the YesN-like response regulator might be under dual control, one in which the cognate histidine kinase controls phosphorylation of the receiver domain, and another mechanism potentially controls the function of the insert region (133). However, Hancock and Perego propose an alternative explanation. Due to the variability and length of the 'linker' region, they suggest that it may serve solely as a linker to tether the receiver and effector domains together (91). Which author's theory is correct still remains up for debate, as no experimental evidence presented here in this dissertation is concrete evidence for or against either model.

In support of Lange's hypothesis, the STRING 8.3 bioinformatics program, a predictor of protein-protein interactions, has predicted that TrxR may have a binding partner in M5005_Spy_1062 (TCS5R), the 5th response regulator in the genome. Although many of the TCSs in GAS have been characterized, little is known about TCS5. An NCBI search of TCS5R predicts a role for the protein in maltodextrose utilization, although no direct connections between TCS5R and maltodextrin have been reported thus far. Numerous studies have implicated a role of maltodextrose in GAS oropharynx infections (220, 221, 223), and the major virulence regulator CovR has also been shown to positively regulate TCS5 while negatively regulating TrxSR (81). Is it therefore possible that unphosphorylated CovR activates TCS5R in response to maltodextrose, and leads to the binding of TCS5R to basal amounts of TrxR present in the cell, all before CovR becomes phosphorylated and has a chance to relieve its own repression of *trxR*? Thus, could TCS5R interact with TrxR in a separate, independent manner from either TrxS or CovR, and could this 'linker' region be an important binding domain for TCS5R to control TrxR's activity? With such a complex hypothesis, ascertaining the validity of this theory would begin with determining whether a separate function exists for the 'linker' region of TrxR. Further experimentation aimed at understanding the overall domain structure and regulation of TrxR will potentially shed light on the complexities of this unique protein.

Interestingly, phosphorylation data may also indicate a multifaceted function for the TrxR protein within the GAS cell. Our data suggest that phosphorylation of TrxR's catalytic aspartate is not necessary for its gene activation of *emm, sic* or *opuAA in vivo*. Both the D55A and D55E catalytic mutants of TrxR were able to rescue a *trxR*$^{-}$

phenotype, indicating that the phosphorylation status at D55 of TrxR is not critical to its ascribed function. Why does TrxR participate in a phosphorelay with TrxS, then, if the phosphorylated form of TrxR acts no differently than its unphosphorylated counterpart to regulate gene expression? Is it possible that TrxR is activated by a mechanism other than phosphorylation at D55? Could there be a second site of phosphorylation in TrxR? Unfortunately, at the present time, answers to either of these questions remain unclear. If, for example, TrxR acted in a similar fashion to CheY of *E. coli* (7), then there may be a second site of possible phosphorylation at the N-terminal serine residue, Ser-54, in the absence of an aspartate at residue 55 in our TrxR D55A protein. The adjacent serine residue may retain the ability to act as a ligand for Mg^{2+}, due to its carbonyl residue, and thus could provide a second site for phosphorylation-induced activity in our TrxR D55A protein as it did for CheY's D57N protein (7). Additional experiments on such mutant proteins are necessary in order to assess the importance of this neighboring residue, and determine its significance to the *in vitro* phosphorylation and *in vivo* activity of TrxR.

Global influence of TrxSR on regulation in GAS

GAS has the ability to cause a variety of diseases within the human host, and can infect different sites/tissues such as the respiratory tract, skin, and the bloodstream. In order to infect such a wide range of environments, GAS coordinately regulates its factors for survival in these unique locations. This study presents evidence suggesting that TrxSR represents a new pathway within GAS to influence disease progression. Not only has it been shown that TrxSR is regulated by the CovRS TCS, but evidence presented

here also links TrxSR to Mga, a transcriptional regulator of the core virulence genes of GAS.

The stand-alone regulator Mga activates a defined set of "core" virulence genes encoding factors important for early stages of colonization and resistance to the host immune response (103). Although the Mga regulon is induced by growth conditions such as logarithmic growth and elevated iron or CO_2 levels, only a few regulatory networks have been linked to *mga* regulation. The metal-dependent MtsR regulator can directly bind to P*mga* and activate *mga* expression, suggesting a link between iron/metal homeostasis and the Mga regulon (256). The stationary phase-associated stand-alone regulators Rgg/RopB, RofA, and Nra are known to repress *mga* expression, either directly or indirectly, providing a mechanism for shutting the Mga regulon down. In addition, RivR/RALP4 appears to work with the Mga protein to directly enhance Mga activation of its target gene promoters, possibly through protein-protein interactions, and RivX, a small RNA, acts at the *mga* promoter to activate transcription of Mga regulon genes (210). This work adds TrxSR to the list of regulators interacting with the Mga regulon. Additionally, TrxSR not only represents the first TCS to regulate Mga expression, but it does so in a direct, activating manner.

We can now begin to model the complex interactions that occur between different regulatory pathways in GAS that influence disease progression (Fig 22). The CovRS TCS plays a central role in this process by negatively regulating genes (*ska, has*, and *sag*) as well as several TCS regulatory loci linked to virulence, in response to stress and possibly other signals. CovR also represses expression of *rivR* and *rivX*, encoding a stand-alone regulator and small RNA, respectively, which enhance transcriptional

activation by another stand-alone response regulator, Mga (Fig 22). The newly defined virulence-associated TCS, TrxSR, is also able to directly activate transcription of *mga* and Mga-regulated genes in response to an as of yet unidentified *in vivo* signal (13). Therefore, there are two distinct pathways by which CovR downregulates Mga regulon expression and two separate opportunities for distinct signal input to control expression of these virulence genes. The Mga virulence regulon is controlled by conditions conducive to productive growth such as CO_2 levels and sugars (103). Recent evidence suggests that the GAS phosphoenolpyruvate:carbohydrate phosphotransferase system and carbon catabolite repression through CcpA play a major role in this regulation. Further identification of regulatory links between these virulence networks will help to better elucidate their contribution to pathogenesis and the complex interplay that occurs *in vivo* during GAS disease.

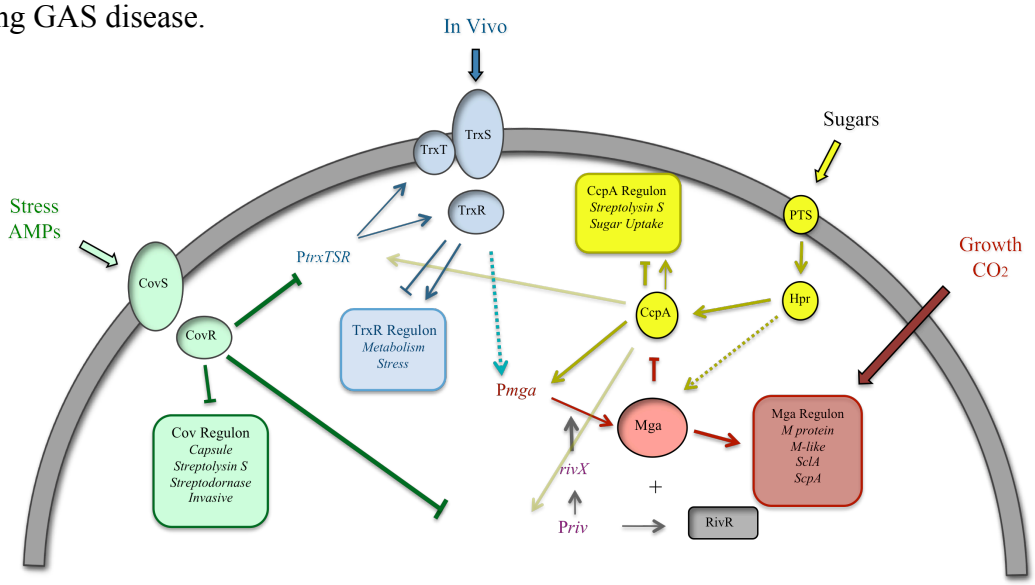

FIGURE 22. **Model for interacting virulence regulation in GAS.** Schematic representation of components for the CovRS TCS (green) and TrxSR TCS (blue) are shown. Stand-alone regulators Mga (red) and RivR/RivX (purple) as well as CcpA (yellow) are shown within the context of a GAS cell. Thin arrows show production of gene product(s) from the indicated promoter. Thick arrowheads indicate activation, and thick flat ends reflect repression by the connected regulator. Solid lines indicate direct regulation, while dashed lines indicate either indirect or unknown regulation. Known or predicted external signals for the regulatory pathways are shown.

Interestingly, our transcriptome study that revealed these new interactions between the aforementioned virulence regulatory networks was completed at late logarithmic phase, a point in growth at which numerous transcriptional changes take place during the transition from exponential growth to stationary phase. In addition to TrxR's effect on *mga* at this growth point, TrxR also represses a small number of various genes involved in such processes as amino acid biosynthesis and the stress response. In total, 29 gene transcripts were significantly affected. Although this number appears low, it does not appear to be abnormal, as for example relatively few GAS genes (28) were affected by the Ihk/Irr TCS at a time period of 30 minutes post addition of the bacteria to PMNs (267). However, the number of Irr-regulated genes increased at later time points in growth, growing the total Irr-regulon to well over 200 genes. Additionally, as seen with the CovR response regulator, gene transcript levels varied widely across growth, with 98 and 229 gene transcripts affected in late-exponential and stationary phases of growth, respectively (81). Because it appears that many RRs of GAS regulate different sets of genes at various points in growth, it's possible that we may discover a larger TrxR regulon when transcriptome analyses at other points in growth are performed.

As such, our P*trxT-luc* experiments that assayed expression from P*trxT* across growth (Fig 7), showed two points within growth where expression was maximal from this promoter. The first point within growth, which showed high transcriptional expression from P*trxT,* was late-logarithmic phase, the same time point chosen for the microarray. Not only does this validate our reasoning for choosing this point for the microarray, but it also confirms our assumption that TrxR has an important role in the cell at this time. The second peak seen in the P*trxT-luc* expression profile appeared

roughly 60-90 minutes into stationary phase, and represents a point at which both CovR and SptR affect transcription of a wider range of genes than they do at any other period (81, 222). Since we can only predict that TrxR might have a similar role in stationary phase, based upon its peak in transcriptional expression from the luciferase assay, it would be of interest to complete a transcriptome study in stationary phase to get a broader look at the overall TrxR regulon.

Could TrxR be linked to such genes utilized in sugar metabolism early in stationary phase? The position of *trxTSR* in the GAS chromosome may suggest that it could. Not only is *trxTSR* located immediately downstream of an ABC sugar transport system, but *trxR* is located immediately upstream of and found to be sometimes co-transcribed with β-galactosidase, an enzyme involved in the catabolism of lactose within the bacterial cell (Fig 5). This central location of *trxTSR* between genes involved in sugar metabolism suggests a potential role or relationship for the TrxSR TCS with sugar transport and metabolism. In fact, this entire *trx* region was found to be upregulated in an *in vivo* murine chamber infection model (13), suggesting that these systems may in fact be linked in some way during infection. Consequently, when a second stationary-phase transcriptome study is complete, and a broader TrxR-regulon is described, we may begin to establish a link for other TrxR-regulated genes found in late-exponential phase and clarify the role of TrxR to the GAS cell.

Summary

In conclusion, the results of this work have identified the role of the TrxSR TCS in the activation of the Mga-regulated virulence factors. Beyond direct regulation of

these factors through interaction with P*mga*, it was found that TrxR is a multifaceted protein with many complexities, including its requirement for phosphorylation. Overall, the results provided within this dissertation have established TrxSR as a major contributor in the network of virulence regulation utilized by GAS to adapt to host niches.

REFERENCES:

1. **Akao, T., T. Takahashi, and K. Kobashi.** 1992. Purification and characterization of a peptide essential for formation of streptolysin S by *Streptococcus pyogenes*. Infection and Immunity **60:**4777-80.
2. **Akesson, P., K. H. Schmidt, J. Cooney, and L. Bjorck.** 1994. M1 protein and protein H: IgGFc- and albumin-binding streptococcal surface proteins encoded by adjacent genes. Biochemistry Journal **300 (Pt 3):**877-86.
3. **Akira, S., and K. Takeda.** 2004. Toll-like receptor signalling. Nature Reviews Immunology **4:**499-511.
4. **Almengor, A. C., T. L. Kinkel, S. J. Day, and K. S. McIver.** 2007. The catabolite control protein CcpA binds to P*mga* and influences expression of the virulence regulator Mga in the group A streptococcus. Journal of Bacteriology **189:**8405-8416.
5. **Andre, I., J. Persson, A. M. Blom, H. Nilsson, T. Drakenberg, G. Lindahl, and S. Linse.** 2006. Streptococcal M protein: structural studies of the hypervariable region, free and bound to human C4BP. Biochemistry **45:**4559-68.
6. **Anthony, B. F.** 2000. Streptococcal pyoderma, p. 144-151. *In* D. L. Stevens and E. L. Kaplan (ed.), Streptococcal Infections: Clinical Aspects, Microbiology, and Molecular Pathogenesis. Oxford University Press, New York.
7. **Appleby, J. L., and R. B. Bourret.** 1999. Activation of CheY mutant D57N by phosphorylation at an alternative site, Ser-56. Molecular Microbiology **34:**915-25.
8. **Appleby, J. L., and R. B. Bourret.** 1998. Proposed signal transduction role for conserved CheY residue Thr87, a member of the response regulator active-site quintet. Journal of Bacteriology **180:**3563-9.
9. **Ashbaugh, C. D., H. B. Warren, V. J. Carey, and M. R. Wessels.** 1998. Molecular analysis of the role of the group A streptococcal cysteine protease, hyaluronic acid capsule, and M protein in a murine model of human invasive soft-tissue infection. Journal of Clinical Investigations **102:**550-60.
10. **Ashbaugh, C. D., and M. R. Wessels.** 2001. Absence of a cysteine protease effect on bacterial virulence in two murine models of human invasive group A streptococcal infection. Infection and Immunity **69:**6683-8.
11. **Ausubel, F., R. Brent, R. Kingston, D. Moore, J. Seidman, J. Smith, and K. Struhl (ed.).** 1997. Short Protocols in Molecular Biology, 3rd ed. John Wiley & Sons, Inc., New York.
12. **Aziz, R. K., R. A. Edwards, W. W. Taylor, D. E. Low, A. McGeer, and M. Kotb.** 2005. Mosaic prophages with horizontally acquired genes account for the emergence and diversification of the globally disseminated M1T1 clone of *Streptococcus pyogenes*. Journal of Bacteriology **187:**3311-8.
13. **Aziz, R. K., R. Kansal, B. J. Aronow, W. L. Taylor, S. L. Rowe, M. Kubal, G. S. Chhatwal, M. J. Walker, and M. Kotb.** 2010. Microevolution of group A streptococci in vivo: capturing regulatory networks engaged in sociomicrobiology, niche adaptation, and hypervirulence. PLoS One **5:**e9798.
14. **Aziz, R. K., M. J. Pabst, A. Jeng, R. Kansal, D. E. Low, V. Nizet, and M. Kotb.** 2004. Invasive M1T1 group A Streptococcus undergoes a phase-shift in

vivo to prevent proteolytic degradation of multiple virulence factors by SpeB. Molecular Microbiology **51:**123-34.

15. **Bader, M. W., S. Sanowar, M. E. Daley, A. R. Schneider, U. Cho, W. Xu, R. E. Klevit, H. Le Moual, and S. I. Miller.** 2005. Recognition of antimicrobial peptides by a bacterial sensor kinase. Cell **122:**461-72.
16. **Bates, C. S., C. Toukoki, M. N. Neely, and Z. Eichenbaum.** 2005. Characterization of MtsR, a new metal regulator in group A streptococcus, involved in iron acquisition and virulence. Infection and Immunity **73:**5743-53.
17. **Beall, B., R. Facklam, and T. Thompson.** 1996. Sequencing *emm*-specific PCR products for routine and accurate typing of group A streptococci. Journal of Clinical Microbiology **34:**953-8.
18. **Beall, B., G. Gherardi, M. Lovgren, R. R. Facklam, B. A. Forwick, and G. J. Tyrrell.** 2000. emm and sof gene sequence variation in relation to serological typing of opacity-factor-positive group A streptococci. Microbiology **146 (Pt 5):**1195-209.
19. **Beckert, S., B. Kreikemeyer, and A. Podbielski.** 2001. Group A streptococcal *rofA* gene is involved in the control of several virulence genes and eukaryotic cell attachment and internalization. Infection and Immunity **69:**534-537.
20. **Beres, S. B., E. W. Richter, M. J. Nagiec, P. Sumby, S. F. Porcella, F. R. DeLeo, and J. M. Musser.** 2006. Molecular genetic anatomy of inter- and intraserotype variation in the human bacterial pathogen group A Streptococcus. Proceedings of the National Academy of Sciences of the United States of America **103:**7059-64.
21. **Bernish, B., and I. van de Rijn.** 1999. Characterization of a two-component system in *Streptococcus pyogenes* which is involved in regulation of hyaluronic acid production. Journal of Biological Chemistry **274:**4786-93.
22. **Bessen, D., K. F. Jones, and V. A. Fischetti.** 1989. Evidence for two distinct classes of streptococcal M protein and their relationship to rheumatic fever. Journal of Experimental Medicine **169:**269-283.
23. **Bessen, D. E.** 2009. Population biology of the human restricted pathogen, Streptococcus pyogenes. Infection, Genetics, and Evolution **9:**581-93.
24. **Bessen, D. E., A. Manoharan, F. Luo, J. E. Wertz, and D. A. Robinson.** 2005. Evolution of transcription regulatory genes is linked to niche specialization in the bacterial pathogen *Streptococcus pyogenes*. Journal of Bacteriology **187:**4163-72.
25. **Bilwes, A. M., L. A. Alex, B. R. Crane, and M. I. Simon.** 1999. Structure of CheA, a signal-transducing histidine kinase. Cell **96:**131-41.
26. **Bisno, A. L., M. O. Brito, and C. M. Collins.** 2003. Molecular basis of group A streptococcal virulence. Lancet Infectious Diseases **3:**191-200.
27. **Bisno, A. L., and D. L. Stevens.** 1996. Streptococcal infections of skin and soft tissues. New England Journal of Medicine **334:**240-5.
28. **Borkovich, K. A., L. A. Alex, and M. I. Simon.** 1992. Attenuation of sensory receptor signaling by covalent modification. Proceedings of the National Academy of Sciences of the United States of America **89:**6756-60.
29. **Boyle, M. D., R. Raeder, A. Flosdorff, and A. Podbielski.** 1998. Role of emm and mrp genes in the virulence of group A streptococcal isolate 64/14 in a mouse model of skin infection. Journal of Infectious Disease **177:**991-997.

30. **Bricker, A. L., V. J. Carey, and M. R. Wessels.** 2005. Role of NADase in virulence in experimental invasive group A streptococcal infection. Infection and Immunity **73:**6562-6.
31. **Bricker, A. L., C. Cywes, C. D. Ashbaugh, and M. R. Wessels.** 2002. NAD+-glycohydrolase acts as an intracellular toxin to enhance the extracellular survival of group A streptococci. Molecular Microbiology **44:**257-69.
32. **Brunskill, E. W., and K. W. Bayles.** 1996. Identification and molecular characterization of a putative regulatory locus that affects autolysis in Staphylococcus aureus. Journal of Bacteriology **178:**611-8.
33. **Buchanan, J. T., A. J. Simpson, R. K. Aziz, G. Y. Liu, S. A. Kristian, M. Kotb, J. Feramisco, and V. Nizet.** 2006. DNase expression allows the pathogen group A Streptococcus to escape killing in neutrophil extracellular traps. Current Biology **16:**396-400.
34. **Burbulys, D., K. A. Trach, and J. A. Hoch.** 1991. Initiation of sporulation in B. subtilis is controlled by a multicomponent phosphorelay. Cell **64:**545-52.
35. **Caparon, M. G., R. T. Geist, J. Perez-Casal, and J. R. Scott.** 1992. Environmental regulation of virulence in group A streptococci: transcription of the gene encoding M protein is stimulated by carbon dioxide. Journal of Bacteriology **174:**5693-5701.
36. **Carapetis, J. R., A. C. Steer, E. K. Mulholland, and M. Weber.** 2005. The global burden of group A streptococcal diseases. The Lancet Infectious Diseases **5:**685-94.
37. **Caron, J., L. M. Coffield, and J. R. Scott.** 1989. A plasmid-encoded regulatory gene, rns, required for expression of the CS1 and CS2 adhesins of enterotoxigenic Escherichia coli. Proceedings of the National Academy of Sciences of the United States of America **86:**963-7.
38. **Carr, A., D. D. Sledjeski, A. Podbielski, M. D. Boyle, and B. Kreikemeyer.** 2001. Similarities between complement-mediated and streptolysin S-mediated hemolysis. Journal of Biological Chemistry **276:**41790-6.
39. **Caswell, C. C., R. Han, K. M. Hovis, P. Ciborowski, D. R. Keene, R. T. Marconi, and S. Lukomski.** 2008. The Scl1 protein of M6-type group A Streptococcus binds the human complement regulatory protein, factor H, and inhibits the alternative pathway of complement. Molecular Microbiology **67:**584-96.
40. **Chang, C., and R. C. Stewart.** 1998. The two-component system. Regulation of diverse signaling pathways in prokaryotes and eukaryotes. Plant Physiology **117:**723-31.
41. **Chassy, B. M.** 1976. A gentle method for the lysis of oral streptococci. Biochemical and Biophysical Research Communication **68:**603-8.
42. **Chaussee, M. A., E. A. Callegari, and M. S. Chaussee.** 2004. Rgg regulates growth phase-dependent expression of proteins associated with secondary metabolism and stress in *Streptococcus pyogenes*. Journal of Bacteriology **186:**7091-9.
43. **Chaussee, M. S., D. Ajdic, and J. J. Ferretti.** 1999. The *rgg* gene of *Streptococcus pyogenes* NZ131 positively influences extracellular SPE B production. Infection and Immunity **67:**1715-22.

44. **Chaussee, M. S., G. A. Somerville, L. Reitzer, and J. M. Musser.** 2003. Rgg coordinates virulence factor synthesis and metabolism in *Streptococcus pyogenes*. Journal of Bacteriology **185:**6016-24.
45. **Chaussee, M. S., G. L. Sylva, D. E. Sturdevant, L. M. Smoot, M. R. Graham, R. O. Watson, and J. M. Musser.** 2002. Rgg influences the expression of multiple regulatory loci to coregulate virulence factor expression in *Streptococcus pyogenes*. Infection and Immunity **70:**762-70.
46. **Chen, C., N. Bormann, and P. P. Cleary.** 1993. VirR and Mry are homologous trans-acting regulators of M protein and C5a peptidase expression in group A streptococci. Molecular and General Genetics **241:**685-693.
47. **Chen, S. M., Y. S. Tsai, C. M. Wu, S. K. Liao, L. C. Wu, C. S. Chang, Y. H. Liu, and P. J. Tsai.** 2010. Streptococcal collagen-like surface protein 1 promotes adhesion to the respiratory epithelial cell. BMC Microbiology **10:**320.
48. **Cleary, P. P., Y. V. Matsuka, T. Huynh, H. Lam, and S. B. Olmsted.** 2004. Immunization with C5a peptidase from either group A or B streptococci enhances clearance of group A streptococci from intranasally infected mice. Vaccine **22:**4332-41.
49. **Cleary, P. P., U. Prahbu, J. B. Dale, D. E. Wexler, and J. Handley.** 1992. Streptococcal C5a peptidase is a highly specific endopeptidase. Infection and Immunity **60:**5219-23.
50. **Collin, M., M. D. Svensson, A. G. Sjoholm, J. C. Jensenius, U. Sjobring, and A. Olsen.** 2002. EndoS and SpeB from Streptococcus pyogenes inhibit immunoglobulin-mediated opsonophagocytosis. Infection and Immunity **70:**6646-51.
51. **Connolly, K. L., A. L. Roberts, R. C. Holder, and S. D. Reid.** 2011. Dispersal of Group A Streptococcal Biofilms by the Cysteine Protease SpeB Leads to Increased Disease Severity in a Murine Model. PLoS One **6:**e18984.
52. **Courtney, H. S., J. B. Dale, and D. I. Hasty.** 1996. Differential effects of the streptococcal fibronectin-binding protein, FBP54, on adhesion of group A streptococci to human buccal cells and HEp-2 tissue culture cells. Infection and Immunity **64:**2415-9.
53. **Courtney, H. S., D. L. Hasty, Y. Li, H. C. Chiang, J. L. Thacker, and J. B. Dale.** 1999. Serum opacity factor is a major fibronectin-binding protein and a virulence determinant of M type 2 *Streptococcus pyogenes*. Molecular Microbiology **32:**89-98.
54. **Courtney, H. S., Y. M. Zhang, M. W. Frank, and C. O. Rock.** 2006. Serum opacity factor, a streptococcal virulence factor that binds to apolipoproteins A-I and A-II and disrupts high density lipoprotein structure. Journal of Biological Chemistry **281:**5515-21.
55. **Cunningham, M. W.** 2000. Pathogenesis of group A streptococcal infections. Clinical Microbiology Reviews **13:**470-511.
56. **Dale, J. B., and E. H. Beachey.** 1985. Epitopes of streptococcal M proteins shared with cardiac myosin. Journal of Experimental Medicine **162:**583-91.
57. **Dalton, T. L., R. I. Hobb, and J. R. Scott.** 2006. Analysis of the role of CovR and CovS in the dissemination of Streptococcus pyogenes in invasive skin disease. Microbial Pathogenesis **40:**221-7.

58. **Dalton, T. L., and J. R. Scott.** 2004. CovS inactivates CovR and is required for growth under conditions of general stress in *Streptococcus pyogenes*. Journal of Bacteriology **186:**3928-37.
59. **Datta, V., S. M. Myskowski, L. A. Kwinn, D. N. Chiem, N. Varki, R. G. Kansal, M. Kotb, and V. Nizet.** 2005. Mutational analysis of the group A streptococcal operon encoding streptolysin S and its virulence role in invasive infection. Molecular Microbiology **56:**681-95.
60. **Denny, F. W., Jr.** 2000. History of hemolytic streptococci and associated diseases, p. 1-18. *In* D. L. Stevens and E. L. Kaplan (ed.), Streptococcal Infections: Clinical Aspects, Microbiology, and Molecular Pathogenesis. Oxford University Press, New York.
61. **Doern, C. D., A. L. Roberts, W. Hong, J. Nelson, S. Lukomski, W. E. Swords, and S. D. Reid.** 2009. Biofilm formation by group A Streptococcus: a role for the streptococcal regulator of virulence (Srv) and streptococcal cysteine protease (SpeB). Microbiology **155:**46-52.
62. **Dorman, C. J.** 1992. The VirF protein from Shigella flexneri is a member of the AraC transcription factor superfamily and is highly homologous to Rns, a positive regulator of virulence genes in enterotoxigenic Escherichia coli. Molecular Microbiology **6:**1575-6.
63. **Dumon-Seignovert, L., G. Cariot, and L. Vuillard.** 2004. The toxicity of recombinant proteins in Escherichia coli: a comparison of overexpression in BL21(DE3), C41(DE3), and C43(DE3). Protein Expression and Purification **37:**203-6.
64. **Dutta, R., and M. Inouye.** 1996. Reverse phosphotransfer from OmpR to EnvZ in a kinase-/phosphatase+ mutant of EnvZ (EnvZ.N347D), a bifunctional signal transducer of Escherichia coli. Journal of Biological Chemistry **271:**1424-9.
65. **Eberhard, T. H., D. D. Sledjeski, and M. D. Boyle.** 2001. Mouse skin passage of a *Streptococcus pyogenes* Tn917 mutant of *sagA/pel* restores virulence, beta-hemolysis and *sagA/pel* expression without altering the position or sequence of the transposon. BMC Microbiology **1:**33.
66. **Edwards, R. J., G. W. Taylor, M. Ferguson, S. Murray, N. Rendell, A. Wrigley, Z. Bai, J. Boyle, S. J. Finney, A. Jones, H. H. Russell, C. Turner, J. Cohen, L. Faulkner, and S. Sriskandan.** 2005. Specific C-terminal cleavage and inactivation of interleukin-8 by invasive disease isolates of Streptococcus pyogenes. Journal of Infectious Diseases **192:**783-90.
67. **Eriksson, A., and M. Norgren.** 2003. Cleavage of antigen-bound immunoglobulin G by SpeB contributes to streptococcal persistence in opsonizing blood. Infection and Immunity **71:**211-7.
68. **Fabret, C., V. A. Feher, and J. A. Hoch.** 1999. Two-component signal transduction in Bacillus subtilis: how one organism sees its world. Journal of Bacteriology **181:**1975-83.
69. **Federle, M. J., K. S. McIver, and J. R. Scott.** 1999. A response regulator that represses transcription of several virulence operons in the group A streptococcus. Journal of Bacteriology **181:**3649-3657.
70. **Fernie-King, B. A., D. J. Seilly, A. Davies, and P. J. Lachmann.** 2002. Streptococcal inhibitor of complement inhibits two additional components of the

mucosal innate immune system: secretory leukocyte proteinase inhibitor and lysozyme. Infection and Immunity **70:**4908-16.

71. **Fernie-King, B. A., D. J. Seilly, C. Willers, R. Wurzner, A. Davies, and P. J. Lachmann.** 2001. Streptococcal inhibitor of complement (SIC) inhibits the membrane attack complex by preventing uptake of C567 onto cell membranes. Immunology **103:**390-8.
72. **Fogg, G. C., C. M. Gibson, and M. G. Caparon.** 1994. The identification of *rofA*, a positive-acting regulatory component of *prtF* expression: use of an m-gamma-delta-based shuttle mutagenesis strategy in *Streptococcus pyogene*s. Molecular Microbiology **11:**671-684.
73. **Foussard, M., S. Cabantous, J.-D. Pedelacq, V. Guillet, S. Tranier, L. Mourey, C. Birck, and J.-P. Samama.** 2001. The Molecular Puzzle of Two-Component Signaling Cascades. Microbes and Infection **3:**417-424.
74. **Frick, I. M., P. Akesson, M. Rasmussen, A. Schmidtchen, and L. Bjorck.** 2003. SIC, a secreted protein of *Streptococcus pyogenes* that inactivates antibacterial peptides. Journal of Biological Chemistry **278:**16561-6.
75. **Gallegos, M. T., R. Schleif, A. Bairoch, K. Hofmann, and J. L. Ramos.** 1997. Arac/XylS family of transcriptional regulators. Microbiology and Molecular Biology Reviews **61:**393-410.
76. **Galperin, M. Y.** 2006. Structural classification of bacterial response regulators: diversity of output domains and domain combinations. Journal of Bacteriology **188:**4169-82.
77. **Gao, R., and A. M. Stock.** 2009. Biological insights from structures of two-component proteins. Annual Review of Microbiology **63:**133-54.
78. **Garcia, A. F., L. M. Abe, G. Erdem, C. L. Cortez, D. Kurahara, and K. Yamaga.** 2010. An insert in the covS gene distinguishes a pharyngeal and a blood isolate of Streptococcus pyogenes found in the same individual. Microbiology **156:**3085-95.
79. **Gerlach, D., K. H. Schmidt, and B. Fleischer.** 2001. Basic streptococcal superantigens (SPEX/SMEZ or SPEC) are responsible for the mitogenic activity of the so-called mitogenic factor (MF). FEMS Immunology and Medical Microbiology **30:**209-16.
80. **Ginsburg, I.** 1999. Is streptolysin S of group A streptococci a virulence factor? Acta Pathologica, Microbiologica et Immunologica Scandinavica **107:**1051-9.
81. **Graham, M. R., L. M. Smoot, C. A. Migliaccio, K. Virtaneva, D. E. Sturdevant, S. F. Porcella, M. J. Federle, G. J. Adams, J. R. Scott, and J. M. Musser.** 2002. Virulence control in group A streptococcus by a two-component gene regulatory system: global expression profiling and in vivo infection modeling. Proceedings of the National Academy of Sciences of the United States of America **99:**13855-60.
82. **Graham, M. R., K. Virtaneva, S. F. Porcella, W. T. Barry, B. B. Gowen, C. R. Johnson, F. A. Wright, and J. M. Musser.** 2005. Group A Streptococcus transcriptome dynamics during growth in human blood reveals bacterial adaptive and survival strategies. American Journal of Pathology **166:**455-65.
83. **Graham, M. R., K. Virtaneva, S. F. Porcella, D. J. Gardner, R. D. Long, D. M. Welty, W. T. Barry, C. A. Johnson, L. D. Parkins, F. A. Wright, and J. M.**

Musser. 2006. Analysis of the transcriptome of group A Streptococcus in mouse soft tissue infection. American Journal of Pathology **169:**927-42.

84. **Grebe, T. W., and J. B. Stock.** 1999. The histidine protein kinase superfamily. Advances in Microbial Physiology **41:**139-227.
85. **Griffiths, B. B., and O. McClain.** 1988. The role of iron in the growth and hemolysin (Streptolysin S) production in Streptococcus pyogenes. Journal of Basic Microbiology **28:**427-36.
86. **Gryllos, I., J. C. Levin, and M. R. Wessels.** 2003. The CsrR/CsrS two-component system of group A streptococcus responds to environmental Mg_{2+}. Proceedings of the National Academy of Sciences of the United States of America **100:**4227-32.
87. **Guzman, C. A., S. R. Talay, G. Molinari, E. Medina, and G. S. Chhatwal.** 1999. Protective immune response against Streptococcus pyogenes in mice after intranasal vaccination with the fibronectin-binding protein SfbI. Journal of Infectious Diseases **179:**901-6.
88. **Haanes, E. J., D. G. Heath, and P. P. Cleary.** 1992. Architecture of the *vir* regulons of group A streptococci parallels opacity factor phenotype and M protein class. Journal of Bacteriology **174:**4967-4976.
89. **Hallas, G., and J. P. Widdowson.** 1982. The opacity factor of group-A streptococci. Journal of Medical Microbiology **15:**451-64.
90. **Hanahan, D., and M. Meselson.** 1983. Plasmid screening at high colony density. Methods in Enzymology **100:**333-42.
91. **Hancock, L., and M. Perego.** 2002. Two-component signal transduction in Enterococcus faecalis. Journal of Bacteriology **184:**5819-25.
92. **Hancock, L. E., and M. Perego.** 2004. Systematic inactivation and phenotypic characterization of two-component signal transduction systems of Enterococcus faecalis V583. Journal of Bacteriology **186:**7951-8.
93. **Hanski, E., and M. Caparon.** 1992. Protein F, a fibronectin-binding protein, is an adhesin of the group A streptococcus *Streptococcus pyogenes*. Proceedings of the National Academy of Sciences of the United States of America **89:**6172-6176.
94. **Hastings, C. A., S. Y. Lee, H. S. Cho, D. Yan, S. Kustu, and D. E. Wemmer.** 2003. High-resolution solution structure of the beryllofluoride-activated NtrC receiver domain. Biochemistry **42:**9081-90.
95. **Hasty, D. L., I. Ofek, H. S. Courtney, and R. J. Doyle.** 1992. Multiple adhesins of streptococci. Infection and Immunity **60:**2147-52.
96. **Hava, D. L., and A. Camilli.** 2002. Large-scale identification of serotype 4 *Streptococcus pneumoniae* virulence factors. Molecular Microbiology **45:**1389-406.
97. **Heath, A., V. J. DiRita, N. L. Barg, and N. C. Engleberg.** 1999. A two-component regulatory system, CsrR-CsrS, represses expression of three *Streptococcus pyogenes* virulence factors, hyaluronic acid capsule, streptolysin S, and pyrogenic exotoxin B. Infection and Immunity **67:**5298-5305.
98. **Ho, S. N., H. D. Hunt, R. M. Horton, J. K. Pullen, and L. R. Pease.** 1989. Site-directed mutagenesis by overlap extension using the polymerase chain reaction. Gene **77:**51-9.

99. **Hoe, N. P., R. M. Ireland, F. R. DeLeo, B. B. Gowen, D. W. Dorward, J. M. Voyich, M. Liu, E. H. Burns, Jr., D. M. Culnan, A. Bretscher, and J. M. Musser.** 2002. Insight into the molecular basis of pathogen abundance: group A streptococcus inhibitor of complement inhibits bacterial adherence and internalization into human cells. Proceedings of the National Academy of Sciences of the United States of America **99:**7646-51.
100. **Hollingshead, S. K., V. A. Fischetti, and J. R. Scott.** 1987. Size variation in group A streptococcal M protein is generated by homologous recombination between intragenic repeats. Molecular and General Genetics **207:**196-203.
101. **Hollingshead, S. K., T. L. Readdy, D. L. Yung, and D. E. Bessen.** 1993. Structural heterogeneity of the *emm* gene cluster in group A streptococci. Molecular Microbiology **8:**707-17.
102. **Holm, S. E., A. Nordstrand, D. L. Stevens, and M. Norgreen.** 2000. Acute poststreptococcal glomerulonephritis, p. 152-62. *In* D. L. Stevens and E. L. Kaplan (ed.), Streptococcal Infections: Clinical Aspects, Microbiology, and Molecular Pathogenesis. Oxford University Press, New York.
103. **Hondorp, E. R., and K. S. McIver.** 2007. The Mga virulence regulon: infection where the grass is greener. Molecular Microbiology **66:**1056-65.
104. **Horstmann, R. D., H. J. Sievertsen, J. Knobloch, and V. A. Fischetti.** 1988. Antiphagocytic activity of streptococcal M protein: selective binding of complement control protein factor H. Proceedings of the National Academy of Sciences of the United States of America **85:**1657-61.
105. **Horstmann, R. D., H. J. Sievertsen, M. Leippe, and V. A. Fischetti.** 1992. Role of fibrinogen in complement inhibition by streptococcal M protein. Infection and Immunity **60:**5036-41.
106. **Hsing, W., and T. J. Silhavy.** 1997. Function of conserved histidine-243 in phosphatase activity of EnvZ, the sensor for porin osmoregulation in Escherichia coli. Journal of Bacteriology **179:**3729-35.
107. **Hu, M. C., M. A. Walls, S. D. Stroop, M. A. Reddish, B. Beall, and J. B. Dale.** 2002. Immunogenicity of a 26-valent group A streptococcal vaccine. Infection and Immunity **70:**2171-7.
108. **Jaffe, J., S. Natanson-Yaron, M. G. Caparon, and E. Hanski.** 1996. Protein F2, a novel fibronectin-binding protein from *Streptococcus pyogenes*, possesses two binding domains. Molecular Microbiology **21:**373-84.
109. **Jeng, A., V. Sakota, Z. Li, V. Datta, B. Beall, and V. Nizet.** 2003. Molecular genetic analysis of a group A streptococcus operon encoding serum opacity factor and a novel fibronectin-binding protein, SfbX. Journal of Bacteriology **185:**1208-17.
110. **Ji, Y., B. Carlson, A. Kondagunta, and P. P. Cleary.** 1997. Intranasal immunization with C5a peptidase prevents nasopharyngeal colonization of mice by the group A streptococcus. Infection and Immunity **65:**2080-2087.
111. **Ji, Y., L. McLandsborough, A. Kondagunta, and P. P. Cleary.** 1996. C5a peptidase alters clearance and trafficking of group A streptococci by infected mice. Infection and Immunity **64:**503-10.
112. **Karasawa, T., S. Takasawa, K. Yamakawa, H. Yonekura, H. Okamoto, and S. Nakamura.** 1995. NAD(+)-glycohydrolase from Streptococcus pyogenes

shows cyclic ADP-ribose forming activity. FEMS Microbiology Letters **130:**201-4.

113. **Karimova, G., J. Pidoux, A. Ullmann, and D. Ladant.** 1998. A bacterial two-hybrid system based on a reconstituted signal transduction pathway. Proceedings of the National Academy of Sciences of the United States of America **95:**5752-6.
114. **Katerov, V., P. E. Lindgren, A. A. Totolian, and C. Schalen.** 2000. Streptococcal opacity factor: a family of bifunctional proteins with lipoproteinase and fibronectin-binding activities. Current Microbiology **40:**149-56.
115. **Kawamukai, M., K. Ferguson, M. Wigler, and D. Young.** 1991. Genetic and biochemical analysis of the adenylyl cyclase of Schizosaccharomyces pombe. Cell Regulation **2:**155-64.
116. **Keener, J., and S. Kustu.** 1988. Protein kinase and phosphoprotein phosphatase activities of nitrogen regulatory proteins NTRB and NTRC of enteric bacteria: roles of the conserved amino-terminal domain of NTRC. Proceedings of the National Academy of Sciences of the United States of America **85:**4976-80.
117. **Kern, D., B. F. Volkman, P. Luginbuhl, M. J. Nohaile, S. Kustu, and D. E. Wemmer.** 1999. Structure of a transiently phosphorylated switch in bacterial signal transduction. Nature **402:**894-8.
118. **Kihlberg, B. M., J. Cooney, M. G. Caparon, A. Olsen, and L. Bjorck.** 1995. Biological properties of a *Streptococcus pyogenes* mutant generated by Tn916 insertion in *mga*. Microbial Pathogenesis **19:**299-315.
119. **Kinkel, T. L., and K. S. McIver.** 2008. CcpA-mediated repression of streptolysin S expression and virulence in the group A streptococcus. Infection and Immunity **76:**3451-63.
120. **Kizy, A. E., and M. N. Neely.** 2009. First Streptococcus pyogenes signature-tagged mutagenesis screen identifies novel virulence determinants. Infection and Immunity **77:**1854-65.
121. **Klenk, M., D. Koczan, R. Guthke, M. Nakata, H. J. Thiesen, A. Podbielski, and B. Kreikemeyer.** 2005. Global epithelial cell transcriptional responses reveal Streptococcus pyogenes Fas regulator activity association with bacterial aggressiveness. Cellular Microbiology **7:**1237-50.
122. **Kotb, M.** 1995. Bacterial pyrogenic exotoxins as superantigens. Clinical Microbiology Reviews **8:**411-426.
123. **Kreikemeyer, B., S. Beckert, A. Braun-Kiewnick, and A. Podbielski.** 2002. Group A streptococcal RofA-type global regulators exhibit a strain-specific genomic presence and regulation pattern. Microbiology **148:**1501-11.
124. **Kreikemeyer, B., M. D. Boyle, B. A. Buttaro, M. Heinemann, and A. Podbielski.** 2001. Group A streptococcal growth phase-associated virulence factor regulation by a novel operon (Fas) with homologies to two-component-type regulators requires a small RNA molecule. Molecular Microbiology **39:**392-406.
125. **Kreikemeyer, B., D. R. Martin, and G. S. Chhatwal.** 1999. SfbII protein, a fibronectin binding surface protein of group A streptococci, is a serum opacity factor with high serotype-specific apolipoproteinase activity. FEMS Microbiology Letters **178:**305-11.
126. **Kreikemeyer, B., M. Nakata, T. Koller, H. Hildisch, V. Kourakos, K. Standar, S. Kawabata, M. O. Glocker, and A. Podbielski.** 2007. The

Streptococcus pyogenes serotype M49 Nra-Ralp3 transcriptional regulatory network and its control of virulence factor expression from the novel *eno ralp3 epf sagA* pathogenicity region. Infection and Immunity **75:**5698-5710.

127. **Kreikemeyer, B., M. Nakata, S. Oehmcke, C. Gschwendtner, J. Normann, and A. Podbielski.** 2005. *Streptococcus pyogenes* collagen type I-binding Cpa surface protein. Expression profile, binding characteristics, biological functions, and potential clinical impact. Journal of Biological Chemistry **280:**33228-39.
128. **Kreikemeyer, B., S. R. Talay, and G. S. Chhatwal.** 1995. Characterization of a novel fibronectin-binding surface protein in group A streptococci. Molecular Microbiology **17:**137-45.
129. **Krell, T., J. Lacal, A. Busch, H. Silva-Jimenez, M. E. Guazzaroni, and J. L. Ramos.** 2010. Bacterial sensor kinases: diversity in the recognition of environmental signals. Annual Review of Microbiology **64:**539-59.
130. **Kwinn, L. A., A. Khosravi, R. K. Aziz, A. M. Timmer, K. S. Doran, M. Kotb, and V. Nizet.** 2007. Genetic characterization and virulence role of the RALP3/LSA locus upstream of the streptolysin s operon in invasive M1T1 Group A Streptococcus. Journal of Bacteriology **189:**1322-9.
131. **Lancefield, R. C.** 1933. A serological differentiation of human and other groups of hemolytic streptococci. Journal of Experimental Medicine **57:**571-95.
132. **Lancefield, R. C.** 1962. Current knowledge of type-specific M antigens of group A streptococci. Journal of Immunology **89:**307-313.
133. **Lange, R., C. Wagner, A. de Saizieu, N. Flint, J. Molnos, M. Stieger, P. Caspers, M. Kamber, W. Keck, and K. E. Amrein.** 1999. Domain organization and molecular characterization of 13 two-component systems identified by genome sequencing of *Streptococcus pneumoniae*. Gene **237:**223-34.
134. **Laub, M. T., E. G. Biondi, and J. M. Skerker.** 2007. Phosphotransfer profiling: systematic mapping of two-component signal transduction pathways and phosphorelays. Methods in Enzymology **423:**531-48.
135. **Leday, T. V., K. M. Gold, T. L. Kinkel, S. A. Roberts, J. R. Scott, and K. S. McIver.** 2008. TrxR, a new CovR-repressed response regulator that activates the Mga virulence regulon in the Group A Streptococcus. Infect Immunity **76:**4659-68.
136. **Lee, V. T., J. M. Matewish, J. L. Kessler, M. Hyodo, Y. Hayakawa, and S. Lory.** 2007. A cyclic-di-GMP receptor required for bacterial exopolysaccharide production. Molecular Microbiology **65:**1474-84.
137. **Lei, B., F. R. DeLeo, N. P. Hoe, M. R. Graham, S. M. Mackie, R. L. Cole, M. Liu, H. R. Hill, D. E. Low, M. J. Federle, J. R. Scott, and J. M. Musser.** 2001. Evasion of human innate and acquired immunity by a bacterial homolog of CD11b that inhibits opsonophagocytosis. Nature Medicine **7:**1298-305.
138. **Lertcanawanichakul, M.** 2007. Construction of plasmid vector for expression of bacteriocin N15-encoding gene and effect of engineered bacteria on Enterococcus faecalis. Current Microbiology **54:**108-12.
139. **Levin, J. C., and M. R. Wessels.** 1998. Identification of *csrR*/*csrS*, a genetic locus that regulates hyaluronic acid capsule synthesis in group A streptococcus. Molecular Microbiology **30:**209-219.

140. **Li, Z., D. D. Sledjeski, B. Kreikemeyer, A. Podbielski, and M. D. Boyle.** 1999. Identification of *pel*, a *Streptococcus pyogenes* locus that affects both surface and secreted proteins. Journal of Bacteriology **181:**6019-6027.
141. **Limbago, B., V. Penumalli, B. Weinrick, and J. R. Scott.** 2000. Role of streptolysin O in a mouse model of invasive group A streptococcal disease. Infection and Immunity **68:**6384-90.
142. **Logsdon, L. K., A. P. Hakansson, G. Cortes, and M. R. Wessels.** 2011. Streptolysin o inhibits clathrin-dependent internalization of group a streptococcus. MBio **2:**00332-10.
143. **Lottenberg, R., D. Minning-Wenz, and M. D. Boyle.** 1994. Capturing host plasmin(ogen): a common mechanism for invasive pathogens? Trends in Microbiology **2:**20-4.
144. **Loughman, J. A., and M. Caparon.** 2006. Regulation of SpeB in Streptococcus pyogenes by pH and NaCl: a model for in vivo gene expression. Journal of Bacteriology **188:**399-408.
145. **Lukomski, S., N. P. Hoe, I. Abdi, J. Rurangirwa, P. Kordari, M. Liu, S. J. Dou, G. G. Adams, and J. M. Musser.** 2000. Nonpolar inactivation of the hypervariable streptococcal inhibitor of complement gene (*sic*) in serotype M1 *Streptococcus pyogenes* significantly decreases mouse mucosal colonization. Infection and Immunity **68:**535-42.
146. **Lukomski, S., C. A. Montgomery, J. Rurangirwa, R. S. Geske, J. P. Barrish, G. J. Adams, and J. M. Musser.** 1999. Extracellular cysteine protease produced by *Streptococcus pyogenes* participates in the pathogenesis of invasive skin infection and dissemination in mice. Infection and Immunity **67:**1779-88.
147. **Lukomski, S., K. Nakashima, I. Abdi, V. J. Cipriano, R. M. Ireland, S. D. Reid, G. G. Adams, and J. M. Musser.** 2000. Identification and characterization of the *scl* gene encoding a group A streptococcus extracellular protein virulence factor with similarity to human collagen. Infection and Immunity **68:**6542-6553.
148. **Lukomski, S., S. Sreevatsan, C. Amberg, W. Reichardt, M. Woischnik, A. Podbielski, and J. M. Musser.** 1997. Inactivation of Streptococcus pyogenes extracellular cysteine protease significantly decreases mouse lethality of serotype M3 and M49 strains. Journal of Clinical Investigations **99:**2574-80.
149. **Luo, F., S. Lizano, and D. E. Bessen.** 2008. Heterogeneity in the Polarity of Nra Regulatory Effects on Streptococcal Pilus Gene Transcription and Virulence. Infection and Immunity **76:**2490-7.
150. **Lynskey, N. N., R. A. Lawrenson, and S. Sriskandan.** 2011. New understandings in Streptococcus pyogenes. Current Opinion in Infectious Diseases **24:**196-202.
151. **Lyon, W. R., C. M. Gibson, and M. G. Caparon.** 1998. A role for trigger factor and an *rgg*-like regulator in the transcription, secretion and processing of the cysteine proteinase of *Streptococcus pyogenes*. EMBO Journal **17:**6263-6275.
152. **MacFarlane, S. A., and M. Merrick.** 1985. The nucleotide sequence of the nitrogen regulation gene ntrB and the glnA-ntrBC intergenic region of Klebsiella pneumoniae. Nucleic Acids Research **13:**7591-606.

153. **Magassa, N., S. Chandrasekaran, and M. G. Caparon.** 2010. Streptococcus pyogenes cytolysin-mediated translocation does not require pore formation by streptolysin O. EMBO Reports **11:**400-5.
154. **Magner, L. N.** 1992. A History of Medicine. New York Marcel Dekker, Inc.
155. **Malke, H., and J. J. Ferretti.** 2007. CodY-affected transcriptional gene expression of Streptococcus pyogenes during growth in human blood. Journal of Medical Microbiology **56:**707-14.
156. **Malke, H., K. Steiner, W. M. McShan, and J. J. Ferretti.** 2006. Linking the nutritional status of *Streptococcus pyogenes* to alteration of transcriptional gene expression: the action of CodY and RelA. International Journal of Medical Microbiology **296:**259-75.
157. **Mangold, M., M. Siller, B. Roppenser, B. J. Vlaminckx, T. A. Penfound, R. Klein, R. Novak, R. P. Novick, and E. Charpentier.** 2004. Synthesis of group A streptococcal virulence factors is controlled by a regulatory RNA molecule. Molecular Microbiology **53:**1515-27.
158. **Manzanera, M., S. Marques, and J. L. Ramos.** 2000. Mutational analysis of the highly conserved C-terminal residues of the XylS protein, a member of the AraC family of transcriptional regulators. FEBS Letters **476:**312-7.
159. **Markowitz, M., and E. L. Kaplan.** 2000. Rheumatic Fever, p. 133-151. *In* D. L. Stevens and E. L. Kaplan (ed.), Streptococcal Infections: Clinical Aspects, Microbiology, and Molecular Pathogenesis. Oxford University Press, New York.
160. **Martin, R. G., and J. L. Rosner.** 2001. The AraC transcriptional activators. Current Opinions in Microbiology **4:**132-7.
161. **Mascher, T., J. D. Helmann, and G. Unden.** 2006. Stimulus perception in bacterial signal-transducing histidine kinases. Microbiology and Molecular Biology Review **70:**910-38.
162. **Mashburn-Warren, L., D. A. Morrison, and M. J. Federle.** 2010. A novel double-tryptophan peptide pheromone controls competence in Streptococcus spp. via an Rgg regulator. Molecular Microbiology **78:**589-606.
163. **Matsuka, Y. V., S. Pillai, S. Gubba, J. M. Musser, and S. B. Olmsted.** 1999. Fibrinogen cleavage by the Streptococcus pyogenes extracellular cysteine protease and generation of antibodies that inhibit enzyme proteolytic activity. Infection and Immunity **67:**4326-33.
164. **McArthur, J., E. Medina, A. Mueller, J. Chin, B. J. Currie, K. S. Sriprakash, S. R. Talay, G. S. Chhatwal, and M. J. Walker.** 2004. Intranasal vaccination with streptococcal fibronectin binding protein Sfb1 fails to prevent growth and dissemination of Streptococcus pyogenes in a murine skin infection model. Infection and Immunity **72:**7342-5.
165. **McArthur, J. D., and M. J. Walker.** 2006. Domains of group A streptococcal M protein that confer resistance to phagocytosis, opsonization and protection: implications for vaccine development. Molecular Microbiology **59:**1-4.
166. **McCormick, J. K., A. A. Pragman, J. C. Stolpa, D. Y. Leung, and P. M. Schlievert.** 2001. Functional characterization of streptococcal pyrogenic exotoxin J, a novel superantigen. Infection and Immunity **69:**1381-8.
167. **McIver, K. S., A. S. Heath, and J. R. Scott.** 1995. Regulation of virulence by environmental signals in group A streptococci: influence of osmolarity,

temperature, gas exchange, and iron limitation on *emm* transcription. Infection and Immunity **63:**4540-4542.

168. **McIver, K. S., and R. L. Myles.** 2002. Two DNA-binding domains of Mga are required for virulence gene activation in the group A streptococcus. Molecular Microbiology **43:**1591-1602.
169. **McIver, K. S., and J. R. Scott.** 1997. Role of *mga* in growth phase regulation of virulence genes of the group A streptococcus. Journal of Bacteriology **179:**5178-5187.
170. **Meehl, M. A., and M. G. Caparon.** 2004. Specificity of streptolysin O in cytolysin-mediated translocation. Molecular Microbiology **52:**1665-76.
171. **Metzgar, D., D. Baynes, C. J. Hansen, E. A. McDonough, D. R. Cabrera, M. M. Ellorin, P. J. Blair, K. L. Russell, and D. J. Faix.** 2009. Inference of antibiotic resistance and virulence among diverse group A Streptococcus strains using emm sequencing and multilocus genotyping methods. PLoS One **4:**e6897.
172. **Mitchell, T. J.** 2003. The pathogenesis of streptococcal infections: from tooth decay to meningitis. Nature Reviews. Microbiology **1:**219-30.
173. **Miyoshi-Akiyama, T., D. Takamatsu, M. Koyanagi, J. Zhao, K. Imanishi, and T. Uchiyama.** 2005. Cytocidal effect of *Streptococcus pyogenes* on mouse neutrophils in vivo and the critical role of streptolysin S. Journal of Infectious Disease **192:**107-16.
174. **Molinari, G., M. Rohde, S. R. Talay, G. S. Chhatwal, S. Beckert, and A. Podbielski.** 2001. The role played by the group A streptococcal negative regulator Nra on bacterial interactions with epithelial cells. Molecular Microbiology **40:**99-114.
175. **Mora, M., G. Bensi, S. Capo, F. Falugi, C. Zingaretti, A. G. Manetti, T. Maggi, A. R. Taddei, G. Grandi, and J. L. Telford.** 2005. Group A streptococcus produce pilus-like structures containing protective antigens and Lancefield T antigens. Proceedings of the National Academy of Sciences of the United States of America **102:**15641-6.
176. **Muller-Alouf, H., T. Proft, T. M. Zollner, D. Gerlach, E. Champagne, P. Desreumaux, C. Fitting, C. Geoffroy-Fauvet, J. E. Alouf, and J. M. Cavaillon.** 2001. Pyrogenicity and cytokine-inducing properties of Streptococcus pyogenes superantigens: comparative study of streptococcal mitogenic exotoxin Z and pyrogenic exotoxin A. Infection and Immunity **69:**4141-5.
177. **Musser, J. M., and F. R. DeLeo.** 2005. Toward a genome-wide systems biology analysis of host-pathogen interactions in group A Streptococcus. American Journal of Pathology **167:**1461-72.
178. **Nataro, J. P., D. Yikang, D. Yingkang, and K. Walker.** 1994. AggR, a transcriptional activator of aggregative adherence fimbria I expression in enteroaggregative Escherichia coli. J Bacteriol **176:**4691-9.
179. **Nelson, D., R. Schuch, P. Chahales, S. Zhu, and V. A. Fischetti.** 2006. PlyC: a multimeric bacteriophage lysin. Proceedings of the National Academy of Sciences of the United States of America **103:**10765-70.
180. **Nizet, V., B. Beall, D. J. Bast, V. Datta, L. Kilburn, D. E. Low, and J. C. De Azavedo.** 2000. Genetic locus for streptolysin S production by group A streptococcus. Infection & Immunity **68:**4245-4254.

181. **Nobbs, A. H., R. J. Lamont, and H. F. Jenkinson.** 2009. Streptococcus adherence and colonization. Microbiol Mol Biol Rev **73:**407-50.
182. **Nordstrand, A., M. Norgren, J. J. Ferretti, and S. E. Holm.** 1998. Streptokinase as a mediator of acute post-streptococcal glomerulonephritis in an experimental mouse model. Infection and Immunity **66:**315-21.
183. **Novick, R. P.** 2003. Autoinduction and signal transduction in the regulation of staphylococcal virulence. Molecular Microbiology **48:**1429-49.
184. **O'Hara, B. P., R. A. Norman, P. T. Wan, S. M. Roe, T. E. Barrett, R. E. Drew, and L. H. Pearl.** 1999. Crystal structure and induction mechanism of AmiC-AmiR: a ligand-regulated transcription antitermination complex. EMBO Journal **18:**5175-86.
185. **Oehmcke, S., A. Podbielski, and B. Kreikemeyer.** 2004. Function of the fibronectin-binding serum opacity factor of *Streptococcus pyogenes* in adherence to epithelial cells. Infection and Immunity **72:**4302-8.
186. **Ohlsen, K. L., J. K. Grimsley, and J. A. Hoch.** 1994. Deactivation of the sporulation transcription factor Spo0A by the Spo0E protein phosphatase. Proceedings of the National Academy of Sciences of the United States of America **91:**1756-60.
187. **Olsen, R. J., I. Sitkiewicz, A. A. Ayeras, V. E. Gonulal, C. Cantu, S. B. Beres, N. M. Green, B. Lei, T. Humbird, J. Greaver, E. Chang, W. P. Ragasa, C. A. Montgomery, J. Cartwright, Jr., A. McGeer, D. E. Low, A. R. Whitney, P. T. Cagle, T. L. Blasdel, F. R. DeLeo, and J. M. Musser.** 2010. Decreased necrotizing fasciitis capacity caused by a single nucleotide mutation that alters a multiple gene virulence axis. Proceedings of the National Academy of Sciences of the United States of America **107:**888-93.
188. **Opdyke, J. A., J. R. Scott, and C. P. Moran.** 2001. A secondary RNA polymerase sigma factor from *Streptococcus pyogenes*. Molecular Microbiology **42:**495-502.
189. **Pahlman, L. I., P. F. Marx, M. Morgelin, S. Lukomski, J. C. Meijers, and H. Herwald.** 2007. Thrombin-activatable fibrinolysis inhibitor binds to Streptococcus pyogenes by interacting with collagen-like proteins A and B. Journal of Biological Chemistry **282:**24873-81.
190. **Pahlman, L. I., A. I. Olin, J. Darenberg, M. Morgelin, M. Kotb, H. Herwald, and A. Norrby-Teglund.** 2008. Soluble M1 protein of Streptococcus pyogenes triggers potent T cell activation. Cellular Microbiology **10:**404-14.
191. **Park, H., and M. Inouye.** 1997. Mutational analysis of the linker region of EnvZ, an osmosensor in Escherichia coli. Journal of Bacteriology **179:**4382-90.
192. **Perego, M., C. Hanstein, K. M. Welsh, T. Djavakhishvili, P. Glaser, and J. A. Hoch.** 1994. Multiple protein-aspartate phosphatases provide a mechanism for the integration of diverse signals in the control of development in B. subtilis. Cell **79:**1047-55.
193. **Perez, N., J. Trevino, Z. Liu, S. C. Ho, P. Babitzke, and P. Sumby.** 2009. A genome-wide analysis of small regulatory RNAs in the human pathogen group A Streptococcus. PLoS One **4:**e7668.
194. **Perez-Casal, J., M. G. Caparon, and J. R. Scott.** 1991. Mry, a trans-acting positive regulator of the M protein gene of *Streptococcus pyogenes* with similarity

to the receptor proteins of two-component regulatory systems. Journal of Bacteriology **173:**2617-2624.

195. **Perez-Casal, J., J. A. Price, E. Maguin, and J. R. Scott.** 1993. An M protein with a single C repeat prevents phagocytosis of *Streptococcus pyogenes*: use of a temperature-sensitive shuttle vector to deliver homologous sequences to the chromosome of *S. pyogenes*. Molecular Microbiology **8:**809-819.
196. **Phillips, G. N., Jr., P. F. Flicker, C. Cohen, B. N. Manjula, and V. A. Fischetti.** 1981. Streptococcal M protein: alpha-helical coiled-coil structure and arrangement on the cell surface. Proceedings of the National Academy of Sciences of the United States of America **78:**4689-93.
197. **Podbielski, A., M. Woischnik, B. A. Leonard, and K. H. Schmidt.** 1999. Characterization of *nra*, a global negative regulator gene in group A streptococci. Molecular Microbiology **31:**1051-64.
198. **Rakonjac, J. V., J. C. Robbins, and V. A. Fischetti.** 1995. DNA sequence of the serum opacity factor of group A streptococci: identification of a fibronectin-binding repeat domain. Infection and Immunity **63:**622-31.
199. **Rasmussen, M., and L. Bjorck.** 2002. Proteolysis and its regulation at the surface of *Streptococcus pyogenes*. Molecular Microbiology **43:**537-544.
200. **Rasmussen, M., and L. Bjorck.** 2001. Unique regulation of SclB - a novel collagen-like surface protein of Streptococcus pyogenes. Molecular Microbiology **40:**1427-38.
201. **Rasmussen, M., H. P. Muller, and L. Bjorck.** 1999. Protein GRAB of *Streptococcus pyogenes* regulates proteolysis at the bacterial surface by binding a2-macroglobulin. Journal of Biological Chemistry **274:**15336-44.
202. **Rasmussen, R., A. Eden, and L. Bjorck.** 2000. SclA, a novel collagen-like surface protein of *Streptococcus pyogenes*. Infection and Immunity **68:**6370-6377.
203. **Reid, S. D., M. S. Chaussee, C. D. Doern, M. A. Chaussee, A. G. Montgomery, D. E. Sturdevant, and J. M. Musser.** 2006. Inactivation of the group A Streptococcus regulator srv results in chromosome wide reduction of transcript levels, and changes in extracellular levels of Sic and SpeB. FEMS Immunology and Medical Microbiology **48:**283-92.
204. **Reid, S. D., A. G. Montgomery, and J. M. Musser.** 2004. Identification of *srv*, a PrfA-like regulator of group A streptococcus that influences virulence. Infection and Immunity **72:**1799-803.
205. **Rhee, S., R. G. Martin, J. L. Rosner, and D. R. Davies.** 1998. A novel DNA-binding motif in MarA: the first structure for an AraC family transcriptional activator. Proceedings of the National Academy of Sciences of the United States of America **95:**10413-8.
206. **Ribardo, D. A., T. J. Lambert, and K. S. McIver.** 2004. Role of *Streptococcus pyogenes* two-component response regulators in the temporal control of Mga and the Mga-regulated virulence gene *emm*. Infection and Immunity **72:**3668-73.
207. **Ribardo, D. A., and K. S. McIver.** 2006. Defining the Mga regulon: comparative transcriptome analysis reveals both direct and indirect regulation by Mga in the group A streptococcus. Molecular Microbiology **62:**491-508.

208. **Roberts, A. L., K. L. Connolly, C. D. Doern, R. C. Holder, and S. D. Reid.** 2010. Loss of the group A Streptococcus regulator Srv decreases biofilm formation in vivo in an otitis media model of infection. Infection and Immunity **78:**4800-8.
209. **Roberts, S. A., G. G. Churchward, and J. R. Scott.** 2007. Unraveling the regulatory network in *Streptococcus pyogenes*: the global response regulator CovR represses *rivR* directly. Journal of Bacteriology **189:**1459-63.
210. **Roberts, S. A., and J. R. Scott.** 2007. RivR and the small RNA RivX: the missing links between the CovR regulatory cascade and the Mga regulon. Molecular Microbiology **66:**1506-22.
211. **Robinson, V., D. Buckler, and A. Stock.** 2000. A Tale of Two Components: A Novel Kinase and Regulatory Switch. Nature Structural Biology **7:**626-633.
212. **Rocha, C. L., and V. A. Fischetti.** 1999. Identification and characterization of a novel fibronectin-binding protein on the surface of group A streptococci. Infection and Immunity **67:**2720-8.
213. **Rodgers, M. E., and R. Schleif.** 2009. Solution structure of the DNA binding domain of AraC protein. Proteins **77:**202-8.
214. **Sabharwal, H., F. Michon, D. Nelson, W. Dong, K. Fuchs, R. C. Manjarrez, A. Sarkar, C. Uitz, A. Viteri-Jackson, R. S. Suarez, M. Blake, and J. B. Zabriskie.** 2006. Group A streptococcus (GAS) carbohydrate as an immunogen for protection against GAS infection. Journal of Infectious Diseases **193:**129-35.
215. **Sanders, D. A., B. L. Gillece-Castro, A. M. Stock, A. L. Burlingame, and D. E. Koshland, Jr.** 1989. Identification of the site of phosphorylation of the chemotaxis response regulator protein, CheY. Journal of Biological Chemistry **264:**21770-8.
216. **Schrager, H. M., S. Alberti, C. Cywes, G. J. Dougherty, and M. R. Wessels.** 1998. Hyaluronic acid capsule modulates M protein-mediated adherence and acts as a ligand for attachment of group A streptococcus to CD44 on human keratinocytes. Journal of Clinical Investigation **101:**1708-16.
217. **Schrager, H. M., J. G. Rheinwald, and M. R. Wessels.** 1996. Hyaluronic acid capsule and the role of streptococcal entry into keratinocytes in invasive skin infection. Journal of Clinical Investigation **98:**1954-1958.
218. **Scott, J. R., P. Cleary, M. G. Caparon, M. Kehoe, L. Heden, J. M. Musser, S. Hollingshead, and A. Podbielski.** 1995. New name for the positive regulator of the M protein of group A streptococcus. Molecular Microbiology **17:**799.
219. **Shatursky, O., A. P. Heuck, L. A. Shepard, J. Rossjohn, M. W. Parker, A. E. Johnson, and R. K. Tweten.** 1999. The mechanism of membrane insertion for a cholesterol-dependent cytolysin: a novel paradigm for pore-forming toxins. Cell **99:**293-9.
220. **Shelburne, S. A., 3rd, D. Keith, N. Horstmann, P. Sumby, M. T. Davenport, E. A. Graviss, R. G. Brennan, and J. M. Musser.** 2008. A direct link between carbohydrate utilization and virulence in the major human pathogen group A Streptococcus. Proceedings of the National Academy of Sciences of the United States of America **105:**1698-703.
221. **Shelburne, S. A., 3rd, D. B. Keith, M. T. Davenport, N. Horstmann, R. G. Brennan, and J. M. Musser.** 2008. Molecular characterization of group A

Streptococcus maltodextrin catabolism and its role in pharyngitis. Molecular Microbiology **69:**436-52.

222. **Shelburne, S. A., 3rd, P. Sumby, I. Sitkiewicz, C. Granville, F. R. DeLeo, and J. M. Musser.** 2005. Central role of a bacterial two-component gene regulatory system of previously unknown function in pathogen persistence in human saliva. Proceedings of the National Academy of Sciences of the United States of America **102:**16037-42.
223. **Shelburne, S. A., M. T. Davenport, D. B. Keith, and J. M. Musser.** 2008. The role of complex carbohydrate catabolism in the pathogenesis of invasive streptococci. Trends in Microbiology **16:**318-25.
224. **Shu, C. J., and I. B. Zhulin.** 2002. ANTAR: an RNA-binding domain in transcription antitermination regulatory proteins. Trends in Biochemical Sciences **27:**3-5.
225. **Shulman, S. T., R. R. Tanz, and M. A. Gerber.** 2000. Streptococcal Pharyngitis, p. 76-101. *In* D. L. Stevens and E. L. Kaplan (ed.), Streptococcal Infections: Clinical Aspects, Microbiology, and Molecular Pathogenesis. Oxford University Press, New York.
226. **Sidote, D. J., C. M. Barbieri, T. Wu, and A. M. Stock.** 2008. Structure of the Staphylococcus aureus AgrA LytTR domain bound to DNA reveals a beta fold with an unusual mode of binding. Structure **16:**727-35.
227. **Simpson, W. A., and E. H. Beachey.** 1983. Adherence of group A streptococci to fibronectin on oral epithelial cells. Infection and Immunity **39:**275-9.
228. **Singh, M., B. Berger, P. S. Kim, J. M. Berger, and A. G. Cochran.** 1998. Computational learning reveals coiled coil-like motifs in histidine kinase linker domains. Proceedings of the National Academy of Sciences of the United States of America **95:**2738-43.
229. **Sitkiewicz, I., and J. M. Musser.** 2006. Expression microarray and mouse virulence analysis of four conserved two-component gene regulatory systems in group a streptococcus. Infection and Immunity **74:**1339-51.
230. **Smoot, L. M., J. K. McCormick, J. C. Smoot, N. P. Hoe, I. Strickland, R. L. Cole, K. D. Barbian, C. A. Earhart, D. H. Ohlendorf, L. G. Veasy, H. R. Hill, D. Y. Leung, P. M. Schlievert, and J. M. Musser.** 2002. Characterization of two novel pyrogenic toxin superantigens made by an acute rheumatic fever clone of Streptococcus pyogenes associated with multiple disease outbreaks. Infection and Immunity **70:**7095-104.
231. **Soncini, F. C., E. G. Vescovi, and E. A. Groisman.** 1995. Transcriptional autoregulation of the Salmonella typhimurium phoPQ operon. Journal of Bacteriology **177:**4364-71.
232. **Steer, A. C., M. R. Batzloff, K. Mulholland, and J. R. Carapetis.** 2009. Group A streptococcal vaccines: facts versus fantasy. Curr Opin Infect Dis **22:**544-52.
233. **Stevens, D. L.** 2000. Group A beta-hemolytic streptococci: virulence factors, pathogenesis, and spectrum of clinical infections, p. 37-56. *In* D. L. Stevens and E. L. Kaplan (ed.), Streptococcal Infections: Clinical Aspects, Microbiology, and Molecular Pathogenesis. Oxford University Press, New York.
234. **Stevens, D. L.** 1992. Invasive group A streptococcus infections. Clinical Infectious Diseases **14:**2-11.

235. **Stevens, D. L.** 2000. Life-threatening streptococcal infections: scarlet fever, necrotizing fasciitis, myositis, bacteremia, and streptococcal toxic shock syndrome, p. 163-79. *In* D. L. Stevens and E. L. Kaplan (ed.), Streptococcal Infections: Clinical Aspects, Microbiology, and Molecular Pathogenesis. Oxford University Press, New York.
236. **Stock, A., T. Chen, D. Welsh, and J. Stock.** 1988. CheA protein, a central regulator of bacterial chemotaxis, belongs to a family of proteins that control gene expression in response to changing environmental conditions. Proceedings of the National Academy of Sciences of the United States of America **85:**1403-7.
237. **Stock, A., V. Robinson, and G. P.** 2000. Two-Component Signal Transduction. Annual Review of Biochemistry **69:**183-215.
238. **Stock, A. M., J. M. Mottonen, J. B. Stock, and C. E. Schutt.** 1989. Three-dimensional structure of CheY, the response regulator of bacterial chemotaxis. Nature **337:**745-9.
239. **Stock, J. B., A. M. Stock, and J. M. Mottonen.** 1990. Signal transduction in bacteria. Nature **344:**395-400.
240. **Studier, F. W.** 2005. Protein production by auto-induction in high density shaking cultures. Protein Expression and Purification **41:**207-34.
241. **Sumby, P., K. D. Barbian, D. J. Gardner, A. R. Whitney, D. M. Welty, R. D. Long, J. R. Bailey, M. J. Parnell, N. P. Hoe, G. G. Adams, F. R. Deleo, and J. M. Musser.** 2005. Extracellular deoxyribonuclease made by group A streptococcus assists pathogenesis by enhancing evasion of the innate immune response. Proceedings of the National Academy of Sciences of the United States of America **102:**1679-84.
242. **Sumby, P., S. F. Porcella, A. G. Madrigal, K. D. Barbian, K. Virtaneva, S. M. Ricklefs, D. E. Sturdevant, M. R. Graham, J. Vuopio-Varkila, N. P. Hoe, and J. M. Musser.** 2005. Evolutionary origin and emergence of a highly successful clone of serotype M1 group A streptococcus involved multiple horizontal gene transfer events. Journal of Infectious Diseases **192:**771-82.
243. **Sumby, P., A. R. Whitney, E. A. Graviss, F. R. DeLeo, and J. M. Musser.** 2006. Genome-wide analysis of group a streptococci reveals a mutation that modulates global phenotype and disease specificity. PLoS Pathogens **2:**e5.
244. **Sun, H., U. Ringdahl, J. W. Homeister, W. P. Fay, N. C. Engleberg, A. Y. Yang, L. S. Rozek, X. Wang, U. Sjobring, and D. Ginsburg.** 2004. Plasminogen is a critical host pathogenicity factor for group A streptococcal infection. Science **305:**1283-6.
245. **Sung, K., S. A. Khan, M. S. Nawaz, and A. A. Khan.** 2003. A simple and efficient Triton X-100 boiling and chloroform extraction method of RNA isolation from Gram-positive and Gram-negative bacteria. FEMS Microbiology Letters **229:**97-101.
246. **Surette, M. G., M. Levit, Y. Liu, G. Lukat, E. G. Ninfa, A. Ninfa, and J. B. Stock.** 1996. Dimerization is required for the activity of the protein histidine kinase CheA that mediates signal transduction in bacterial chemotaxis. Journal of Biological Chemistry **271:**939-45.

247. **Swift, H. F., A. T. Wilson, and R. C. Lancefield.** 1943. Typing group A hemolytic streptococci by M precipitin reactions in capillary pipettes. Journal of Experimental Medicine **78:**127-33.
248. **Tanford, C.** 1984. Twenty questions concerning the reaction cycle of the sarcoplasmic reticulum calcium pump. CRC Critical Reviews in Biochemistry **17:**123-51.
249. **Tao, L., S. K. Hollingshead, A. N. Suvorov, J. J. Ferretti, and W. M. McShan.** 1995. Construction of a Streptococcus pyogenes recA mutant via insertional inactivation, and cloning and sequencing of the complete recA gene. Gene **162:**59-62.
250. **Terao, Y., S. Kawabata, E. Kunitomo, J. Murakami, I. Nakagawa, and S. Hamada.** 2001. Fba, a novel fibronectin-binding protein from *Streptococcus pyogenes*, promotes bacterial entry into epithelial cells, and the *fba* gene is positively transcribed under the Mga regulator. Molecular Microbiology **42:**75-86.
251. **Terao, Y., S. Kawabata, M. Nakata, I. Nakagawa, and S. Hamada.** 2002. Molecular characterization of a novel fibronectin-binding protein of *Streptococcus pyogenes* strains isolated from toxic shock-like syndrome patients. Journal of Biological Chemistry **277:**47428-35.
252. **Throup, J. P., K. K. Koretke, A. P. Bryant, K. A. Ingraham, A. F. Chalker, Y. Ge, A. Marra, N. G. Wallis, J. R. Brown, D. J. Holmes, M. Rosenberg, and M. K. Burnham.** 2000. A genomic analysis of two-component signal transduction in *Streptococcus pneumoniae*. Molecular Microbiology **35:**566-76.
253. **Tillett, W. S., and R. L. Garner.** 1933. The fibrinolytic activity of hemolytic streptococci. Journal of Experimental Medicine **58:**485-502.
254. **Todd, E. W., and L. F. Hewitt.** 1932. A new culture medium for the production of antigenic streptococcal haemolysin. Journal of Pathology and Bacteriology **35:**973.
255. **Toppel, A. W., M. Rasmussen, M. Rohde, E. Medina, and G. S. Chhatwal.** 2003. Contribution of protein G-related a2-macroglobulin-binding protein to bacterial virulence in a mouse skin model of group A streptococcal infection. Journal of Infectious Diseases **187:**1694-703.
256. **Toukoki, C., K. M. Gold, K. S. McIver, and Z. Eichenbaum.** 2010. MtsR is a dual regulator that controls virulence genes and metabolic functions in addition to metal homeostasis in the group A streptococcus. Molecular Microbiology **76:**971-89.
257. **Turner, C. E., P. Kurupati, M. D. Jones, R. J. Edwards, and S. Sriskandan.** 2009. Emerging role of the interleukin-8 cleaving enzyme SpyCEP in clinical Streptococcus pyogenes infection. Journal of Infectious Diseases **200:**555-63.
258. **Ulrich, L. E., E. V. Koonin, and I. B. Zhulin.** 2005. One-component systems dominate signal transduction in prokaryotes. Trends in Microbiology **13:**52-6.
259. **Ulrich, R. G.** 2008. Vaccine based on a ubiquitous cysteinyl protease and streptococcal pyrogenic exotoxin A protects against Streptococcus pyogenes sepsis and toxic shock. Journal of Immune Based Therapies and Vaccines **6:**8.

260. **Unnikrishnan, M., J. Cohen, and S. Sriskandan.** 1999. Growth-phase-dependent expression of virulence factors in an M1T1 clinical isolate of *Streptococcus pyogenes*. Infection and Immunity **67:**5495-9.
261. **Vahling, C. M., and K. S. McIver.** 2005. Identification of residues responsible for the defective virulence gene regulator Mga produced by a natural mutant of *Streptococcus pyogenes*. Journal of Bacteriology **187**.
262. **Vincent, W. F., and K. J. Lisiewski.** 1969. Improved growth medium for group A streptococci. Applied Microbiology **18:**954-5.
263. **Virtaneva, K., S. F. Porcella, M. R. Graham, R. M. Ireland, C. A. Johnson, S. M. Ricklefs, I. Babar, L. D. Parkins, R. A. Romero, G. J. Corn, D. J. Gardner, J. R. Bailey, M. J. Parnell, and J. M. Musser.** 2005. Longitudinal analysis of the group A streptococcus transcriptome in experimental pharyngitis in cynomolgus macaques. Proceedings of the National Academy of Sciences of the United States of America **102:**9014-9.
264. **Visai, L., S. Bozzini, G. Raucci, A. Toniolo, and P. Speziale.** 1995. Isolation and characterization of a novel collagen-binding protein from Streptococcus pyogenes strain 6414. Journal of Biological Chemistry **270:**347-53.
265. **von Pawel-Rammingen, U., B. P. Johansson, and L. Bjorck.** 2002. IdeS, a novel streptococcal cysteine proteinase with unique specificity for immunoglobulin G. The EMBO Journal **21:**1607-15.
266. **Voyich, J. M., K. R. Braughton, D. E. Sturdevant, C. Vuong, S. D. Kobayashi, S. F. Porcella, M. Otto, J. M. Musser, and F. R. DeLeo.** 2004. Engagement of the pathogen survival response used by group A streptococcus to avert destruction by innate host defense. Journal of Immunology **173:**1194-201.
267. **Voyich, J. M., D. E. Sturdevant, K. R. Braughton, S. D. Kobayashi, B. Lei, K. Virtaneva, D. W. Dorward, J. M. Musser, and F. R. DeLeo.** 2003. Genome-wide protective response used by group A streptococcus to evade destruction by human polymorphonuclear leukocytes. Proceedings of the National Academy of Sciences of the United States of America **100:**1996-2001.
268. **Walker, M. J., A. Hollands, M. L. Sanderson-Smith, J. N. Cole, J. K. Kirk, A. Henningham, J. D. McArthur, K. Dinkla, R. K. Aziz, R. G. Kansal, A. J. Simpson, J. T. Buchanan, G. S. Chhatwal, M. Kotb, and V. Nizet.** 2007. DNase Sda1 provides selection pressure for a switch to invasive group A streptococcal infection. Nature Medicine **13:**981-5.
269. **Wei, L., V. Pandiripally, E. Gregory, M. Clymer, and D. Cue.** 2005. Impact of the SpeB protease on binding of the complement regulatory proteins factor H and factor H-like protein 1 by Streptococcus pyogenes. Infection and Immunity **73:**2040-50.
270. **Wessels, M. R., and M. S. Bronze.** 1994. Critical role of the group A streptococcal capsule in pharyngeal colonization and infection in mice. Proceedings of the National Academy of Sciences of the United States of America **91:**12238-42.
271. **West, A., and A. Stock.** 2001. Histidine Kinases and Response Regulator Proteins in Two-Component Signaling Systems. Trends in Biochemical Sciences **26:**369-376.

272. **Widdowson, J. P., W. R. Maxted, and D. L. Grant.** 1970. The production of opacity in serum by group A streptococci and its relationship with the presence of M antigen. The Journal of General Microbiology **61:**343-53.
273. **Zhang, S., A. Reeves, R. L. Woodbury, and W. G. Haldenwang.** 2005. Coexpression patterns of sigma(B) regulators in Bacillus subtilis affect sigma(B) inducibility. J Bacteriol **187:**8520-5.
274. **Zhu, X., J. Rebello, P. Matsumura, and K. Volz.** 1997. Crystal structures of CheY mutants Y106W and T87I/Y106W. CheY activation correlates with movement of residue 106. J Biol Chem **272:**5000-6.
275. **Zinkernagel, A. S., A. M. Timmer, M. A. Pence, J. B. Locke, J. T. Buchanan, C. E. Turner, I. Mishalian, S. Sriskandan, E. Hanski, and V. Nizet.** 2008. The IL-8 protease SpyCEP/ScpC of group A Streptococcus promotes resistance to neutrophil killing. Cell Host Microbe **4:**170-8.